JIMMA UNIVERSITY

JIMMA INSTITUTE OF TECHNOLOGY

SCHOOL OF POST GRADUATE STUDIES

FACULTY OF CIVIL AND ENVIRONMENTAL ENGINEERING

DEPARTMENT OF HYDRAULIC AND WATER RESOURCE ENGINEERING

HYDROLOGY AND HYDRAULIC ENGINEERING CHAIR

MASTERS PROGRAM IN HYDRAULIC ENGINEERING

Evaluation of Impact of Climate Change on Streamflow, A Case of Mojo River, Upper Awash Basin, Ethiopia

A final thesis Submitted to the School of Post Graduate Studies of Jimma University, Jimma Institute of Technology Faculty of Civil and Environmental Engineering in Partial Fulfillment of the Requirement for the Degree of Masters of Science in Hydraulic Engineering**.**

By

SORESSA FITA IJIGU

January, 2022

Jimma, Ethiopia

JIMMA UNIVERSITY

JIMMA INSTITUTE OF TECHNOLOGY

SCHOOL OF POST GRADUATE STUDIES FACULTY OF CIVIL AND ENVIRONMENTAL ENGINEERING

DEPARTMENT OF HYDRAULIC AND WATER RESOURCE ENGINEERING

MASTERS PROGRAM IN HYDRAULIC ENGINEERING

Evaluation of Impact of Climate Change on Streamflow, A Case of Mojo River, Upper Awash Basin, Ethiopia

A final thesis Submitted to the School of Post Graduate Studies of Jimma University, Jimma Institute of Technology Faculty of Civil and Environmental Engineering in Partial Fulfillment of the Requirement for the Degree of Masters of Science in Hydraulic Engineering

By

SORESSA FITA IJIGU

Advisors:

Advsior Mr. Tolera Abdisa (Assist. Prof.)

Co-advisor Mr. Wana Geyisa (M.Sc.)

January, 2022

Jimma, Ethiopia

DECLARATION

I hereby declare that this is a final thesis, entitled "Evaluation of the impact of climate change on streamflow" using the SWAT model, A case study of Mojo River, upper awash basin, Ethiopia. This is my original work which I submit for partial fulfillment of the degree of Master of Science in Hydraulic Engineering at the school of post graduate studies; Hydrology and Hydraulic Engineering Chair, Jimma Institute of Technology, Jimma University. The thesis was conducted under the guidance of the main advisor, Tolera Abdissa (Asst. Prof.), and Co-Advisor Wana Geyisa (M.Sc.)

Name	Signature	Date
Soressa Fita		24/04/2022

Name	Signature	Date
1. Tolera Abdisso Main Advisor (assist. Prof.)		24/04/2022
2. Wana Geyisa CO – Advisor (M.Sc.)		24/04/22

APPROVALPAGE

This thesis entitled "**Evaluation of the impact of climate change on stream flow" A case study of Mojo River, upper awash basin, Ethiopia."** has been approved by the examiners and submitted as a partial fulfillment for the award of the Degree of Master of Science in Hydraulic Engineering complies with the regulations of the university and meets the accepted standards with respect to originality, content and quality.

Members of the Examining board:

Name	Signature	Date
1.Dr. Adane Abebe External Examiner		24/01/2022
2. Mr. Abebe Chala Internal Examiner		24/01/2022
3. Mr. Nasir Gebi chair person		24/01/2022

ACKNOWLEDGMENT

First of all, I would like to thank the space almighty God. You have given me all the chance, strength, and good health. I would like to express my sincere gratitude to Jimma University (JU), Jimma Institute of Technology (JIT).

I am deeply indebted to my advisors Tolera Abdissa (Asst. Prof.) for this support in supervising my thesis work, providing me with important reference and also my Co-advisor Wana Geyisa (M.Sc.) for their professional guidance, encouragement, and continued support provided throughout my thesis work without them, this work wouldn’t have been realized.

They devoted their precious time and provided me with all the necessary relevant literature and information to carry out the thesis. Finally, I would like to deepen my sincere gratitude to my family my mother (Malkitu Temasgn) and Father, all my brothers, and my sister for encouragement. Last but not least, I would like to thank my friends for their ultimate support and encouragement.

ABSTRACT

The impact of climate change on streamflow is one of the present-day sensitive issues all over the world. The main objective of this study was to evaluate the impact of climate change streamflow in the Mojo River watershed, Upper Awash River basin, Ethiopia. The observed hydro-meteorological data for the baseline period of 1987-2016 was collected from Ethiopian Ministry of Water,Irrigation and Energy (MoWIE) and Ethiopian Meteorological Agency (EMA). Three Regional Climate Models (RCMs),i.e. RACMO22T, RCA4 and CCLM4-8, derived by one MOHC-HadGEM2-ES Global Climate Model (GCM) were downloaded from CORDEX-Africa, under representative concentration pathways (RCPs)4.5 and 8.5. Each climatic parameter was extracted from RCMs using Arc GIS 10.4.1 and the performance of the model was tested by using r, RMSE, PBIAS, and identified RAMCO22T the better performed than the other. Bias corrections was done by power transformation for the precipitation and variance scale for the temperature equation. The trend of precipitation and temperature was significantly increased and decreasing annually. The simulation was carried out by using the Soil and Water Assessment Tool (SWAT) model under historical (1987-2016) and future climatic scenarios that range between (2022-2051) and (2052-2081). Calibration and validation were performed by using sequential uncertainty fitting version-two (SUFI-2) algorithm in SWAT CUP program utilizing recorded streamflow data of (2000-2015). The Performance of the model was evaluated during calibration (R^2 = 0.71, NSE = 0.70, PBAIS = -13.9) and validation (R^2 = 0.71, NSE = 0.64, PBAIS = -4.7). The projected mean annual maximum temperature showed an increasing trend in the future period (2022-2051), and (2052 - 2081) periods under RCP4.5 by 0.14℃ and 0.7℃, and RCP8.5 scenarios by 0.4℃ and 1.3℃ respectively. Whereas, the minimum temperature will be decreasing by (-1.1 and -0.7) for (2022-2051) and increasing by (1.3 and 1.3) for (2052-2081) periods under RCP4.5 and RCP8.5 scenarios respectively. The annual streamflow will increase by 55% and 57.07% under RCP4.5, and by 55.8% and 58% under RCP8.5 with the future periods of (2051), and (2081) respectively.

Keywords: - Arc SWAT, CORDEX, Climate change, MK, RCM RCPs, Streamflow

TABLE OF CONTENTS

LIST OF FIGURE

LIST TABLE

LIST OF ACRONYMS

AR4	the Fourth Assessment Report
CO2	Carbon dioxide
CORDEX	Coordinated regional climate downscaling experiment
CMIP5	Coupled Model Inter-Comparison Project Phase 5
DEM	Model Digital Elevation
GCM	Global climate model
GLUE	Generalized Likelihood Uncertainty Estimation
IPCC	Intergovernmental panel on climate change
HRU	Hydrological Response Unit
LULC	Land use land cover
MKT	Modified Mann-Kendal test
NSE	Nash-Sutcliff Efficiency
SRES	Special Report on Emission Scenarios
r	Pearson product-moment correlation coefficient
R^2	Coefficient of determination
RMSE	Root mean square error
PBIAS	Present of Bias
SUFI-2	Sequential Uncertainty Fitting version-2
SWAT	Soil and Water Assessment Tool
SWATCUP	Soil and Water Assessment Tool Calibration and Uncertainty
RCP	Representative Concentration Pathway climate scenario
WMO	World Metrological Organization
MoWIE	Ministry of Water, Irrigation, and Energy

1 INTRODUCTION

1.1 Back Ground

Climate is weather averaged over an extended period (30-year intervals). The United Nations Framework Convention on Climate Change defines climate change as “a change of climate which is attributed directly or indirectly to human activities that alter the composition of the global atmosphere in addition to the natural climate variability observed over a comparable period” (UNFCC,2011). It is mainly attributed to anthropogenic activities like rising temperature, and sea levels, increase in the emission of greenhouse gases (GHGS), and erratic, unpredictable, and unreliable rainfall patterns (Asare-nuamah and Botchway, 2019)

The world climate has been changing for several years with a widespread impact on human and natural systems. However, its changes have become more rapid and unusual in recent to the past (Conway, 2011; Birara *et al.*, 2018; Moges and Bhat, 2021*)*. According to the Fifth Assessment Report (AR5) of the International Panel on Climate Change (IPCC, 2013), climate change is a well-documented and acknowledged phenomenon that may cause human health problems, water supply shortages, and damage to biodiversity and ecosystems, among other impacts on the economy and the environment. Many parts of the world, particularly countries in sub-Sahara Africa are affected by climate change owing to changing temperature and precipitation patterns (Conway, 2011*)*. The rainfall variability and warming of temperature are being perceived as the two most important variables of climate change, imposing a crippling effect on streamflow in sub-Saharan African countries (Ibe & Amikuzuno, 2019).

Also, the other potential impacts of climate change will be changing frequency, intensity, and predictability of rainfall. This change will ultimately influence water availability which will have reaching consequences on water supply, agriculture, and hydropower generation (Taye & Willems, 2013), and concerning hydrology, climate change can cause a significant impact on streamflow by resulting in changes in the hydrological cycle.

Ethiopia is one of the Sub-Sahara African countries that is extremely vulnerable to the impacts of climate change and variability (Birara *et at., 2018),* it is vulnerable to climate change since the economy of the country mainly depends on agriculture, which is very sensitive to climate change and variations (Kefeni *et al*., 2020). The recurrent droughts combined with changes in the amount and spatial distribution of seasonal and annual rainfall are among the major climate-related disasters in Ethiopia (Addisu *et al.*, 2015; Zeleke *et al.*, 2017; Weldearegay and Tedla, 2018). Though one of the countries which development activities encompass all major river basins. The Awash River basin is the most important, intensively utilized, and environmentally vulnerable in Ethiopia due to the huge agricultural potentials in the awash basin that have been considerable attention (Mahtsente Tibebe Tadese *et al.*, 2019). It is the most developed area with more than 60% of the potential irrigable area has been developed (Kerim *et al., 2016*).

The Mojo River watershed is one of the sources of the Upper Awash River basin and its water resources are an important input for water development projects and the livelihood support of the communities in the basin and it covers a wide climate zone (from humid subtropical to arid). The fact that the impact of different climate change scenarios projected at the global scale, the exact type, and the magnitude of the impact at the catchment scale is not investigated in most parts of the world (Andrew *et al., 2010*). Hence, identifying the local impacts of climate change at the catchment level is quite important for the decision-makers and designers.

Therefore, this research was aimed to evaluate performance of different RCMs models using statistical method and the impact of climate changes on streamflow of Mojo River watershed using the Soil and Water Assessment Tools (SWAT). The driven downscaled future climate projection models were from Hadley Global Environmental Model-2-Earth System (HadGEM2-ES). The downscaled regional climate model was (RAMCO22T, CCLM4-8, RCA4) under two radiactive forcing scenarios (RCPs4.5 and RCP8.5). The two Representative Concentration Pathways (RCPs) together span the most range of all the four (RCPs) scenarios.

1.2 Statement of the Problem

The countries around the world will likely face climate change impacts that affect a wide variety of sectors, from water resources to human health to ecosystems. The impacts are varying from country to country. Many people in developing countries are more vulnerable to climate change impacts than people in developed countries. Africa may be the most vulnerable continent to climate variability and change because of multiple existing pressures and low adaptive capacity. Existing pressures include poverty, food insecurity, political conflicts, and ecosystem degradation**.** Also, it is accelerating from time to time over the earth's surface due to the increase in human activities (Fekadu *et al.*, 2019). The rate increase since 1976 has been approximately three times faster than the century-scale trend (NCDC,2008)**.**

The impact of climate on water resources is high worldwide, because water resources in particular comprise one sector that is highly dependent on and influenced by climate change (Tadesse & Paper, 2010). Future change in overall flow magnitude, variability, and timing of the main flow event is among the most frequently cited hydrological issues (Kaluarachchi & Smakhtin, 2008). It has been adversely affecting water resources in Ethiopia, mainly through rising temperatures, changing rainfall patterns, and increasing atmospheric water demand. Especially semi-arid and arid areas are particularly vulnerable to the impacts of climate change on the water resource. Mojo river is one of the upper awash sub-basin, Awash River basin is a basin that covers a wide climate zone (from humid subtropical to arid), it is a relatively well-developed water source in Ethiopia also several towns in and around it (Bewket *et al.*, 2015*)*. The long-term evaluation of the impacts of climate change on hydrological components such as streamflow and precipitation over the watershed area is necessary to support long-term water resources management and planning. Therefore, changes in streamflow caused by climate change have become the most important topic for future water resources management. But most studies have been done on the impact of climate change either at the country level or river basin scale.

Therefore, the results of these studies are highly aggregated and have little importance in information on the impact of climate change at a smaller watershed scale and this may cause significant problems for any water resources development activities that would be planned the river basins. The Mojo River is one upper Awash River basin and the river that face competition among users. The competition for water among the major users of the river is increasing due to socio-economic development and population growth in the area. Due to this, there is a change in land use and land cover on watershed areas, this is one of the causes of climate change. Therefore, these research aims are to better understand local climate phenomena, and performance of model evaluation. Then the result of the study can be used as a tool for planners and decision-makers and to predict the impact of climate change risk on streamflow and ecosystem to improve response capacity using the SWAT model

1.3 The Objective of the Research

1.3.1 General Objective

The general objective of this study is to evaluate the impact of climate change on the streamflow of the Mojo river watershed by using the soil and water assessment tool (SWAT) model.

1.3.2 Specific Objectives

i. To evaluate the performance of different regional climate models using statistical methods.

ii. To analyze the variability and trends of the precipitation and temperature on an annual and seasonal basis.

iii. To assess the impact of future climate changes on streamflow using the SWAT model.

1.4 Research Questions

1. How do different regional climate models perform over the Mojo River watershed?
2. What are the trends of future precipitation and temperature to climate change in annual and seasonal?
3. What is the response of streamflow of Mojo River to present and future climate change?

1.5 Significance of Study

The impact of climate change on streamflow and precipitation is increased over the entire world today. Climate change has significantly impacted water resources. The Awash River basin is one of the twelve river basins in Ethiopia that is subjected to high climate variability, experiencing frequent floods and droughts. The basin is already subjected to water stress, with higher water demand than supply. The streamflow naturally varies over a year. So knowing the variation amount of streamflow has important because very high flows can cause erosion and damaging floods, while very low flows would have diminished water quality, harm fish, and reduced the amount of water available for people to use. To know such variation on streamflow and precipitation on the watershed area it needs the climate change impacts studies.

Identifying the impact climate change cause on streamflow and the performance of the models for the watershed area is the important one. Also, clear variation of streamflow, precipitation, and temperature with seasonal for the future and the present are other important. Therefore, knowing such impact was an input for water resource planners, decision-makers, and any concerned body to understand the consequences of climate change impacts on the watershed area in general and streamflow in particular. The results would be compared with ground-based measurements in the watershed based on monthly, seasonally, and annual climate variables. The output of the study helps to evaluate model results in the watershed or regions. They are also important for the understanding of local climate in regions of Ethiopia that have the same properties of streamflow. Furthermore, the study output is would be intended to be used for the evaluation of the impact of climate change on watershed areas.

1.6 Scope of the Research

The purpose of this study was bounded by the objective of the study that aimed to evaluate the impact of climate change on streamflow, precipitation, and temperature on the Mojo River watershed. The evaluation of the impact of climate change was succeeded using the Soil and Water Assessment Tool (SWAT) model and by fulfilling data required such as CORDEX-Africa, DEM, spatial like slope, land use, land use, and soil type. Ongoing work-wise this

SWAT model was used to develop the impact of climate change on mojo watershed for the present and future.

In general, one of the primary reasons for this research was to enable or develop climate change impacts on streamflow, precipitation, and temperature strategies of Mojo River flow. recommendation on the measurement to take to reduce the impact of climate change as a result of the external and internal driving force.

2 LITERATURE REVIEW

2.1 Overview of Climate Change

Climate change has emerged as one of the biggest environmental challenges facing the world (Dervis, 2007). According to IPCC (2007), climate change can be defined as a change in the state of the climate that can be identified (e.g. using statistical tests) by changes in the mean or the variability of its properties, and that persists for an extended period, typically decades or longer. It refers to any change in climate over time, whether due to natural variability or as a result of human activity. So one way of detecting such an influence is through long-term changes in mean conditions, preferably guided by climate model studies as to which variables and how they should change. One of the great challenges of the 21st century is climate change. Due to the shift in the average patterns of weather, climate change and variability are now becoming significant development challenges (Abera, 2011).

The impacts of climate change on water resources are high on the research agenda worldwide. Future changes in flow magnitude, variability, and timing of the flow events are among the most frequently cited hydrologic issues (Yaseen *et al.*, 2014). The impact of climate change on hydrological processes is an issue of high priority for hydrological. The effect of climate change on streamflow conditions has been revealed in different parts of the world (Saharia & Kumar, 2018). These effects will be particularly severe in regions where the climate becomes drier (Wang *et al*., 2011).

Scientists look in many places to find clues about climate change. Like that, they observed historical records, collect measurements, and observe trends in temperature, weather patterns, sea level, and other features of the environment. Because there are so many clues from all over the world that the climate is changing from time to time, to know that climate change is now happening today and it imposed so many problems like changing the temperature and precipitation pattern (Morello, 2011). Recently, there is strong scientific evidence that indicates the average temperature on the earth's atmosphere is continuing to rise due to an increase in greenhouses gases at all levels on the earth's surface.

According to the Intergovernmental Panel on Climate Change (IPCC) Scientific Assessment Report, the global average temperature would rise between 1.4 and 5.8°C by 2100 with the doubling of the CO2 concentration in the atmosphere (Roth *et al.*, 2018);

The fifth Assessment Report (AR5) of the Intergovernmental Panel on Climate Change (IPCC) indicates that rainfall over Eastern Africa has decreased between March and June in the last three decades, while there has been an increase in temperature over East Africa since the beginning of the 1980s (Climate change, 2014). Climate projections also indicate that there will be a likely increase in rainfall amount and extreme rainfall in the region by the end of the 21st century. There will be higher rates of evaporation in Ethiopia due to warming over the country due it is one tropical country. Such changes are expected to impact the economy of East African countries, including Ethiopia, by high climate sensitivity. Regular climate change assessment studies focus on only one hydrological component such as streamflow. However, to gain insights into the variation of streamflow of the basin in the future, all relevant hydrological components should be considered (Uniyal & Jha, 2015). The long-term evaluation of the impacts of climate change on hydrological components such as streamflow, evapotranspiration, and water yield is necessary to support long-term water resources management and planning (Capdevila *et al.*, 2015).

2.2 Impact of Climate Change

The impacts of future climate change on available water resources are critical and affect the quantity and quality of water because of the increased temperature and variability of rainfall intensity and frequency (Bates *et al.*, 2008). Accordingly, the increasing temperature and rainfall variability which varies the climate of the earth will be expected to disturb the hydrological cycle in terms of increasing water stress, increasing the risks of flooding and drought in many areas, and affecting food availability, stability, access, and utilization. This may lead to affect the livelihood of many people. Sub Saharan Africa region has been experiencing increasing natural disasters with a noticeable severe food and drought of 2010 and 2012 respectively in central and western Africa that affected more than 1.5 million people and death of 340 (Ilori & Ajayi, 2020). Ethiopia is one of the African countries whose economy is largely dependent on agriculture. Therefore, the country's economy is subjected to a direct impact of climate change (WaleWorqlul *et al.*, 2018) and Ethiopia is experiencing the impacts of both climate change and variability (Zegeye, 2018).

The estimation of water resources and their future availability under effects of global warming and climatic change, which occur from a direct consequence of warmer temperatures, require multi-disciplinary research, especially when considering hydrology and global water resources, must be based on present world climate patterns (WMO, 2012). Based on the statistically downscaled GCM outputs, assessment of available water resources and impact of climate change in Mara River Basin, Kenya, indicates the hydrologic impact of climate change on water resource availability that often expressed as change in surface flow volume or groundwater table depth (Dessu & Melesse, 2013). In general, all major climate changes, including natural ones, are disruptive. Past climate changes led to the extinction of many species, population migrations, and pronounced changes in the land surface and ocean circulation. The speed of the current climate change is faster than most of the past events, making it more difficult for human societies and the natural world to adapt (Society,2020).

2.2.1 Assessment of Climate Change

Streamflow is a measure of the rate at which water is carried by rivers and streams, and it represents a critical resource for people and the environment. Changes in streamflow can directly influence the supply of drinking water and the amount of water available for irrigating crops, generating electricity, and other needs. In addition, many plants and animals depend on streamflow for habitat and survival. Streamflow naturally varies over a year. For example, rivers and streams in many parts of the country have their highest flow when the snow melts in the spring and their lowest flow in late summer. The knowing amount of streamflow is important because very high flows can cause erosion and damaging floods, while very low flows can diminish water quality, harm fish, and reduce the amount of water available for people to use. The timing of high flow is important because it affects the ability of reservoir managers to store water to meet needs later in the year. In addition, some plants and animals (such as fish that migrate) depend on a particular pattern of streamflow as part of their life cycles. Climate change can affect streamflow in several ways. Changes in the amount of precipitation and air temperatures that influence melting can alter the size and timing of high spring streamflow. More precipitation is expected to cause higher average streamflow in some places, while heavier could lead to larger peak flow. More frequent or severe droughts, however, could reduce streamflow in certain areas (Climate Change Indicators in the United States, 2016).

Most of the climate change impact assessment studies for streamflows have used data from GCM's output only and limited studies are available that implement RCM data. Presents the effects of different climate scenarios in the streamflow and shows that climate change may drastically impact the system to assure energy. It is quite apparent from the diverse scientific literature that to assess the impact of the changing climate at a local scale, it is vital to utilize the results of climate simulation conducted at an advanced resolution like that in RCM.

2.2.2 Climate Change Analysis

Assessing the impact of climate change on streamflows, reservoir volume, soil moisture, groundwater, and other hydrological parameters essentially involves taking projections of climatic variables (e.g. precipitation, temperature, humidity, mean sea level pressure, etc.) at a global scale.

Downscale these global-scale climatic variables to local-scale hydrologic variables and computing hydrological components for water resources variability and risks of hydrologic extremes in the future are the major components. Projections of climatic variables globally have been performed with General Circulations Models (GCMs), which provide projections at large spatial scales. Such large-scale climate Projections must then be downscaled to obtain smaller-scale hydrologic projections using appropriate linkages between the local climates (Wilby and Dawson, 2007).

2.3 Climate Models

Climate models, called general circulation models (GCMs), are used to project the potential climate change for assumed future greenhouse gas emission scenarios. The long time scales and uncertainty due to global change have led analysis to develop ‘scenarios’ of future environmental, social, and economic changes to improve understanding among decision-makers of the potential consequences of their decisions (Iran *et al.*, 2018) and important tools for improving our understanding and predictability of climate behavior on seasonal, annual, decadal, and centennial time scales. Models investigate the degree to which observed climate changes may be due to natural variability, human activity, or a combination of both. There are different climate scenarios from those general circulation model outputs is numerical models (General Circulation Models or GCMs), representing physical processes in the atmosphere, ocean, cryosphere, and land surface, are the most advanced tools currently available for simulating the response of the global climate system to increasing greenhouse gas concentrations. In this study, the numerical models (General Circulation Models or GCMs) was used

2.3.1 General Circulation Model (GCM)

Global climate model (GCM) is a complex mathematical representation of the major climate system components (atmosphere, land surface, ocean, and sea ice), and their interactions. GCMs are critical tools that enable us to improve the understanding and prediction of atmosphere, ocean, and climate behavior. Models allow us to determine the distinct influence of different climate features by providing a way of exploring climate sensitivities with experiments that cannot be performed on the actual earth. Global climate models (GCMs) are tools for the assessment of climate variability and change. Current GCMs have spatial resolution on the order of 100-250 km and have the potential to simulate the main characterizes of general circulation at the range of this scale (Al *et al.*, 2013).

According to many researchers, GCMs are the vital resource used to perform climate change experiments regionally, globally, and very fine-scale up to point climate patterns from which climate change scenarios are derived, but they have main drawbacks because of their course resolution. Most of the time they lack producing of current climate trend including the most important statistical parameters like mean and variance (John, 2018).

Simulations of global climate are conducted with general circulation models (GCMs), which are designed to balance model resolution and physics with computational requirements and limitations. Hence, long climate simulations (centuries to millennia) have necessarily been run at relatively coarse spatial resolutions, which are on the order of a few degrees in latitude and longitude (Alder *et al.*, 2018). Generally, GCMs models produce simulations of current and past large-scale climates that agree with observations. But, it does not allow taking into account fine-scale physical processes (eg., local convection that determines point of precipitation), which are necessary for a good representation of local climate. To overcome this major problem, researchers have developed regional climate models (RCMs).

2.3.2 Regional Climate Model (RCMs)

RCMs have defined the downscale global climate simulations into redefined data, taking into account the local climate features, linked to the coastlines, mountains, lakes, and vegetation, that have a strong influence on the regional climate and regional climate model. The regional climate model is a climate model of higher resolution than a global climate model (GCM). Although regional climate models, in general, can improve on the details of GCM simulations through dynamical downscaling over complex terrain. Regional climate models have been used to conduct climate change experiments for many regions of the world. These methods of obtaining sub-grid scale estimates (commonly down to 50 km resolution or less) can account for important local forcing factors such as surface type and elevation, which conventional GCMs are unable to resolve (Filippo, 2019).

2.3.2.1 Bias Correction of Downscaled Climate Model

Climate change studies are conducted using data from general circulation models (GCMs); however, since the GCMs have a coarse resolution, they are not suitable for regional climate change impact studies. Rather, regional climate models (RCMs) have been used to dynamically downscale GCM output to scales more suitable to end regional applications. Therefore, GCM-driven RCM output may provide valuable information to climate adaptation practices, risk assessment studies, and policy planning. Such efforts enabled the application of RCM outputs to understand the impacts of climate change in local climates that are influenced by complex topographies and landscapes (Mengistu, 2021).

Several bias correction methods are applicable to account for differences between the climate model data and the measurement data (Piani *et al.*, 2010; Teutschbein *et al.*, 2011). In many climate change impact studies, two groups of bias correction methods (e.g. linear scaling, delta-change approach,) and sophisticated (distribution mapping, power transformation), have to be applied (Teutschbein & Seibert, 2012; Troin *et al.*, 2015). However, individual bias correction methods reduce the deviations between model and measurements in unique ways, resulting in different absolute values as well as a different variability (C. Teutschbein & Seibert, 2013). Although GCMs are regarded as the best tools available for the projection of climate change into the future, there are biases in GCM outputs. GCM bias is simply explained as the deviation of GCM outputs from the observations. However, in more elaborated terms, incorrect reproduction of extreme temperatures, prediction of the excess number of wet days with low-intensity rainfalls, under or over-prediction of climatic variables, incorrect seasonal variations, and so on are some of the forms of biases prevailing in GCM outputs (Claudia Teutschbein & Seibert, 2012).

Bias correction procedures employ a transformation algorithm for adjusting climate model output. The underlying idea is to identify bias between observed and simulated historical climate variables to parametrize a bias correction algorithm that is used to correct simulated historical climate data. Bias correction methods are assumed to be stationary. The correction algorithm and its parametrization for current climate conditions are assumed to be valid for future conditions as well. Thus, the same correction algorithm is applied to future climate data. however, it is unknown how well a bias correction method performs for conditions different from those used for parametrization. A good performance during the evaluation period does not guarantee a good performance under change future conditions. Teutschbein and Seibert (2012) provide a detailed discussion and state that a method that performs well for the current condition is likely to perform better for the changed condition than a method that already performs poorly for the current condition

2.4 Climate Change Scenarios

A climate scenario was a plausible indication of what the future could be like over a long period of centuries, giving a specific assumption. These assumptions include future trends in energy demand, emissions of greenhouse gases, land-use change as well as assumptions about the behavior of the climate system over long time scales. It is largely the uncertainty surrounding this assumption that determines the range of possible scenarios (Carter *et al*., 2016).

2.4.1 Representative Concentration Pathway (RCPs)

One of the climate change scenarios was Representative Concentration Pathways (RCPs). RCPs scenarios are the latest generation of scenarios that provide input to climate models participating in Coordinated Regional Climate Downscaling Experiment (CORDEX) and span the range of plausible irradiative forcing scenarios (Vuuren *et al.*, 2011) and (IPCC, 2013).

They are prescribed pathways for greenhouse gas and aerosol concentrations, together with land-use change, that is consistent with a set of broad climate outcomes used by the climate modeling community. The pathways are characterized by the radioactive forcing produced by the end of the 21st Century (IPCC, 2013).

There are four types of RCPs to predict future climate change. These are one (RCPs 8.5) the strongest forcing scenario, two stabilization scenarios (RCPs 4.5 and 6.0), and the other are mitigation scenarios leading to the weakest forcing level (RCPs2.6) (IPCC, 2012).

The World Climate Research Program (WCRP) has developed, international project Coordinated Regional Climate Downscaling Experiment (CORDEX) regional climate projections, for the majority of the Worlds region. According to the report of (Gutowski *et al.*, 2016), Africa was designated as the target area of CORDEX due to three major reasons. The high vulnerability of this region in many sectors follows from climate variability, the relatively low adaptive capacity of its economies, and significant changes in temperature and precipitation patterns. Besides, there is a fewer availability of simulations based on regional climate downscaling (RCD) tools for Africa (Dibaba *et al.*, 2019).

Previous work about RCMs in Ethiopia has examined the performance of multimodal numerical simulations and multi observational databases focusing on seasonal cycles and spatial variations of precipitation over Ethiopia. Most of the studies used globally available gridded data sets and satellite-based data sets as a reference to evaluate the CORDEX-Africa RCMs output. Besides, some of the studies are based on a single parameter to represent the overall model performance. All the RCMs are not found to be equally important in all regions. (Endris *et al*., 2013) indicated the RCMs rainfall simulation varies along the regions, performing good in some and poorly in others. A recent study by (Van Vooren *et al*., 2019) indicated RCMs estimation is sensitive to elevation producing higher biases for higher elevation. This study is being initiated to evaluate the performance of a set of RCMs from CORDEX- RCMs is driven by the European Centre for Medium Weather Forecasting (ECMWF) Interim reanalysis (ERA-Interim) in simulating the current climatic variables over mojo catchment. In many aspects, RACMO22T simulates rainfall over most stations better than the CLM4-8 and RCA4 other models. The highest biases are associated with the highest error in simulating maximum and minimum temperature with the highest biases in high elevation areas. So for this study use RACMO22Tmodel RCMs.

2.4.2 Special Report on Emission Scenario (SRES)

One of the primary reasons for developing emissions scenarios is to enable coordinated studies of climate change, climate impacts, and mitigation options and strategies. A classification scheme is presented here to assist the reader in understanding the links between driving forces and scenario outputs. This scheme can also be used to help select appropriate scenarios for further analysis (IPCC, SRES). The SRES scenarios were developed as quantitative interpretations of the four alternative storylines that represent possible futures with different combinations of driving forces. These broad scenario families are broken down further into seven scenario groups, used here to classify the input driving forces.

The scenario outputs of most interest are emissions of GHGs, SO_2, and other radiactive important gases. However, the categorization of scenarios based on emissions of multiple gases is quite difficult. All gases that contribute to radiactive forcing should be considered, but methods of combining gases such as the use of global warming potentials (GWP) are appropriate only for near-term GHG inventories.

In addition, emission trajectories may display different dynamics, from monotonic increases to non-linear trajectories in which a subsequent decline from a maximum occurs. This particularly diminishes the significance of a focus on any given year, such as 2100. In light of these difficulties, the classification approach presented here uses cumulative CO_2 emissions between 1990 and 2100. CO_2 is the dominant GHG and cumulative CO_2 emissions are expected to be roughly proportional to CO_2 radiactive forcing over the time scale considered (Houghton *et al.* 1996). The scenario is classification according to scenario family and cumulative total carbon dioxide emissions (fossil, industrial, and net deforestation) from 1990 to 2100, and there is four families of Emissions Scenario A1 (A1C, A1G, A1B, A1T), A2 (A2), B1 (B1) and B2 (B2).

The potential future evolution of anthropogenic emission of greenhouse gases and other radiactive forcing substances is depicted according to a set of scenarios spanning alternative future development. The past generation of climate projections, in particular experiments issued from the CMIP3 and integrated with the IPCC Fourth Assessment Report (AR4, IPCC 2007), were based on the family of green gas emission storylines (Rolf, 2005). In particular, medium to high range emissions according to the SRES A1B scenarios was the focus of the discussions and climate impact research. The different types of emission scenarios are will be used in climate research to assess the long-term impact of atmospheric greenhouse gases and pollutants based on the assumptions of population growth, economic development level.

2.4.3 Climatological Base Line

Four grid points that lie near the select record meteorological stations was been chooses. The historical data from (1987-2016) was taken as a baseline period and two consecutive periods near-term (2022-2051) and long-term (2052-2082) future periods were considered as future scenarios periods under RCP4.5 and RCP8.5. Bias correction was done the downloaded selected climate variables before being transferred to hydrological model to simulate flows for selected future periods.

2.5 Regional Climate Model (RCMs) Performance Evaluation.

The three statistical method performance evaluation criteria were used; to evaluate how the simulating precipitation RCMs models performed with observed precipitation. The parameter used was mean bias (PBIAS), root means square error (RMSE), and Pearson correlation coefficient (r). An initial evaluation was taken on how the mean annual precipitation simulated by individual RCMs and their mean ensemble varied spatially concerning observed precipitation over the watershed area and also the spatial distribution map of the observed rainfall, RCMs output, and mean ensemble were developed.

$$PBIAS = \frac{1}{n}\sum_{i=1}^{n}(Si - Oi)\text{...}2.1$$

$$RMSE = \sqrt{\frac{\sum_{i=1}^{n}(Si - Oi)^2}{n}}\text{...}2.2$$

$$r = \frac{\sum_{i=1}^{n}(Si - Sm)(Oi - Om)}{\sqrt{\sum_{i=1}^{n}(Si - Sm)2}\sqrt{\sum_{i=1}^{n}(Oi - Om)2}}\text{...............................}2.3$$

Where S is the simulated value of the RCMs and O is the observed value of the climate variable, i refer to the simulated and observed pairs, n is the total number of pairs and m refers to mean.

2.6 Future Trend Analysis of Precipitation and Temperature.

Trend analysis is a technique used in technical analysis that attempts to predict future variable data change based on recently observed trend data. There is different method of trend analysis: - are Mann–Kendall (MK), modified Mann-Kendall, and Sen’s slope method. Mann–Kendall (MK) (non-parametric) test is usually used to data that no need of autocorrelation and modified Mann Kendall is a (parametrical) test used the data that used autocorrelation both of them is usually test used to detect an upward trend or downward (i.e. monotonic trends) in a series of hydrological data (climate data) and environmental data. The zero hypothesis for this test indicates no trend, whereas the alternative hypothesis indicates a trend in the two-sided test or a one-sided test as an upward trend or downward trend (Pohlert, 2020).

Te Sen's estimator is another non-parametric method used for the trend analysis of the hydro climate data set. It is also used to identify the trend magnitude. Hence, this test computes the linear rate of change (slope) and the intercept as shown in Sen's method (Sen 1968). The Innovative Trend Analysis (ITA) of different climate data analysis graphs for all stations were investigated through Studio (Alemu & Dioha, 2020) in this study month, and seasonally is used modified Mann Kendall test and interannual trend test was used.

Generally, in this study, a modified Mann-Kendall trend test was used to detect the change in precipitation and temperature seasonally and monthly. Mann-Kendall trend test and sen slope were used to evaluate the trend of mean annual temperature and precipitation in the area. The Mann-Kendall statistic of the time series data analysis is the output compared to the critical value to test whether the trend of the hydroclimate variable has been detected or not.

The test statistic *S* and critical test statistics *Z* are described below.

$$S = \sum_{i=1}^{n=1} \sum_{j=i+1}^{n} (Xj - Xi) \qquad 2.4$$

The trend test is applied to *Xi* data values (*i* = 1, 2, …. *n*) and X (*j* = *i* + 1, 2, . . . , *n*). The data values *Xi* are used as reference points to compare with the data values of *Xij*, which are given data below.

Sgn(s) = 1, if (xj-xi) > 0, 0, if (xj-xi) = 0 and -1 if (xj-xi) < 0

where *Xi* and *Xj* are the values in periods *i* and *j* when the number of data series is greater than or equal to 10 (n > 10); the MK test is then characterized by a normal distribution with the mean E(*S*) = 0, and the variance *Var*(*S*) is equated as below equation.

$$\mathrm{var}(s) = \frac{n(n-1)+(2n+5-\sum_{k=1}^{m} tk*(tk-1)+(2tk+5)}{18} \qquad \text{...............2.5}$$

Where *m* is the number of the tied groups in the time series and *tk* is the number of data points in the *k*th tied group. The critical test statistic or significance test *Z* is as follows.

$$Z = \frac{s-1}{\delta} if, s \supset 0, 0 ifs = 0, and \frac{s+1}{\delta} if, s \subset 0 \qquad \text{...............2.6}$$

If $Z > 0$, it indicates an increasing trend. When $Z < 0$, it represents a decreasing trend and the trend is a significance level at the *Z*-score's critical values where it is greater than ±1.65, ±1.96, and ±2.58 at p-value 0.1, 0.05, and 0.01, respectively.

2.7 Impact Climate Change on Streamflow

Climate change can affect streamflow in several ways. Changes in the amount of spring snowpack and air temperatures that influence melting can alter the size and timing of high spring stream flows. More precipitation is expected to cause higher average streamflow in some places, while heavier storms could lead to larger peak flows. More frequent or severe droughts, however, could reduce streamflow in certain areas (Fekadu *et al*., 2019).

Ethiopia is experiencing the impact of both climate variability and change. Climate change has led to recurrent drought and famines, flooding, expansion of desertification, loss of wetlands, loss of biodiversity, a decline in agricultural production and productivity, scarcity of water, and increased incidence of pests and diseases. Climate change is likely to aggravate environmental degradation, food insecurity disease epidemics, and poverty in Ethiopia the above mean change on streamflow (Haileab, 2018). Also, it is expected to increase the surface temperature of the Earth and the oceans, raise sea levels, alter the global distribution of precipitation, affect the direction of ocean currents and major airstreams, and increase the intensity and frequency of extreme weather events. Climate change is already causing loss of life, damaging property, and affecting livelihoods in many parts of the world including Ethiopia. The cause of climate change was wide-ranging effects on the environments, socio-economic conditions, and related sectors, including streamflow, agriculture, and food security, human health, terrestrial ecosystems.

2.8 Hydrological Models

Hydrological modeling is a powerful technique of hydrological systems investigation for both the research hydrologist and practicing water resources engineers involved in the planning and development of an integrated approach for the management of water resources (Melke & Abegaz, 2017). Hydrological modeling is a great method of understanding hydrologic systems for the planning and development of integrated water resources management. The purpose of using a model is to establish baseline characteristics whenever data is not available and to simulate long-term impacts that are difficult to calculate, especially in ecological modeling.

Effective watershed management and ecological restoration require a thorough understanding of hydrologic processes in the watersheds. Spatial and temporal variations in soils, vegetation, and land-use practices make a hydrologic cycle a complex system, therefore, mathematical models and geospatial analyses tools are needed for studying hydrologic processes and hydrologic responses to land use and climatic changes (Dilnesaw, 2006; (Melke & Abegaz, 2017).

2.8.1 Lumped Conceptual Models

Lumped models treat the catchment as a single unit, with state variables that represent average values over the catchment area, such as storage in the saturated zone. Due to the lumped description, the description of the hydrological processes cannot be based directly on the equations that are supposed to be valid for the individual soil columns. Hence, the equations are semi-empirical, but still with a physical basis. For steam flow and reservoir regulation lumped, continuous streamflow simulation models are the best option (U.S ACE, 1987).

2.8.2 Distributed Models

Parameters of distributed models are fully allowed to vary in space at a resolution usually chosen by the user. Distributed modeling approach attempts to incorporate data concerning the spatial distribution of parameter variations together with computational algorithms to evaluate the influence of this distribution on simulated precipitation-runoff behavior. These models generally require a large amount of data. However, the governing physical processes are modeled in detail, and if properly applied, they can provide the highest degree of accuracy.

2.8.3 Semi-Distributed Models

Parameters of semi-distributed models are partially allowed to vary in space by dividing the basin into several smaller sub-basins. The main advantage of these models is that their structure is more physically-based than the structure of lumped models, and they are less demanding on input data than fully distributed models. SWAT is in the domain of semi-distributed hydrological models**.**

2.9 (SWAT) Model Setup

The SWAT model is most versatile and was widely used in various regions and climatic conditions on a daily, monthly, and annual basis and for watersheds of various sizes and scales. The Hydrologic Response Units (HRUs) are used to describe spatial heterogeneity in terms of land cover, soil type, and slope class within a watershed area. The model estimates relevant hydrologic components such as evapotranspiration, surface runoff, and peak runoff, groundwater flows, and sediment yields for each HRUs unit. The SWAT is embedded in a GIS interface. The hydrologic cycle simulated by SWAT is based on the water balance equation. It is a physically-based semi-distributed hydrologic model which routes continuously on an hourly, daily, monthly, and yearly time step. The SWAT model uses an ArcGIS interface for the definition of watershed hydrological features. hydrology, weather, soil types, sediment yields, plant growth, nutrients loss, pesticides, bacterial load, and land-use management.

In addition to the above advantage of the SWAT model were mentioned, hence it's selected by many researchers for hydrological uses. A review of 16 well-known (continental scale) hydrological and land surface models revealed that the SWAT model has a higher potential and suitability for hydrological drought forecasting in Africa. It is the ability to generate missing weather records during simulation or fill in gaps in weather records. That means it is easily applicable in the data-scarce area, and well demonstrated as capable of predicting flow yield and performing further analysis of hydrological response (Akoko *et al.*, 2021). Also SWAT model was able to generate good spatial and temporal simulations of flow throughout the watershed, implying that the model can be highly beneficial in supporting watershed management through the identification of drivers.

2.9.1 The (SWAT) Model Performance Evaluation

To evaluate the model performance relative to the observed data and simulated data the following three performance measures were used.

2.9.1.1 Nash-Sutcliffe Efficiencies

The Nash-Sutcliffe Efficiencies (NSE) is a normalized statistic that determines the relative magnitude of the residual variance ("noise") compared to the measured data variance ("information") (Nash and Sutcliffe, 1970) ENS indicates how well the plot of observed versus simulated data fits.

$$NSE = 1 - \frac{\sum_{i=1}^{n}[(Qi^{obs} - Qi^{sim})]^2}{\sum_{i=1}^{n}[(Qi^{obs} - Qi^{obsmean}]^2} \qquad \text{...2.7}$$

Where N_{SE} is Nash-Sutcliffe Efficiency, Qi^{obs} is i^{th} observed streamflow of day i, Qi^{sim} is simulated streamflow of day i and $Qi^{obs\ mean}$ is mean observed streamflow. The "i" used in the calculation is the period have used (Nash and Sutcliffe, 1970)

2.9.1.2 Coefficient of Determination (R^2)

Another widely used statistical measure is coefficient of determination (R^2) which describes the degree of co-linearity between simulated and measured data. The R^2 describes the proportion of the variance in measured data; its value varies from 0 to 1, with higher values indicating less error variance, and typically values greater than 0.5 are considered acceptable (Santhi *et al*., 2001)

$$R^2 = \frac{\sum_{i=1}^{n} = \quad [(Qi^{obs} - Qobs^{mean})(Qi^{sim} - Qsim^{mean})]^2}{\sum_{i=1}^{n} = [[Qi^{obs} - Qobs^{mean}]^2 \sum_{i=1}^{n} = [Qi^{sim} - Qsim^{mean}]^2]} \text{........2.8}$$

Where Qi^{obs} and Qi^{sim} are observed and simulated streamflow; $Qobs^{mean}$ and $Qsim^{mean}$ are mean observed and simulated streamflow. The coefficient of determination varies from 0 to 1 where a higher value denotes a better fit of the regression line between simulated and observed discharges. When stimulated and observed streamflow exactly match each other, a value of 1 is obtained.

2.9.1.3 Percent of Bias (%)

PBIAS measures the average tendency of the simulated data to be larger or smaller than their observed counterparts. The optimal value of PBIAS is 0.0, with low-magnitude values indicating accurate model simulation. Positive values indicate model underestimation bias, and negative values indicate model overestimation bias and underestimation. Percent bias is calculated by the below equation.

$$PBIAS = [\frac{\sum_{i=1}^{n} (Qi^{obs} - Qi^{sim}) * 100}{\sum_{i=1}^{n} (Qi^{obs})}] \text{..2.9}$$

2.9.2 Sensitivity Analysis

A sensitivity analysis can provide a better understanding of which particular input parameters have a greater effect on model output (Strickland & Bosch, 2013). Generally, local and global sensitivity analysis will be performing and this analysis may yield different results. Local sensitivity analysis will be performed by changing values at a time whereas global sensitivity analysis allows all parameter values to change at a time. The sensitivity of one parameter often depends on the value of other related parameters; hence, the problem with the one-at-a-time analysis is that the correct values of other parameters that are fixed are never known. The disadvantage of the global sensitivity analysis is that it needs many simulations. Both procedures, however, provide insight into the sensitivity of the parameters and are necessary steps in model calibration. After pre-processing of the Mojo river sub-basin data and Arc-SWAT model set up, the simulation will do.

2.9.2.1 Calibration and Validation of SWAT

Model calibration is critical in hydrologic modeling studies to reduce model simulation uncertainty. The purpose of calibration is to achieve an acceptable agreement between measured and model-simulated values by adjusting model parameters within the acceptable range because describing physical processes is natural by the mean mathematical equation is difficult to job. Therefore: the model was calibrated by adjusting model parameters to get the best-fit estimation within the observed one. The model was used to run with input parameters set during the calibrated phase for the validation process.

2.10 Previous Studies Impact of Climate Change on Streamflow

The adverse impact of climate change may worsen the existing social and economic challenges of the whole country. Global climate change is expected to impact future precipitation and surface temperature trends and could alter the local hydrological system (Quansah *et al.*, 2021). One of the most significant potential consequences of climate change in the long term would be a change in the regional hydrological cycle (Kefeni *et al,* 2019). Numerous studies have demonstrated climate and streamflow changes for different basins throughout the world. The streamflow of the same river in the world has decreased and increased significantly due to climate change and intensifying human activity. Investigated the observed trend of global streamflow and reported that runoff reduction occurred in sub-Saharan Africa, southern Europe’s and southern Austral, and runoff of increased like North America, the southeastern quadrant of African, and northern, Australia (Zhang *et al*., 2017).

Climate change and its impact on water resources availability in space and time have put a complex challenge to the African countries. The severity and the magnitude of the impact depend on the geographical area and context (Bodian *et al*., 2018). Ethiopia has one of the sub-Sahara African countries and it has a diverse climate that could result in a water scare zone in the same part of the country (FAO, 2016; Gurara *et al*., 2021). These studies show that climate changes have and will continue to influence streamflow discharge river basins (Tessema *et al*., 2020). For instance,(Taye, 2018) reported an increase in water deficiency in the awash basin over the twenty-first century because due to climate change.

A reduction in precipitation is likely over Northern Africa and the southwester parts of South Africa by the end of the 21^{st} century under the SRES A1B and A2 scenarios (medium to high confidence). Projected rainfall change over sub-sahara Africa in mid-and late 21^{st} century is uncertain. In regions of high or complex topography such as the Ethiopia highland, downscaled projected indicate likely increases in rainfall and extreme rainfall by end of the 21 st century (Niang *et al.*, 2015)

3 MATERIALS AND METHODS

3.1 Description of the Study Area

There are twelve river basins in Ethiopia, among that Awash River basin is one of the most utilized river basins. This study was conducted on the Mojo River watershed which is located in the upper part of the Awash River basin, Ethiopia. Mojo watershed has a total area of 1663.09 km^2 were situated in central Oromia Regional State, Ethiopia, geographically it was located between latitudes of 8° 16´0” - 9° 18´ 0” N and longitude of 37° 57´0” - 39° 17´0” E. The mojo watershed drains finally into the Awash River. The mean annual rainfall of the area ranges from 918.50 to 1226 mm and the mean maximum temperature of the watershed was ranged from 21°C to 27°C. The highest was a record in May and the lowest in July. The mean minimum temperature ranges from 8°C to 12°C where the minimum and maximum are occurring in December and April respectively. The altitude of the watershed ranges from 1592.15 a.m.s.l at the river bed to 3065.49 a.m.s.l at the upper part of the watershed (A.Amin and N.Nuru, 2020). (figure 3.1) show the study area of the mojo catchment.

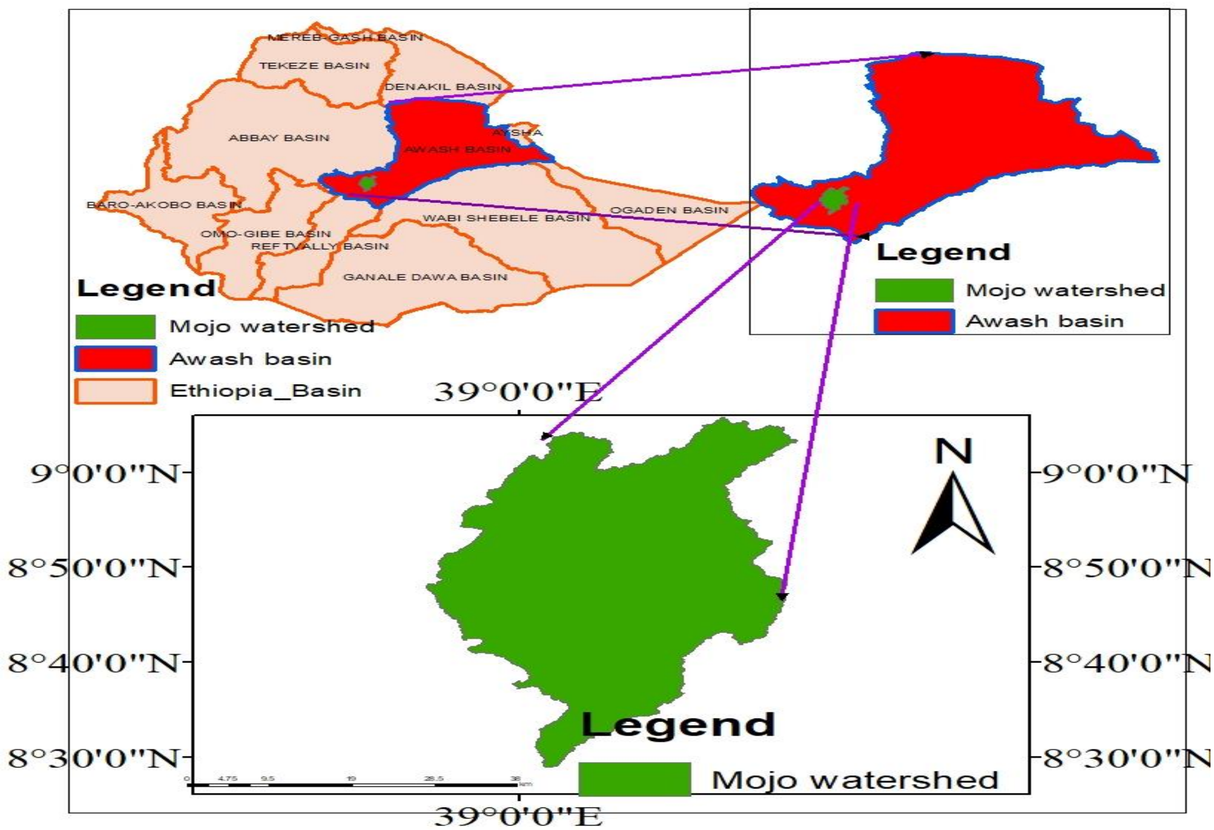

Figure 3.1 Location map of mojo watershed

3.2 Materials Used

ArcGIS10.4.1, Arc SWAT 2012, SWAT-CUP 2019, pcpSTAT, Dew02.exe were used. ArcGIS was used for developing and extracting data from CORDEX-Africa, collecting geographic data, analyzing map information, managing geographic information in a database, and implementation of GIS processing tools (such as extract, map preparation, and spatial analysis). Similarly, the Arc SWAT model was used for the setup of the project, delineation of the watershed area, analyzing HRU, writing all input tables, editing all inputs. Then, it was used to simulate streamflow by discretizing dominant land use, soil, and slope into a homogeneous hydrologic response unit. SWAT-CUP 2019 was used to calibrate the model for better parameterizing the model for a given set of local conditions, there by carefully selected values for model input parameters with in their respective uncertainty ranges by comparing the model prediction for the existing observed data under the same conditions to minimize the probable uncertainty using SUFI-2 algorithm installed in the SWAT-CUP. In addition to the above Microsoft Excel was used in this paper to organize data manipulations like arithmetic operations, display data as line graphs, allow sectioning of data to view its dependencies on various factors for different perspectives (using pivot tables). Similarly, the pcpSTAT software package was used to calculate statistical parameters of daily precipitation data such as average total monthly precipitations, the standard deviation for daily precipitation, the skew coefficient for daily precipitation, probability of wet day following dry day, probability of wet day following wet day and average days of precipitation used by weather generator of SWAT models. Lastly, the dewo2.exe was used to calculate average daily dew point temperature (minimum and maximum daily temperature data), humidity, and dew point per month using daily data to result in a more precise output.

3.3 Data Collection

The soil and water assessment tool model needs input data to process and generate the output. The SWAT input data used for this study were: spatial data (digital elevation model, soil map, and land use/land cover), meteorological data (precipitation, temperature, solar radiation, relative humidity, and wind speed), and hydrological data (streamflow) and climate (CORDEX) data). After data was collected, quality control data was done and performed on the available data mainly preliminary checked, plotted, and removal of errors by spatial and temporal consistency checks to ensure the quality of the data for further investigation.

3.3.1 Meteorological Data

Meteorological data were daily data collected from the meteorological station and used as an input to the model to be processed and generate an output. Meteorological data used were rainfall, maximum and minimum temperature, relative humidity, wind speed, and sun shine. The selection meteorological station was based on the availability of the data and representative of the study of the total study area. The selected meteorological stations were Bishoftu, Chefedonsa, and Mojo. In this study, meteorological data of thirty (30) years period from January 1987 to December 2016 were used evaluation of the impact of climate change analysis.

3.3.1.1 Solar Radiation Data

The SWAT model requires the solar input daily data in global solar radiation. The data from the Ethiopian National Meteorological Agency was available in sunlight hour and it was changed into solar data as required for the SWAT input. Empirical models based on Angstrom-Prescott model were selected to estimate the monthly average daily global solar radiation (Wussah, 2014). The Angstrom-Prescott regression equation is used to estimate the monthly average daily global solar radiation on a horizontal surface. The simplest method commonly used to calculate the hydrological data Ethiopian ministry of irrigation and electricity average global solar radiation on a horizontal surface is the well-known Angstrom, Prescott equation (Suehrcke., 2000). If the solar radiation, is not measured, it can be calculated with the Angstrom formula which relates solar radiation to extraterrestrial radiation and relative sunshine duration (Allen *et al.*, 1998).

$$Rs = (as + bs + \frac{n}{N})Ra \qquad 3.1$$

Where is solar or shortwave radiation (MJ m-2 day-1) n is the actual duration of sunshine (hour), N is the maximum possible duration of sunshine, n/N is relative sunshine duration, Ra is extraterrestrial radiation (MJ m-2 day-1), as and bs regression constant Depending on atmospheric circumstances (humidity, dust) and solar declination (latitude and month), the Angstrom values as and bs will vary. Where no actual solar radiation data are available and no calibration has been carried out to develop as and bs parameters, the values as = 0.25 and bs = 0.50 are recommended (Allen *et al*., 1998).

3.3.2 Hydrological Data

Hydrological data (streamflow data) was collected from the Ministry of Water, Irrigation, and Energy (MoWIE). The hydrological data of the Mojo River from (2000 to 2015) was recorded at the Mojo gauging station at the outlet of the watershed. The recorded streamflow data was required for calibration and validation of the SWAT model. The errors in the streamflow records would affect the ability of the model to represent the actual condition of the watershed. If a model calibrated used data was in error, the model parameter values would be affected and the predictions for other periods, which depend on the calibrated parameter values would be affected. In this study, there is small missing streamflow data.

3.3.3 Spatial Data

The spatial dataset is which used for the prediction of streamflow yield using the SWAT model were land use and land cover, soil type, and digital elevation model. It is obtained from a different source which is brief each described below.

Digital Elevation Model (DEM):

The digital elevation model is one of the essential inputs required for SWAT. The DEM of the study area was produced in 12.5*12.5 m grid resolution. This degree of resolution is more sufficient for hydrological modeling. The digital elevation model of the study area was downloaded from https://asf:alaska.edu. Using ArcGIS 10.4.1 the download digital elevation data was projected with UTM WGS zone 37N and combined with arc tool raster mosaic application. The digital elevation model has to be pre-processed for determination the number of the size of the subbasin based on the threshold area of 3139 ha. The number of subbasins was twenty-five (25) subbasins. The elevation of the study area is shown (fig 3.3).

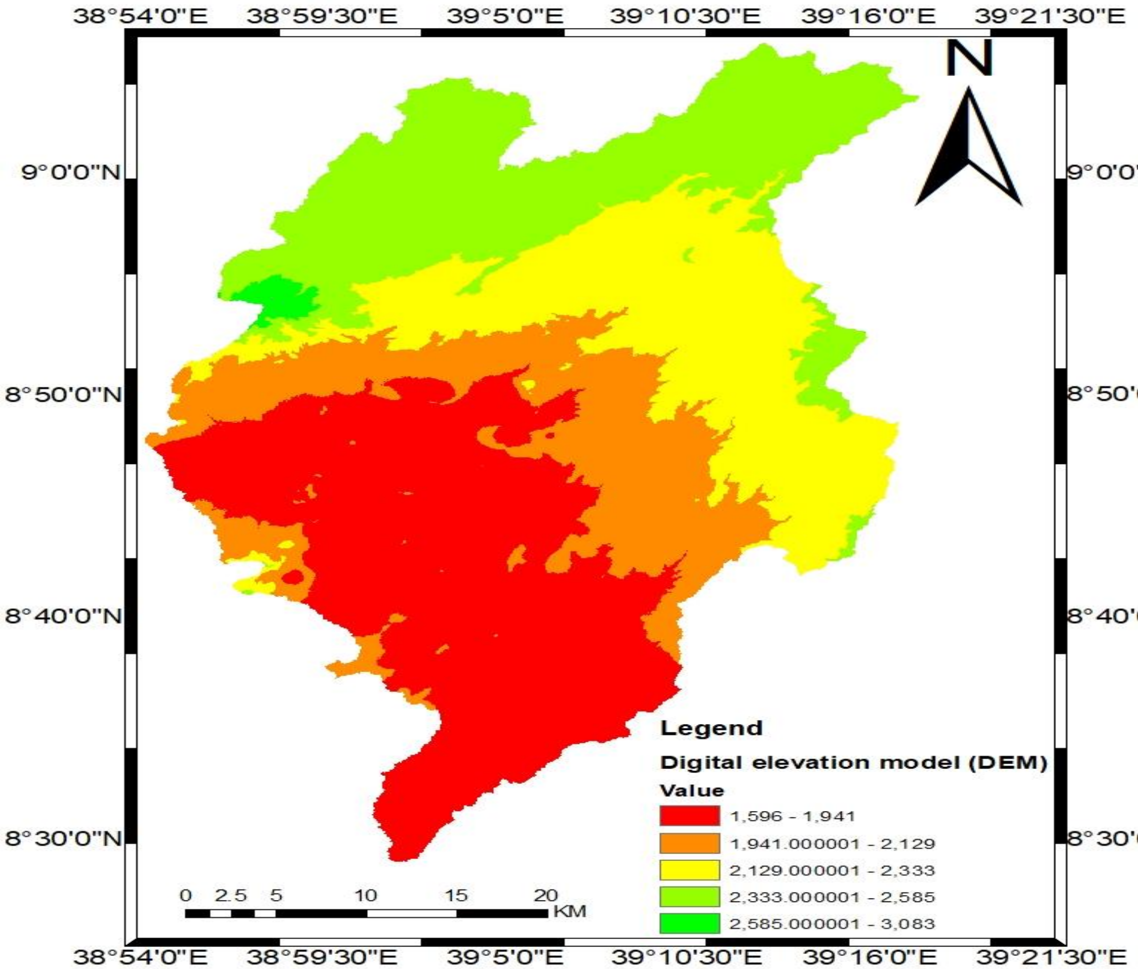

Figure 3.2 Digital elevation model (DEM) of mojo watershed.

Land Use Land Cover: land use and land cover information is important for estimation of actual evapotranspiration by Kristensen and Jensen formulation and to decide manning's roughness coefficient to estimate overland flow (Seibert, 2011)

Land use and land cover map of the Mojo river watershed used in the model was downloaded from https://earthexplorer.usgs.gov.The land sat images were processed and vectorized by using the Geographic coordinate systems of World Geodetic System 1984, to create their vector shapefiles, which were also masked using the shapefile of the study catchment area and analyzed by the ArcGIS 10.4.1 tool. land use and land cover map of Mojo watershed were classified by ArcGIS 10.4.1 in this study area. The watershed area was divided into five (5) major land use and land cover classes (figure 3.4). The major land use land cover was cultivated land, plantation forest, pastureland, degraded (barren) land, settlement (rural and urban), and water bodies. According to SWAT land use and land cover classification, Agriculture (Cultivation) land was the dominant land use in the study area.

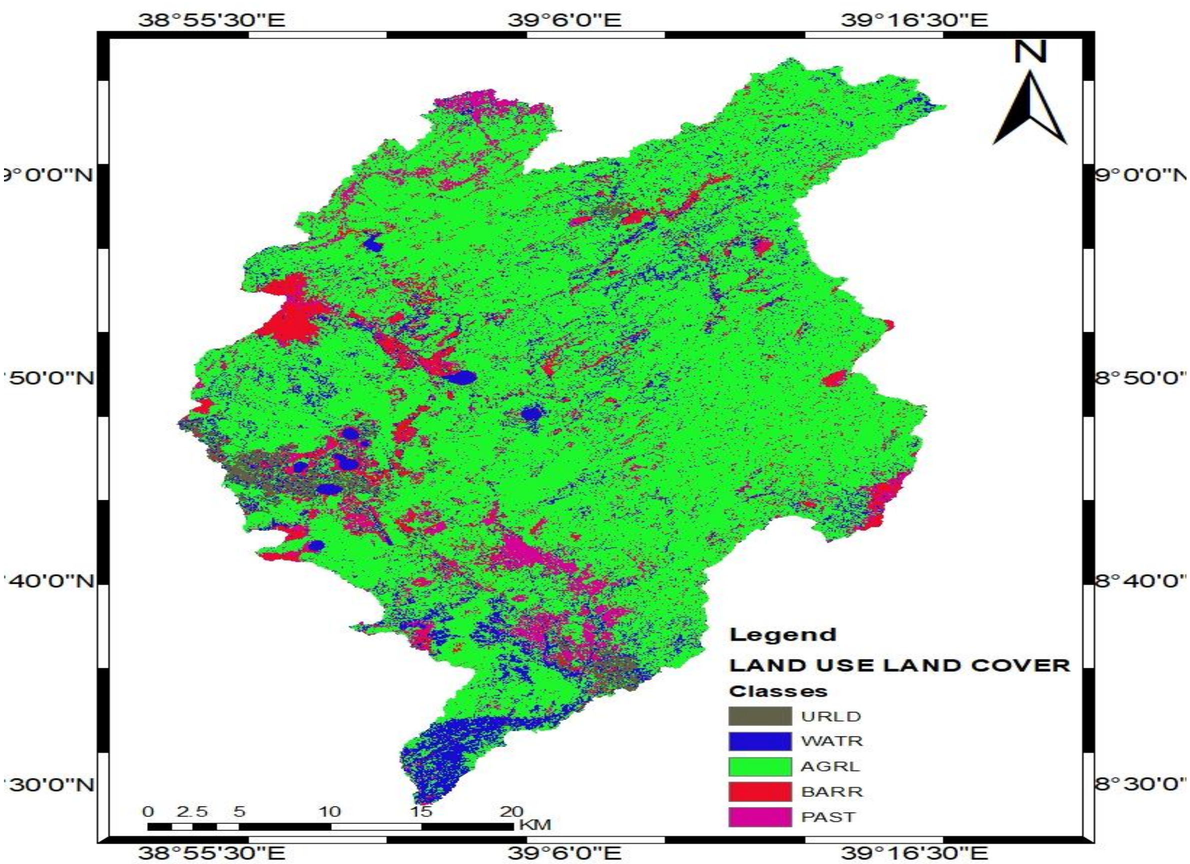

Figure 3.3. Land use land cover Map

Soil type: The soil map used in the SWAT model was made available in the GIS database prepared in this study area was originally developed by (Ethio digital soil database). The soil map represents the dominant soil type in the upper part of the soil column inside the study area there are seven (7) soil type classes (figure 3.5). The dominant soil type as Vertic Combisols and Eutric Vertisols with medium to hard texture. The SWAT model requires soil property data such as the texture, chemical composition, physical properties, available moisture content, hydraulic conductivity, bulk density, and organic carbon content for the different layers of each soil type. A brief description of each soil type is presented in (table 3.1).

Table 3.1 Soil type of watershed area

No	Soil-type	sname	Hydrograph	Texture
1	Vertic combisols	VTCAMBISOLS	D	Clay
2	Mollic Andosols	MOANDOSOLS	B	Loam
3	Luvic phaeozems	LUPHAEOZEM	B	Loam
4	Lithic Leptosols	LTLEPTOSOLS	A	Sandy loam
5	Haplic Luvisols	HPLUVISOLS	B	Loam
6	Eutric Vertisols	EUVERTISOLS	D	Clay
7	Chromic Luvisols	CHLUISOLS	B	Loam

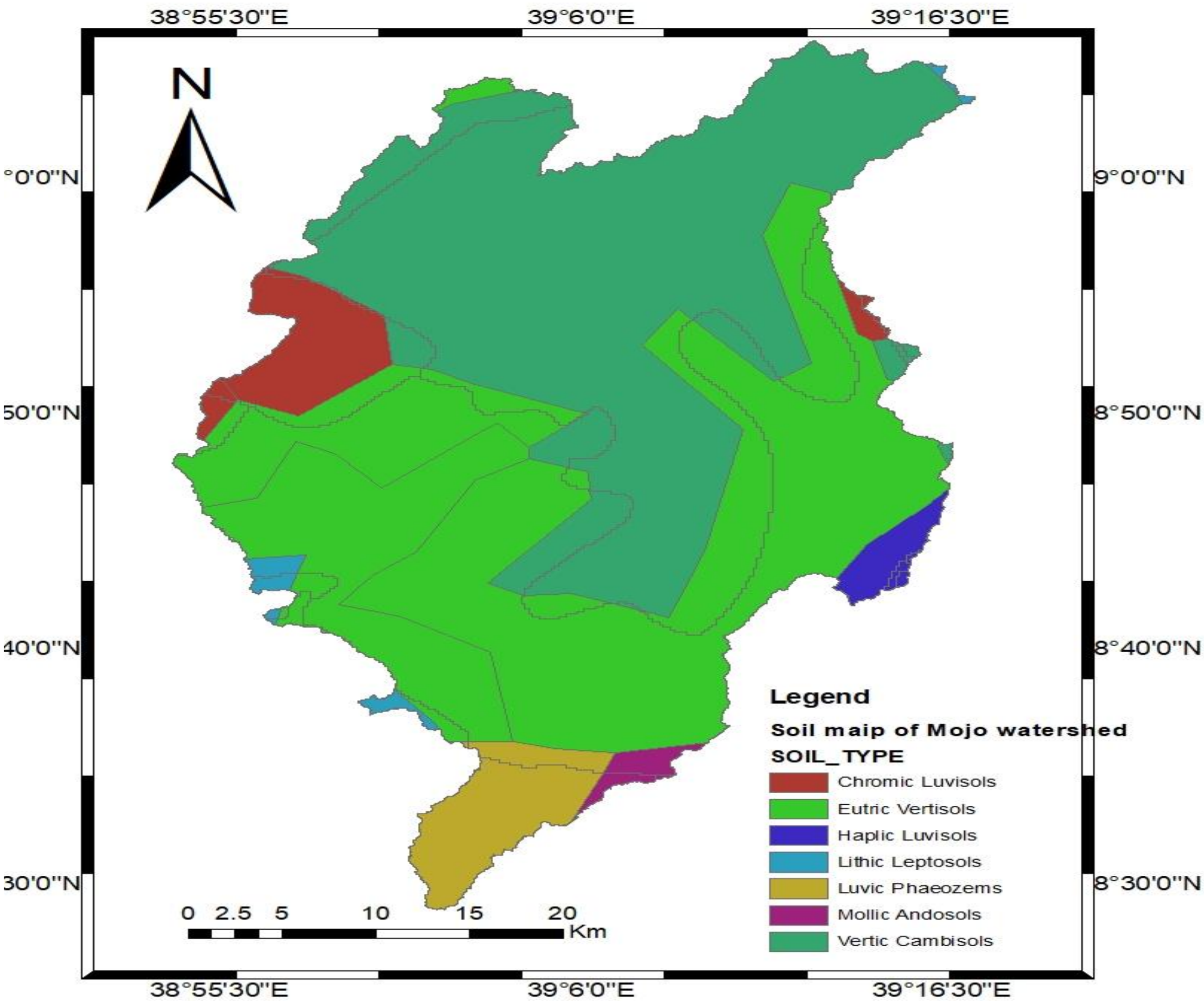

Figure 3.4 Soil map of mojo watershed

Climate data: The climate data is the projected data for CORDEX such as rainfall, snowfall, air temperature, and evaporation data are major climate information needed for the SWAT model. However, for this study precipitation and temperature data were used. RCMs simulation from CORDEX driven by HadGEM-2 ES is obtained from (CORDEX) projected under the African domain with the spatial resolution of -50km (-0.44^{o}). They are different methods of (RCMs) data extraction from CORDEX-African among those ArcGIS was used. Regional climate model data were extracted from the grid of cells covering the Mojo River subbasin by using ArcGIS10.4.1 from CORDEX data and unit conversion was taken.

3.4 Methods

The procedure or methods to conduct the objective of the thesis or research, which includes starting from data collection to result from the analysis was the same as what is clearly shown below.

3.4.1 Data Processing

Before doing any hydrological process and analysis it is important to make sure that data are: reliable, consistent, adequate, and continuous with no missing data. Errors resulting from lack of appropriate data processing are serious because they lead to bias in the final results. In any case, data should be appropriately adjusted for consistency, correct for bias, extend for insufficiency, and fill for missing data by using different techniques based on the percentage of errors**.**

3.4.2 Filling Missing Data

Before the observation data for both temperature and precipitation to use for analysis, data quality control is carried out to get severe errors in the result. This is because the consistency of data was an important prerequisite in any analysis. Inadequate temperature and precipitation data results in impracticable output. Estimation of the missing records of temperature and precipitation data sets is essential since they are utilized to drive and adjust the SWAT model that requires consistent data records. In this study missing observed rainfall and Temperature values are estimated used by multiple regressions using XLSTAT by filling each from its neighboring stations.

3.4.3 Data Quality Test

The data quality was tested by homogeneity, stationary, and consistency of data. figure (3.6) show consistency and stations data using the double mass curve method.

Consistency of recording data for all station stations: To assess the data consistency the double mass curve analysis has been used for the period of (1987-2016). Cumulated values of a given station are plotted against accumulated values of the average value of other stations, over the same time. Through the double mass curve inhomogeneities in the time series (in particular jumps) can be investigated, if for a change in observer record, in rain-gauge type, etc. This is indicated in a double mass plot, showing an inflection point in the straight line. The inconsistent data series can be adjusted to consistent values by proportionality. The plotted figure below for checking of consistency of rainfall.

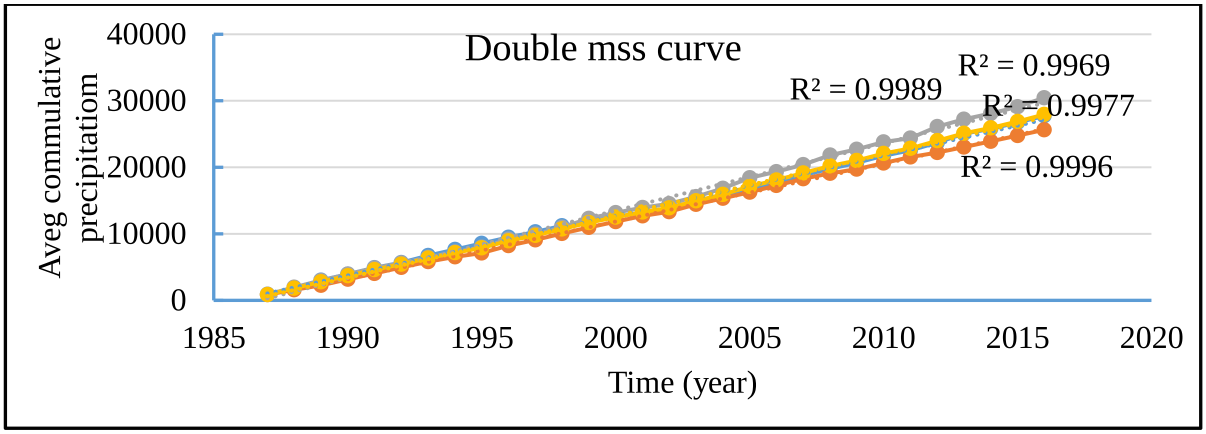

Figure 3.5 Data Consistency test graph for all the stations using double mass curve

Estimation of Areal Precipitation: Numerous area rainfall estimation methods are currently used for averaging rainfall depths collected at the ground station. The isohyetal and Thiessen polygon techniques are conventional techniques that are usually applied to estimate the areal rainfall over the entire basin (Taesombat & Sriwongsitanon, 2009). For this thesis, the Thiessen polygon method was considered because this method is the most important in the engineering context, especially in engineering hydrology. The method weighs each gauge in direct proportion to the area it represents of the total basin without consideration of topography or other basin physical characteristics. Station weights are scalar factors used to transform point precipitation observed at this rainfall gauging station into associated mean precipitation over an area that the station data are assumed to represent (Desta, 2017). If there are n stations with rainfall values P1, P2, P3…Pn and A1, A2, A3…. A cumulative rainfall (mm) cumulative of other stations' rainfall (mm). (figure 3.8 and table 3.2) indicate Thiessen polygons and it's the station area covered.

$$Pav = \sum_{1}^{n} pi \frac{Ai}{A} \qquad 3.8$$

Where $\frac{Ai}{A}$ is the weight factor of each station.

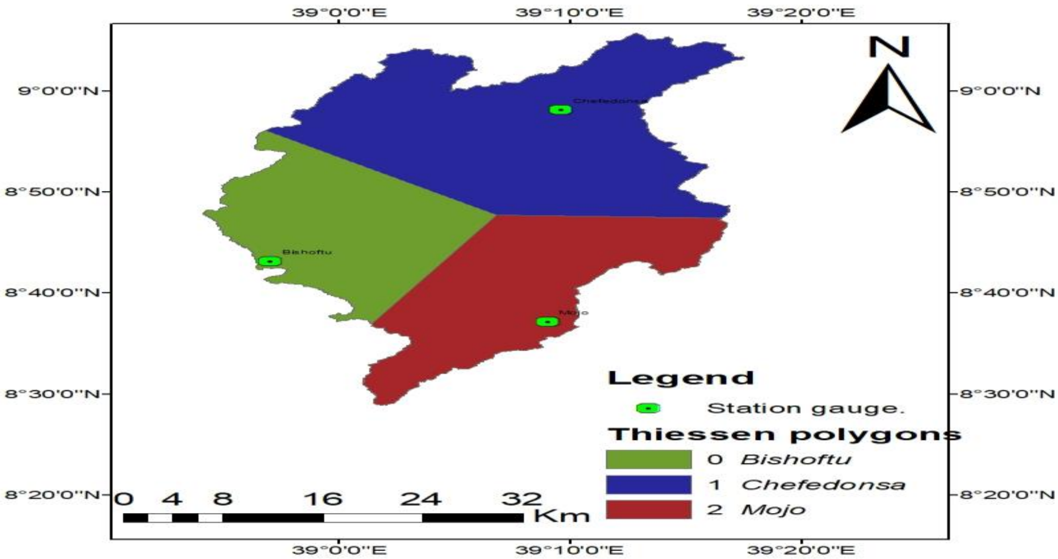

Figure 3.6 Thiessen polygons meteorological station.

Table 3.2 Station name watershed area

No	Station name	Latitude	longitude	elevation	Area(km^2)
1	Chefedonsa	8.97	39.13	2100	743
2	Bishoftu	8.73	38.95	1900	433
3	Mojo	8.62	39.15	1870	487

3.4.4 Regional Climate Model Performance Evaluation.

Several studies have evaluated regional climate model output with CORDEX- projected over Africa. The characteristics of the performance evaluations of projected precipitation of the past and the future in Ethiopia have been highlighted by some of those authors. The recent study by (Dibaba *et al*., 2019) the performance evaluation of a set of 6 RCMs from CORDEX of RCMs driven by the European Centre for Medium Weather Forecasting (ECMWF) interim reanalysis (ERA-interim) in simulating the current climate variable over Didessa and fincha catchment.

These studies were the performance evaluations of three regional climate models projected from CORDEX-Africa driven by Met Office Hadley centre (MOHC) of HadGEM2-ES (GCMs) by statistical analysis using the current observed precipitation vs projected precipitation for the mojo River watershed area. Those performance evaluations were made by (r), RMSE, and PBIAS.

3.4.5 Bias Correction of Climate Data

All way, outputs of regional climate models data were not being directly used for impact analysis as the data compute variables may differ systematically from the observed ones. Bias correction is therefore will be applied to compensate for any tendency to overestimate or underestimate the mean of downscaled variables. The performance of the different bias correction methods is not uniform across space or time (Beyer, Krapp, and Manica, 2020). Bias correction factors are computed from the statistics of observed and simulated variables, for this thesis the methods of bias correction used were power transformation for precipitation and variance scaling for temperature.

Power Transformation for precipitation: The precipitation is usually varied spatially and highly nonlinear. The power transformation method utilizes a non-linear approach in an exponential form aP^b to correct the mean and variance of the precipitation time series (Luo et al., 2018). In this study, the RCM data of precipitation was bias-corrected by using the power transformation method because it corrects the mean, variance, and coefficient of variation (CV), leading to a better copy of observed precipitation. The correction method is applied by comparing the daily observed precipitation at each station with the nearest grid point of the RCM considering the grid points as a single station on the watershed and Unlike the LS method, the PT method further adjusts the bias in standard deviation and variance using an exponential form (Tadese, 2020). The power transformation method is explained in the following equations:

$$p^{*} = a\,p^{b} \text{...} 3.8$$

Where P* is corrected precipitation, P is simulated precipitation. The parameters a and b are estimated by equalizing the coefficient of variation (CV) of the corrected simulations P^b and CV the observed values, both from the calibration/optimization period. Parameter b was first determined iteratively by ensuring that the CV of the corrected precipitation matched that of the observed. Then parameter a, which depends on the value of b, was determined by matching the means of the corrected and observed precipitation.

Variance Scaling for Temperature: The PT method is an effective method to correct both the mean and variance of precipitation, but it cannot be used to correct temperature time series, as the temperature is known to be approximately normally distributed (Yang *et al,* 2015). The Variance scaling method was developed to correct both the mean and variance of normally distributed variables such as temperature (Teutschbein and Seibert, 2012). Temperature is normally corrected using the Variance method.

$$Tcorr = \overline{T}obs + \frac{\delta Tobs}{\delta Trcm}(Trcm - \overline{T}rcm) \text{..........................} 3.8$$

Where: Tcorr the corrected daily temperature, Trcm the uncorrected daily temperature from RCM model, and Tobs the observed daily temperature while $\overline{T}$ is mean observed temperature and is mean simulated temperature and σ standardization.

3.5 Trends Analysis

There are different methods of trend analysis: -those are Mann–Kendall (MK), modified Mann Kendall (mmk), and Sen's slope (S) method. Mann-Kendall: it graphical of or non-numerical method but modified Mann-Kendall it magnitude of trend or numerical value and sen's slope also direction of the trend that means negative or positive trends.

3.6 Hydrological Modeling.

Hydrological modeling is the characterization of a specified watershed by adding a hydrological model under limited data conditions (S. M. Tessema, 2011). The Arc SWAT model can estimate relevant hydrological components such as surface runoff, evapotranspiration, peak rate of runoff, sediment yield, groundwater flow, nutrients, and pesticides for each HRUs unit in the sun-watershed (Sisay, 2017). For this study, the simulation of the hydrological components was by the Arc SWAT model using a water balance equation at the watershed level (Neitsch *et al*. 2011).

$$SWt = SWo + \sum_{i=1}^{t} (Rday - Qsurf - Ea - Wsweep - Wgw.) \qquad 3.9$$

Where SWt is the total water content in (mm), t is period in a day, Rday is the amount of precipitation on specific days i (mm), Qsurf is the amount runoff on specific days i (mm), Ea is evaporation transpiration amount on days i (mm), Wsweep is the water percolaThe simulation was conducted based on the Soil Conservation Service Curve Number (SCSCN) methodted into a vadose zone on a day i (mm), and Wgw is the return amount of flow on the day i (mm).

The SCS curve number method is less data intensive than Green & Ampt infiltration method. Hence, the SCS curve number was used to calculate surface run off in the watershed since available spatial data is limited. In the Soil Conservation Service (SCS) curve number method often called the Curve-Number (CN) method, land use and soil characteristics are lumped into a single parameter.

$$S = \frac{25400}{CN} - 254 \qquad 3.10$$

Where: S-maximum soil retention potential, CN-curve Number

$$Ia = 0.2s \qquad \text{.....} 3.11$$

$$Qsurf = \frac{(p - 0.2s)^2}{p + 0.8s} \qquad \text{.....} 3.12$$

Where : Qsurf is the daily surface runoff in millimeters (mm), *Ia* -initial abstraction (mm), and P-accumulated precipitation

3.7 Description of the Soil and Water Assessment Tool (SWAT) Model

Soil and Water Assessment Tool (SWAT) is a river basin scale model developed to quantify the impact of land management practices in large, complex watersheds and is a public domain hydrology model. The Soil and Water Assessment Tool (SWAT) is a physical-based model used to estimate the runoff, sediment, and chemical yields in gauged and un-gauged basins. For this study, the SWAT model was used to model streamflow.

3.7.1 SWAT Model Setup

The first step was modeling setup to create a new SWAT project in Arc SWAT using Arc SWAT version 2012.

3.7.2 Watershed Delineation

The second step was automatically watershed delineation by adding the digital elevation model of the watershed, this watershed has 25 subbasins and 132 HRU by selecting a threshold area of 3159 ha.

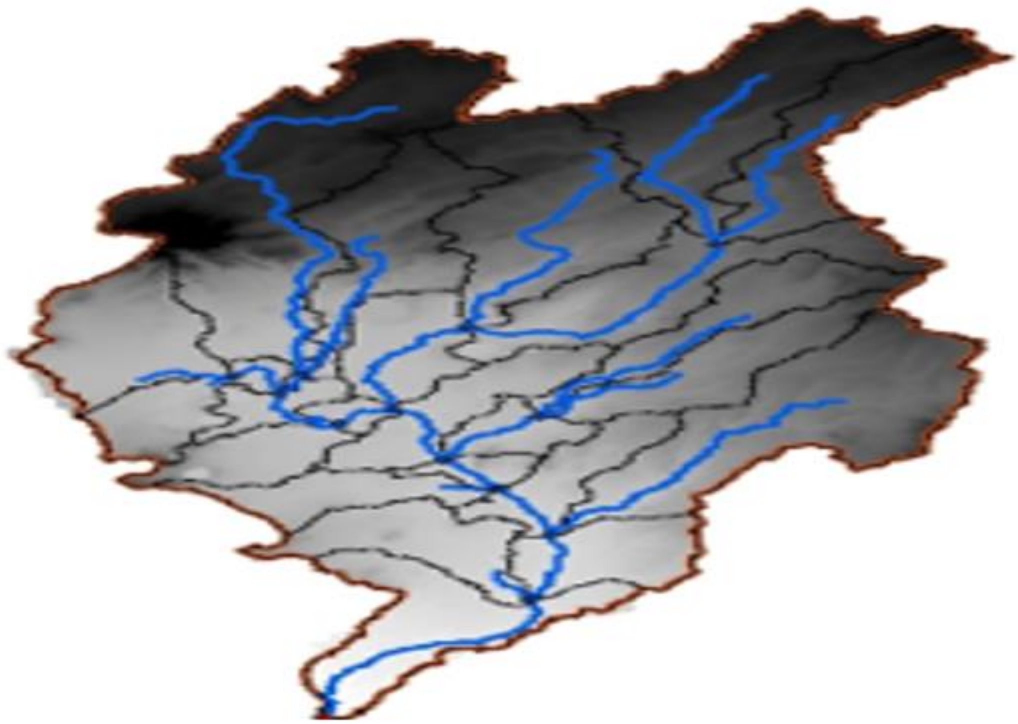

Figure 3.7 Watershed delination and stremflow

3.7.3 Hydrological Response Unity (HRU)

The third step was adding the land use, soil, and slope for subwatershed is divided into HRUs (overlay of specific land-use, soil, and slope). HRUs were defined and mapped using the ArcSWAT interface and the land cover, soil, and slope datasets described above. HRU definition involves selecting minimum area thresholds for land cover classes, soil types, and slope classes within a subwatershed that must be met for HRUs for those classes to be included in the model. The use of thresholds for HRU definition prevents the inclusion of land cover, soil, and slope classes with negligible areas in a sub-watershed, thereby reducing the total number of HRUs and improving model efficiency.

3.7.4 Write Input Table.

The fourth step opens the write input table and adds observed weather data like daily precipitation, maximum and minimum temperature, wind speed, relative humidity, and solar radiation data from stations that were used to run the model. The weather generator file table was prepared using the 24 years daily meteorological data of Bishoftu station as a principal station to calculate and fill all missed daily weather information of other stations and included in the projected file. Generally, the following are the important procedures for modeling the watershed component using SWAT: - Create SWAT project, delineate the designated watershed for modeling,

3.7.5 Model Running Up

After the hydrological response unit was generated write input data table those are weather generator, daily precipitation, maximum and minimum temperature, wind speed, relative humidity, and solar radiation data from stations was input and swat is simulation opened and swat setup run.

3.7.6 SWAT Model Performance Evaluation

There is different method of Soil and Water Assessment Tool (SWAT) model performance evaluation. Among those: - Nash-Sutcliff Efficiency (NSE), Coefficient of Determination (R^2), Percent Bias (PBIAS), and returns the person product-moment correlation coefficient (r) is used in this study;

3.7.6.1 Sensitivity and Uncertainty Analysis

Sensitivity analysis is a mechanism for the evaluation of the input parameters concerning their impact on model output and is useful for model development, model validation, and reduction of uncertainty (Lenhart *et al*., 2002). They are five calibration approaches widely used by the scientific community in SWAT CUP. For this study SWAT-CUP 2012, Sequential Uncertainty Fitting (SUFI2) was used. SWAT-CUP2012, Sufi-2 is advanced with global sensitivity analysis and at one-time sensitivity to identify the most sensitive flow parameters for SWAT hydrological modeling (Gudu *et al.*, 2020). The two types of sensitivity analysis are generally performed. Those are local sensitivity by changing values one at a time and global sensitivity by allowing all parameter values to change.

3.7.6.2 Model Calibration and Validation

Model calibration is the process of iteratively adjusting the model parameter to estimate improve the best fit between model predictions and real-world observations. After calibration, model validation is performed by running the model with the calibrated parameter set and comparing predictions to additional observed data (i.e., observed data not used for calibration). Based on the level of agreement between predictions and these additional observations, the model is either validated for further use or model inputs and parameters are revisited for further calibration(Group, 2018)

3.8 Present and Future Climate Change Impact Analysis

Analysis of the impact of climate change on streamflow involves hydrologic models and projections for future climate variables such as precipitation and temperature from the global climate models (GCMs). However, the coarse spatial resolution (approximately 100−250 km) of the GCM models makes them inadequate for regional studies (Teutschbein and Seibert, 2012). Then RCMs downscaling techniques will be used to extract high-resolution regional or watershed scale climate variables from larger-scale GCM outputs.

3.9 The Overall of Method Framework Model

The methods implemented to evaluate the impact of climate change on mojo streamflow through the SWAT model interface of GIS by using spatial, hydrological, meteorological, and climate model output data. The methods used are data collection, analysis, model simulation, and model performance evaluation. In this study, the overall framework design is given below in fig (3.2).

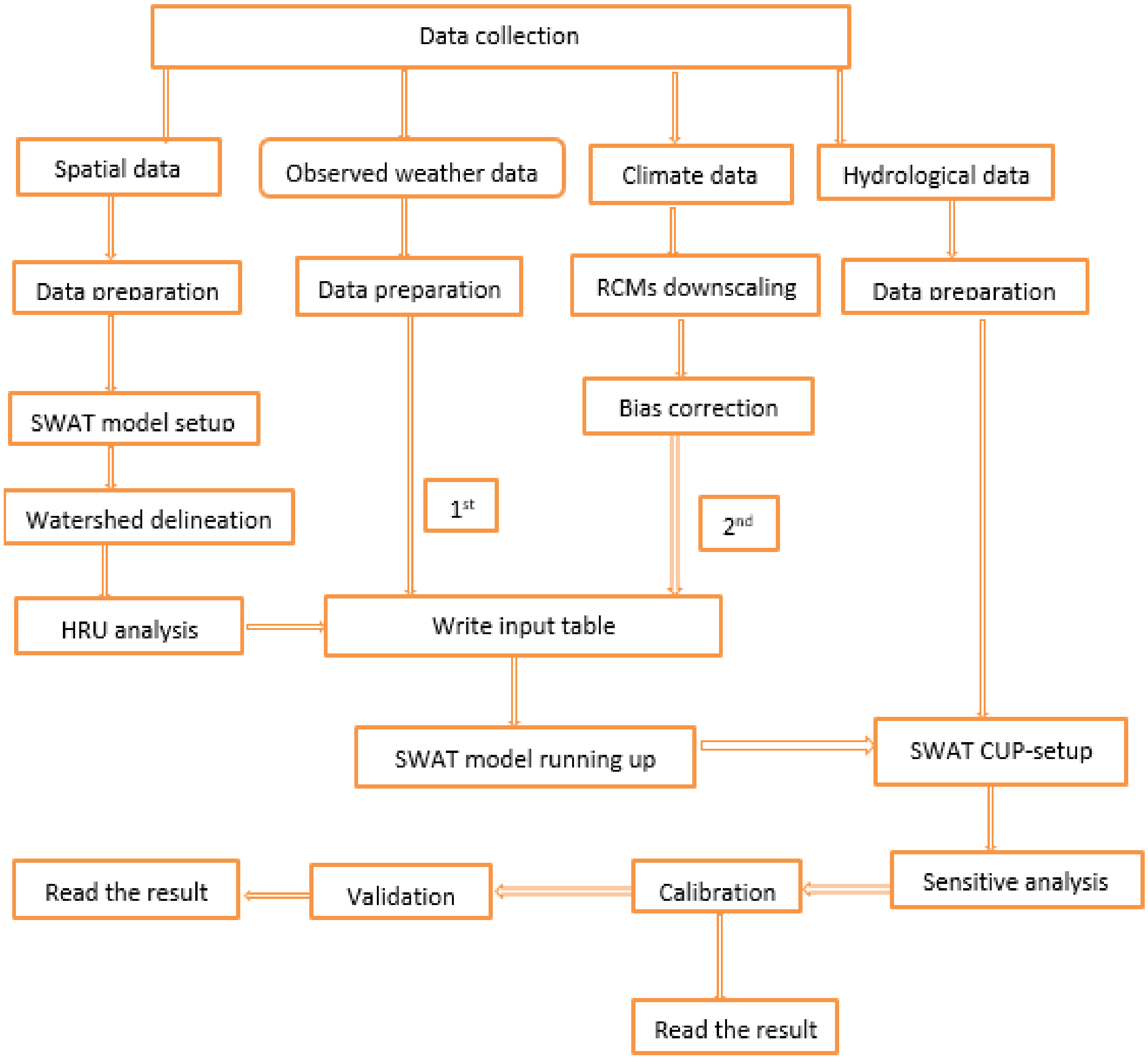

Figure 3.8 Conceptual flow charts of the Studies

4 RESULT AND DISCUSSION

Based on the objective of the research, the result and discussion are presented in three parts. The first part was the performance evaluation of different regional climate models using projected precipitation to identify the changing climate over the watershed area. The second part has focused on the trends of projected precipitation and temperature. Finally, analysis of the future impact of climate change on streamflow of the watershed area.

4.1 Performance Evaluation of Regional Climate Models.

The first aim of this study was the performance evaluation of different regional climate models. using the Coordinated Regional Climate Downscaling Experiment (CORDEX) on the Mojo River watershed. At present many collaboration projects are generating climate simulation from dynamical downscaling for model inter-comparisons and impact assessment. The project includes CORDEX that produces dynamical downscaled climate simulation on all continents. These projects have made available a large number of high-resolution climate simulations that can be used for impact assessment. However, before using climate simulation from dynamical downscaling it is appropriate to evaluate their performance at different spatial scales. This is the most important for choosing the appropriate climate model to be used for impact assessment at the location since the performance of dynamical downscale data differs from location to location from one RCM to another (Niang *et al*., 2015). The evaluation was based on how the RCMs projected precipitation data was performed with observed precipitation data using statistical methods.

Three statistical model performance evaluation criteria were used to evaluate how the projected precipitation under different RCM. Due to it is extremely important for water resource management and natural hazard assessment. Also the discontinuous nature of precipitation in time and space this climate variable perhaps the most challenging one for climate simulate (Airey & Hulme, 1995). The RCMs have adequately captured the reference precipitation probability density function with a few showing towards excessive light rainfall events (Niang et al., 2015). Most researchers such as - (Endrie, 2013, Reda, 2015, Dibaba *et al*., 2019, Tumsa,

2021) evaluated the performance model was by Pearson correlation coefficient (r), mean Bias (PBIAS), and root mean square error (RMSE). An initial evaluation was made on how the mean annual projected precipitation by individual RCMs and their mean ensemble varied spatially concerning observed precipitation over the watershed area. Also for this study, the spatial maps of the observed rainfall, RCMs output, and mean ensemble were developed by the inverse distance method.

Table 4.1 Statistical performance of three regional climate model under RCPs4.5 and RCP8.5 using difference evaluation method

No	Name of RCMs	r	RMSE	PBIAS
1	RAMCO22T	0.5856	1.1333	-0.45348
2	CCLM4-8	0.5626	1.262	-0.48212
3	RAC4	0.5245	1.871	-0.75707
4	Ensemble	0.5557	1.367	-0.56424

RMSE is the absolute error of the climate models is projected climate variables. The smaller absolute value of both PBIAS and RMSE indicates the good performance of the model and vice versa. The correlation coefficient value range can from -1 for perfect negative correlation to 1 for a perfect positive correlation between the RCMs and the observed climate variables. In different cases, there is no single criterion that indicates surely the best RCMs performance of the watershed. Thus, PBIAS, RMSE, and r, are used in combination. The percentage of bias negative indicates all the models are underestimated, while the RAMCO22T model was better performed than other models for this watershed area. But RCA4 showed weak performance and the CCLM4-8 model showed overestimation under higher altitudes. Similar GCMs data downscaled using the RCA4 model showed weak performance in capturing annual rainfall of mojo sub-basin and GCMs downscaled using the CCLM4-8 model showed overestimation in the higher altitudes of the mojo basin (fig 4.1), similar to the study (Endris *et al.*, 2013).

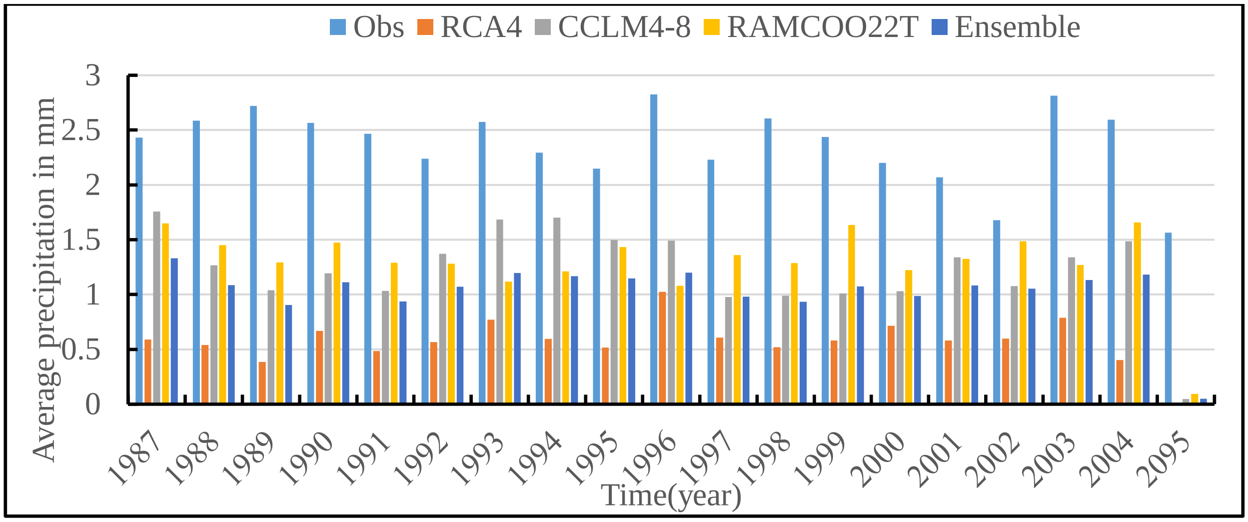

Figure 4.1 Graphical compression simulated and historical precipitation with in different RCPs model under rcp4.5 andrcp8.5

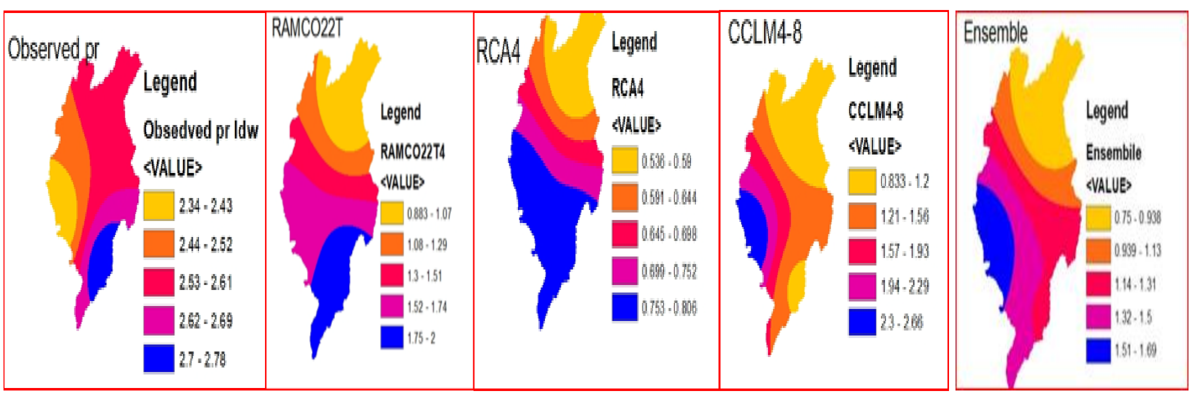

Figure 4.2 The spatial distribution projected and observed precipitation using in mm/day.

The spatial distribution of projected rainfall for different regional climate models was done using the inverse distance method are shown in (fig 4.2) and the RAMCO22T model was well performed than other models. Because among three individual and ensemble of the models, RAMCO22T model projected rainfall was well performed over most the station than the other model. Rainfall bias is likely to be associated with differences in the physical parameter rainfall of watersheds. The model bias is found highest dependent on terrain elevation and the highest is associated with the highest elevation (Dibaba *et al*,.2019).

4.2 Bias Corrected Precipitation

Three bias correction methods were used for historical precipitation data to select a suitable bias correction method because it is important for providing reliable inputs for impact analysis of the watershed. The power transformation method was well performed in hydrological extremes. The result of bias-corrected was at the monthly level, as shown in (fig 4.1), some months have underestimated (RCP) precipitation as compared to the observed precipitation and other months are overestimated especially the three months June, July, September, and October which are found in the main rainy season.

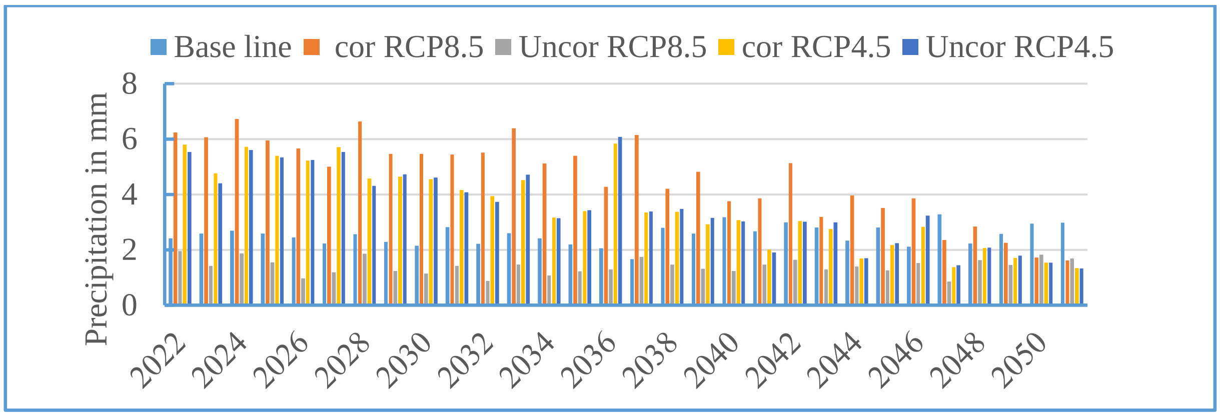

Figure 4.3 Comparison of yearly under RCP4.5 and RCP8.5 of bias-corrected and bias uncorrected with the baseline.

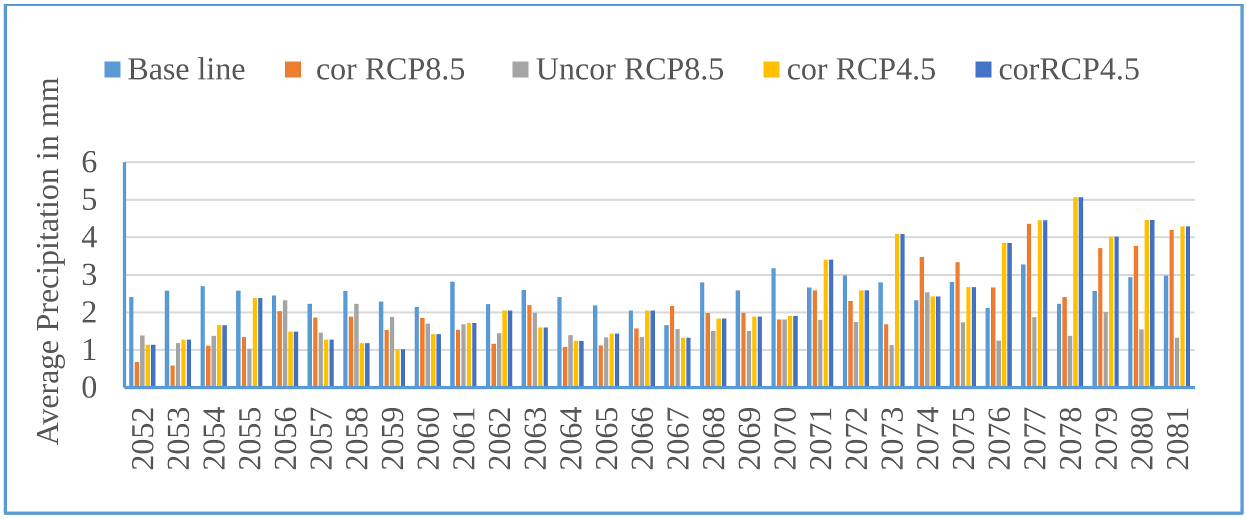

Figure 4.4 Comparison of yearly under RCP4.5 and RCP8.5 of bias-corrected and bias uncorrected precipitation with the baseline.

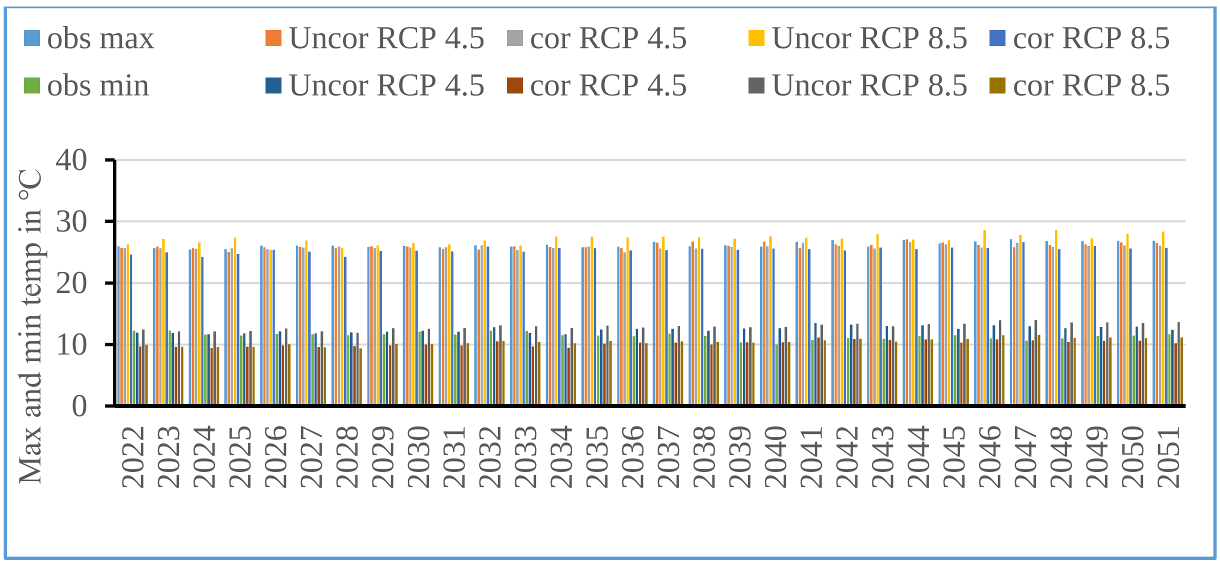

figure 4.5 Comparison of yearly temperature max and min RCP4.5 and RCP8.5 of bias-corrected and bias uncorrected with the baseline.

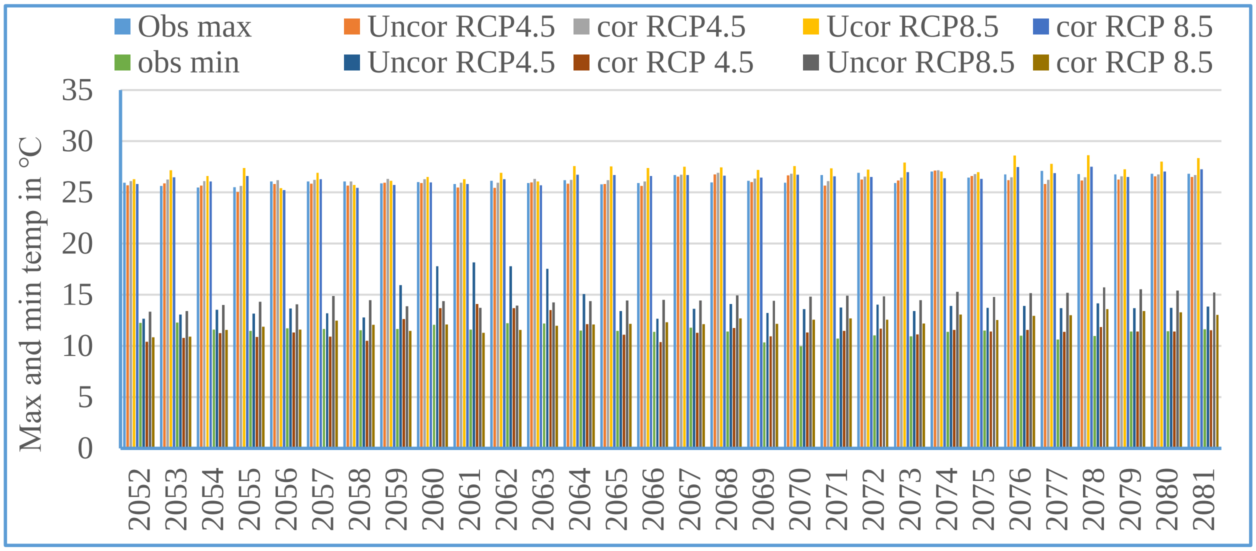

Figure 4.6 Temperature maximum and minimum under RCP4.5 and RCP8.5 of bias-corrected and bias uncorrected with the baseline.

4.3 SWAT Model Simulation and Sensitivity Analysis for Calibration and Validation

The observed and projected data was analyzed for the input (SWAT) model to simulate streamflow and water balance component. The simulated SWAT was rerun for calibration and validation using streamflow as input data and the simulation was executed to check the performance of the model on the watershed area.

4.3.1 Sensitivity Analysis

Sensitivity analysis is a way to identify which model parameter is the most important. For sensitivity analysis of project type used was SUFI-2 algorism provided the same information about the sensitivity of the model parameters. In this study select seventeenth (17) global parameter for calibration depending on previous paper on the study area and out of this only eight (8) most sensitivity parameters with absolute minimum and maximum range in SWAT model for the watershed area for calibration and validation. The initial minimum and maximum limits of the parameters were set based on literature and local knowledge of the watershed (Amin & Nuru, 2020; Biru & Kumar, 2018). The data was split into calibration and validation by sampling were 65% and 35% data for calibration and validation (WaleWorqlul *et al.*, 2018). The selection of the streamflow sensitive parameters was based on their t and p-value. The higher the absolute values of the t and cross ponding with the smaller values of p, the more sensitivity of the streamflow. Based on the t and p values the streamflow sensitive parameters were ranked as in fig (4.7) and table (4.2). The streamflow calibration, the response of the model towards parameter involving. Threshold depth of water in shallow aquifer for revap or percolation to the deep aquifer (REVAMN.gm), Manning's "n" value for (CH_N2), HRU_SLP, and evaporation (ESCO) are very low. On the other hand, parameters involving surface runoff (CN2), Groundwater delay (GW_Delay) surface lag time (R_SURLAG), and Saturated Soil conductivity (mm/h) are the most sensitive parameter in streamflow for calibration and validation respectively.

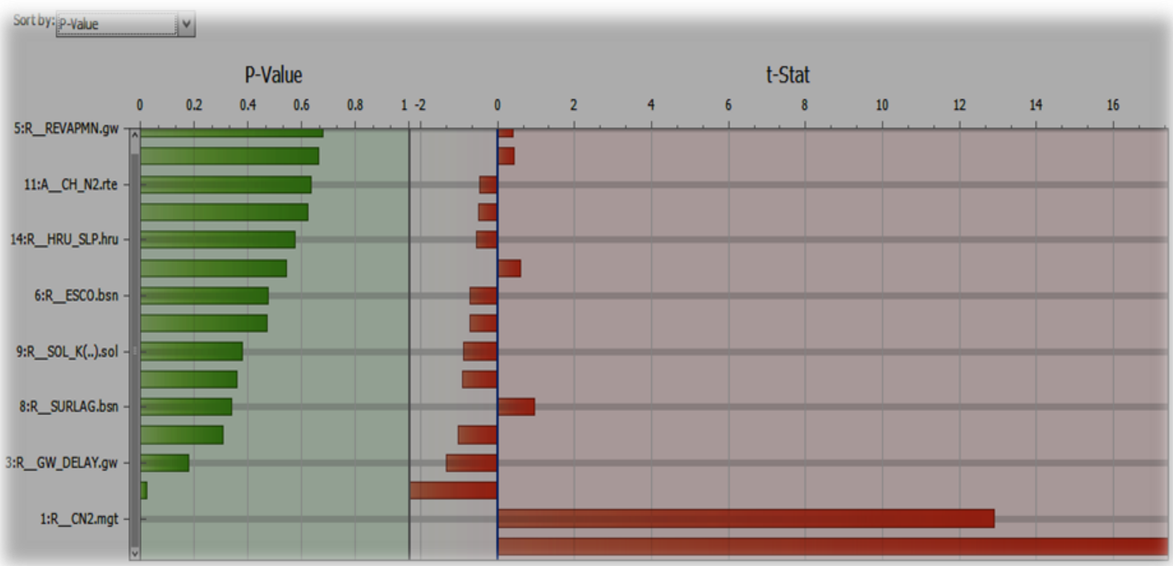

Figure 4.7 The most Sensitivity analysis of flow

Table 4.2 the most sensitivity parameter for the watershed area

No	Sensitive parameter	Description	min	max	p-value	t-value	Rank
1	R_CN2	Initial SCS runoff curve number for moisture condition II	0.22	0.41	0	12.9	1
2	R_GW_DEAY	Ground water delay(days	319.1	462.7	0.023	-1.3	2
3	R_SURLAG	Surface lag time	0.22	0.27	0.337	-0.95	3
4	R_SOL_K	Saturated Soil conductivity (mm/h)	0.40	0.52	0.384	-0.87	4
5	R_ESCO	Soil evaporation compensation factor	1.19	1.24	0.474	-0.71	5
6	R_HRU_SLP	Hydraulic response unit slope	0.133	0.178	0.545	-0.56	6
7	A_CH_N2	Manninig's "n" value for	0.220	0.38	0.667	-0.47	7
8	R_REVAPMN	Threshold depth of water in shallow aquifer for revap or percolation to the deep aquifer	412.4	425.2	0.681	0.41	8

4.3.1.1 Calibration and Validation

Calibration followed sensitivity analysis by considering those model parameters. Calibration involves testing the model with known input data and output data to adjust some parameters, while validation involves comparison of the model results used for calibration with an independent dataset during calibration without any further adjustment of the calibration parameters. Model calibration and validation using SWAT CUP SUFI-2 Al- algorithm, flow predictions period used for calibration (2000 to 2009), and validation (2010 to 2015) monthly flow data. After calibrating for streamflow simulation was completed the hydrographs are well captured. The agreement between the observed and simulation is generally good, which are tested by R^2 , NSE, and percent of bias an acceptable result was obtained according to the model evaluation guideline (Moriasi *et al*., 2007). The results of these tests illustrated that the monthly coefficient of determination, Nash- Sutcliffe coefficient, and Present of bias were 0.71, 0.70, and -13.9 for the calibration period. The calibration and validation period of the model was fifteen years from the (2000 to 2015) period (Figure 4.8) and (Figure 4.10) below respectively.

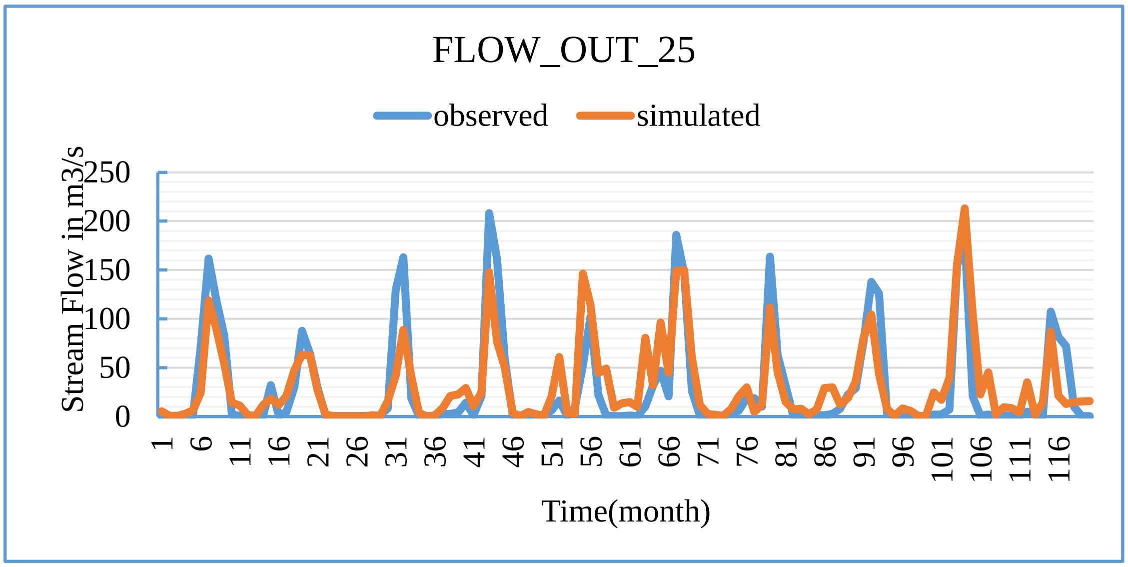

Figure 4.8 Streamflow calibration at Mojo river gauging station

The hydrography plot of the observed versus simulated streamflow also shows the simulated and observed streamflow have a good relation. The R^2 of the observed versus simulated streamflow.

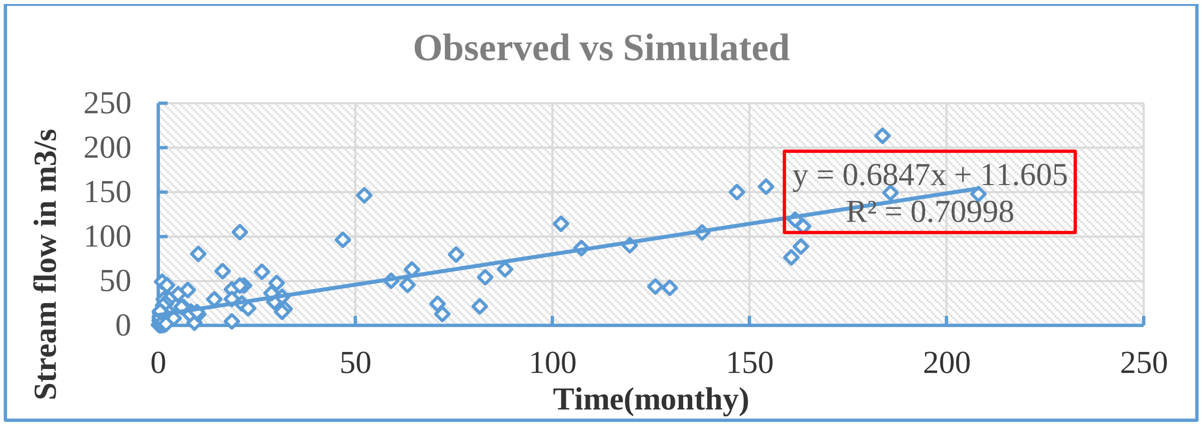

Figure 4.9 The scatter plot of the observed Vs simulated streamflow

4.3.1.2 Streamflow Validation

The model calibration parameters were validated using an independent set of measured flow data which were not used during model calibration. Flow validation was carried out from (2010 to 2015) without further adjustment of the parameters of flows used in calibration. Based a good relationship between monthly observed and simulated flows in the validation period were demonstrated by the R^2 of 0.71, NSE of 0.64, and PBIAS of -4.7. The hydrograph for the validation period of the observed and simulated streamflow in a monthly base estimation shows that the model overestimated the streamflow in the study area.

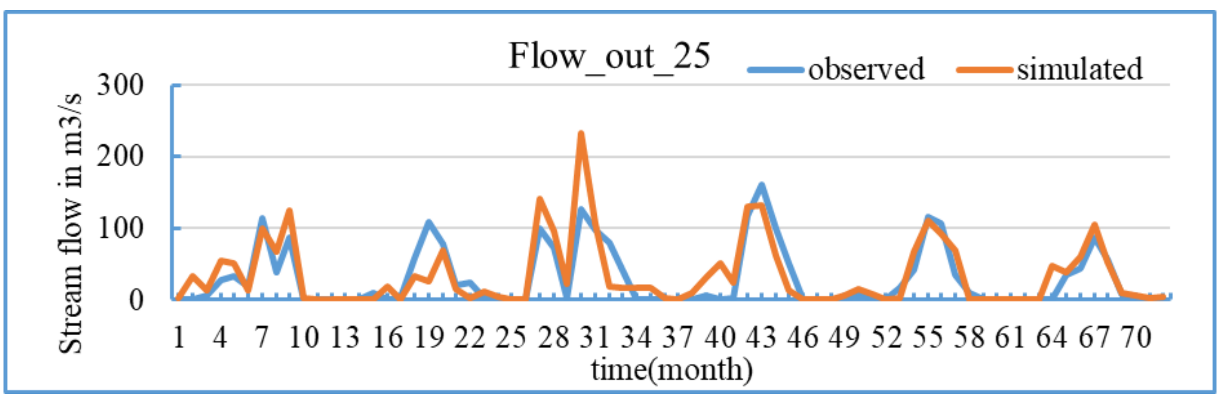

Figure 4.10 Streamflow validation of observed vs simulated

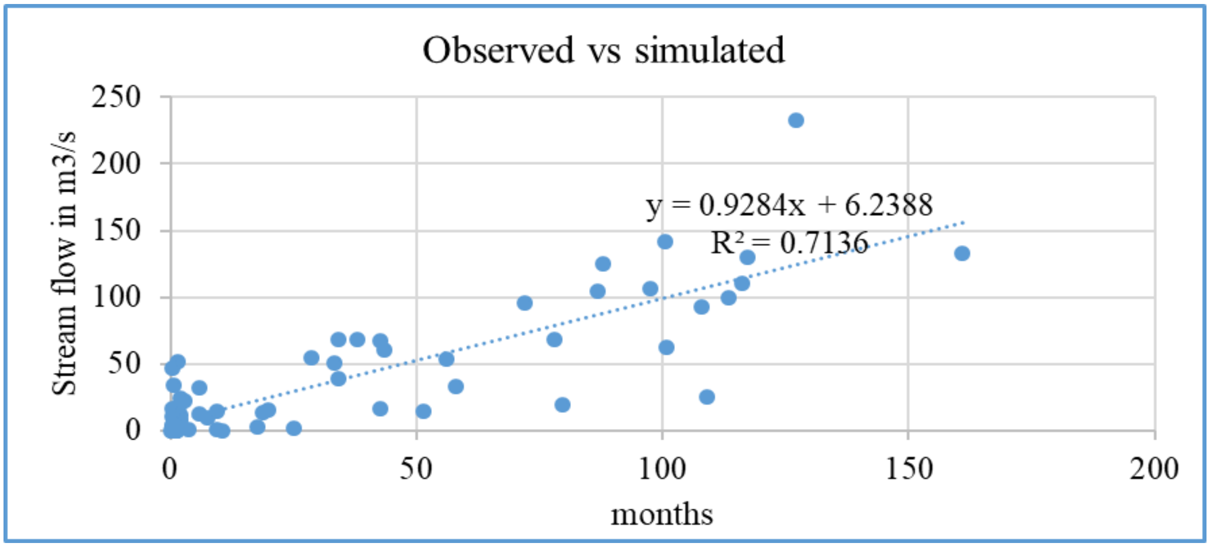

Figure 4.11 The scatter plot of the observed Vs simulated streamflow

Table 4.3 Statistically performance of SWAT model for calibration and validation result.

Statistical parameter	Calibration	Performance Rating	Validation	Performance Rating
R^2	0.71	good	0.70	good
NSE	0.70	good	0.66	good
PBIAS	-13.9	good	-4.7	Very good

4.4 Impact of Climate Change on Precipitation Trends.

One of the common tools for detecting a change in climate and hydrology time series is trend analysis. Several statistical trend tests exist to assess the significance of the trend in time series. For this study non-parametrical and parametrical trend test is the Mann Kendall trend test and the modified Mann Kendall trend test was used. Mann Kendall test is used to determine whether a time series has graphical upward or downward trend only does not tell in numerical and autocorrelation must have done before trend test. Modified Mann Kendall trend test parametrical trend test and it is not needed of per-weighting data time series to test trend.

The projected precipitation of the watershed indicates under RCP4.5 and RCP8.5 there will be a significant change. The average projected precipitation of the watershed will be a significant decreasing trend under RCP4.5 and RCP8.5 scenarios in the future period (2022-2051) climate model. Sen's slope estimate indicates precipitation will be decreasing trend to more than -1.75 mm/annual and -1.9 mm/annual under both intermediate scenario RCP4.5 and high emission scenario RCP8.5. In the period of (2052-2081) the average projected precipitation is significantly increasing, the Sen's slope estimate indicates precipitation will be increasing trend of more than 1.165 mm/annual and 1.02 mm/annual under both RCP4.5 and RCP8.5 scenarios. The average annual precipitation and temperature of the Awash river basin showed a consistently increasing trend (Gedefaw *et al*., 2018). The trend of the Awash river basin showed an increase and decrease in mean annual rainfall (Mahtsente Tibebe Tadese *et al*., 2019).

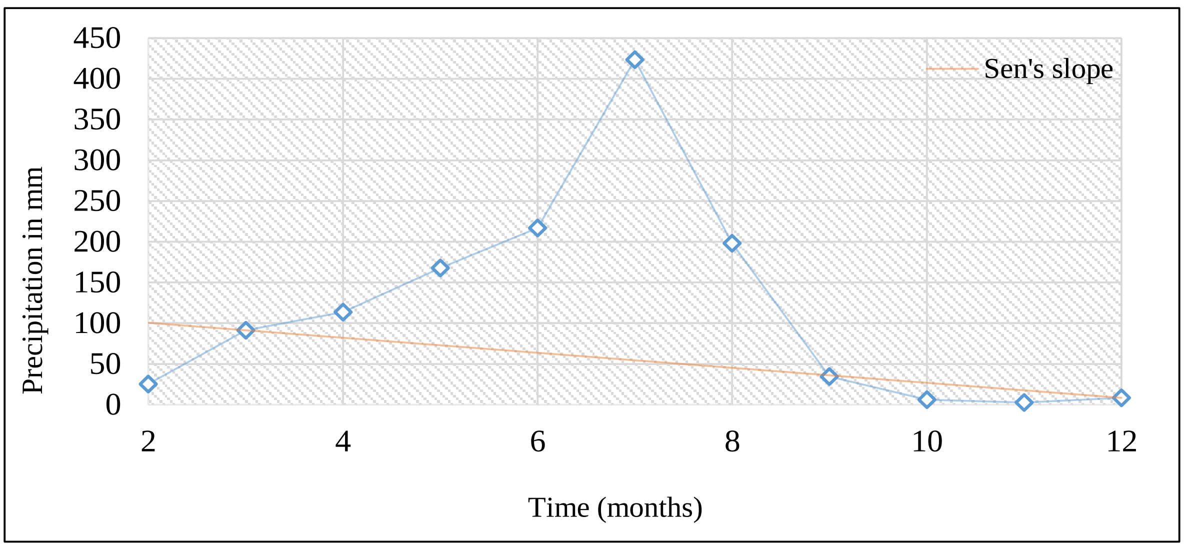

Figure 4.12 Monthly precipitation trends analysis time series for in period (2022-2051) under RCP4.5.

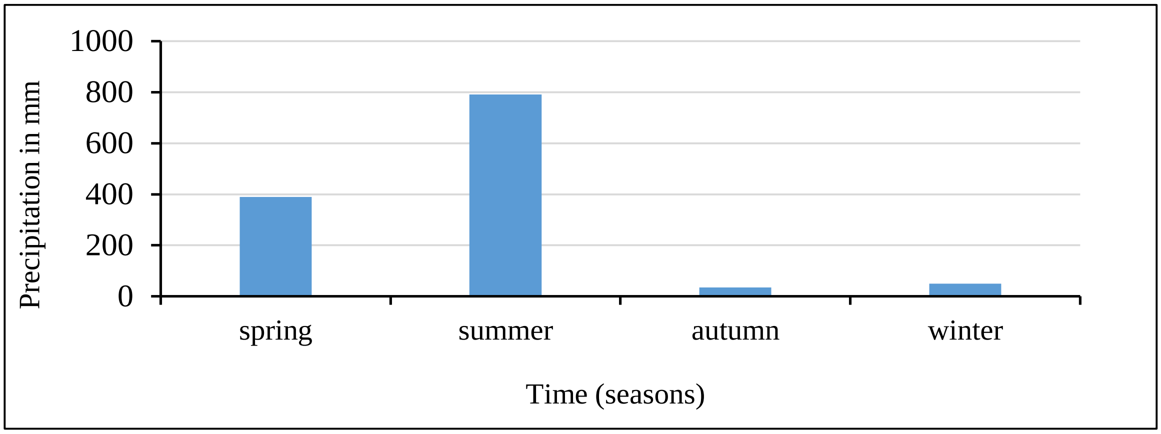

Figure 4.13 Seasonal precipitation trends analysis time series for in period (2022-2051) under RCP4.5.

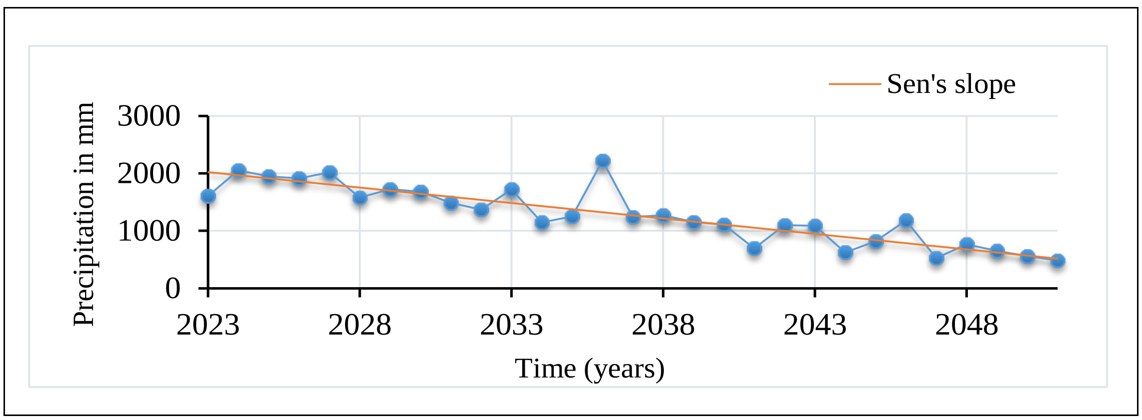

Figure 4.14 Precipitation trends analysis time series for in period (2022-2051) under RCP4.5

Table 4.4 Precipitation trends analysis time series the period of (2022-2051) under RCP4.5

No	Name	$P_{0.05}$	|Z| -value	P-value	Sen's slope	New-variance
1	Spring	1.96	2.90	0.004	10.9	2583.39
2	Summer	1.96	6.28	0.000	-62.28	3141.66
3	Autumn	1.96	1.21	0.225	-0.76	3141.66
4	Winter	1.96	4.81	0.000	-2.91	3141.66
5	Annually	1.96	5.8	0.000	-52.6	3141.66

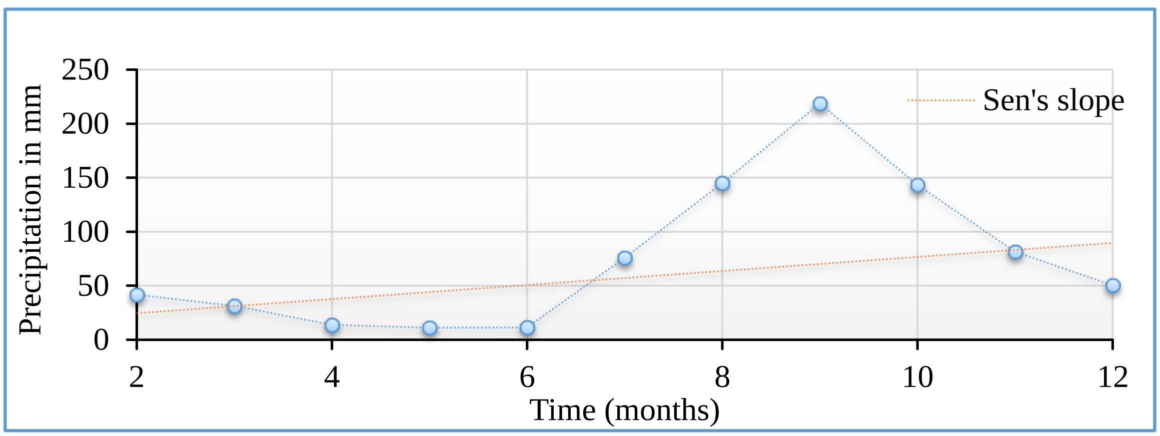

Figure 4.15 Precipitation trends analysis time series for in period (2052-2081) under RCP4.5

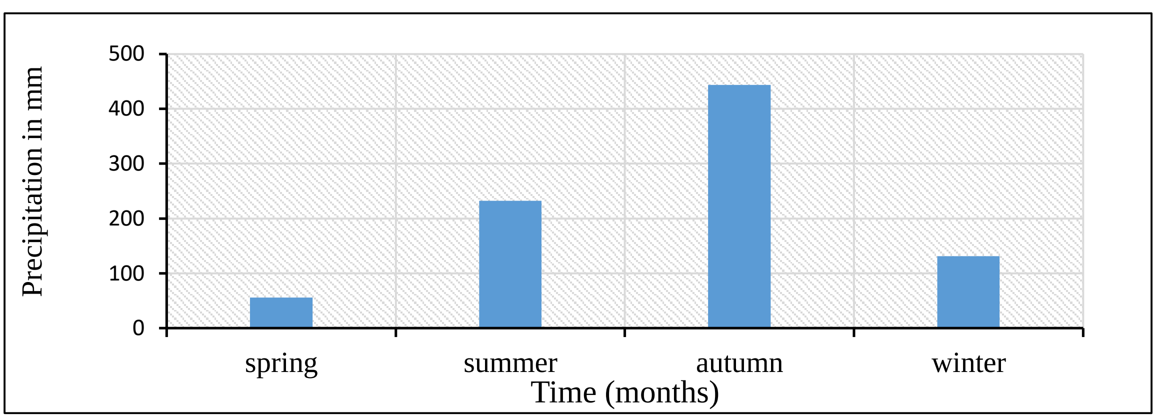

Figure 4.16 Seasonal precipitation trends analysis time series for in period (2052-2081) under RCP4.5

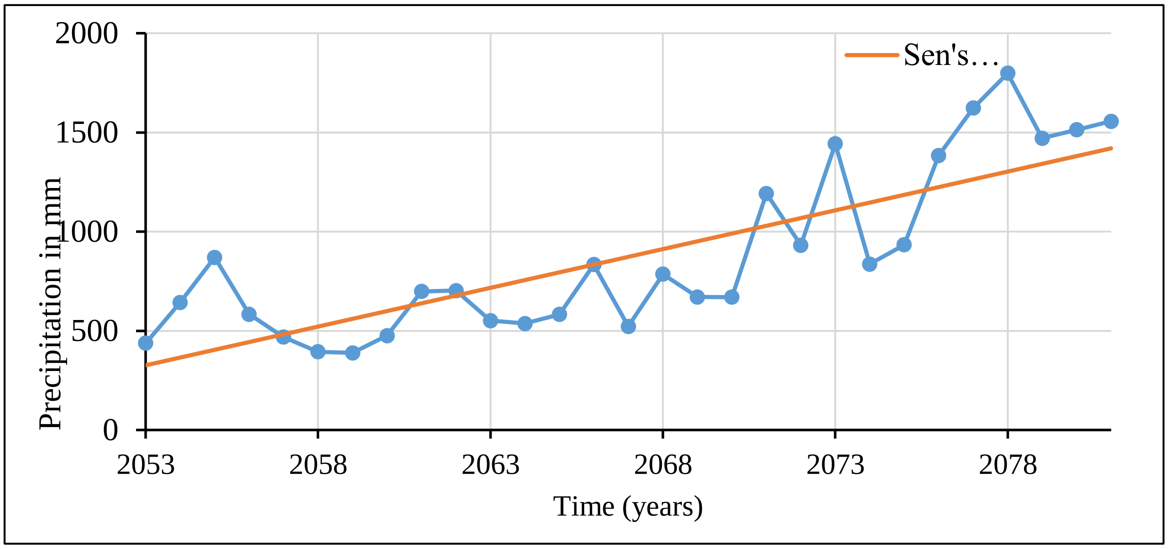

Figure 4.17 Yearly precipitation trends analysis time series for in period (2052-2081) under

Table 4.5 Precipitation trends analysis time series for in period (2052-2081) under RCP4.5

No	Name	$P_{0.05}$	$\lvert Z \rvert$-value	P-value	Sen's slope	New-variance
1	Spring	1.96	4.89	0.000	-3.40	2842
2	Summer	1.96	1.90	0.057	8.46	4322.3
3	Autumn	1.96	3.53	0.0004	34.45	8143.9
4	Winter	1.96	2.04	0.0408	-2.37	2842.0
5	Annually	1.96	3.70	0.0001	34.95	4594.3

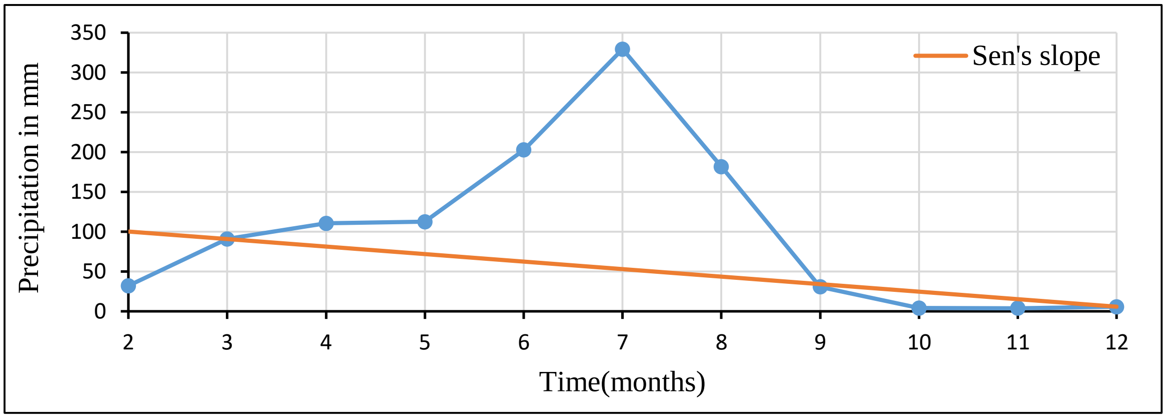

Figure 4.18 Monthly precipitation trends analysis for the period of (2022-2051) under RCP8.5

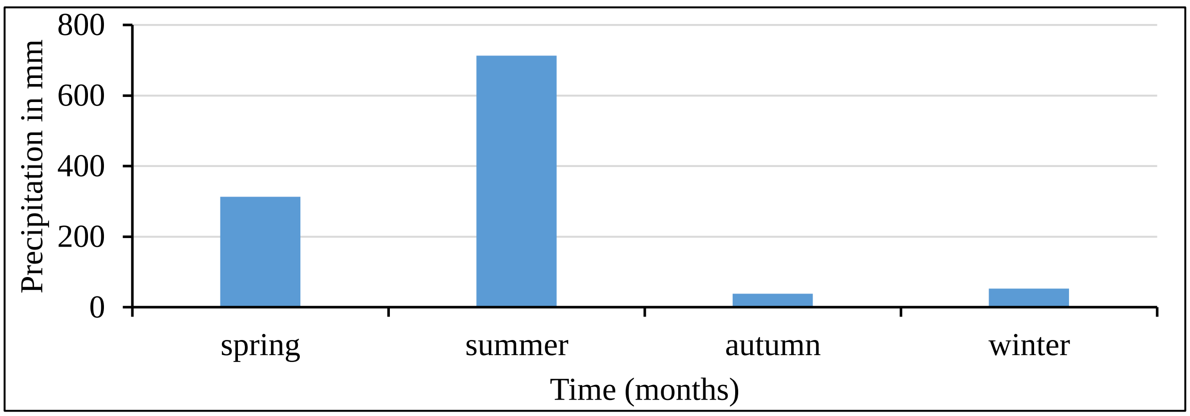

.

Figure 4.19 Seasonal precipitation trends analysis for the period of (2022-2051) under RCP8.5

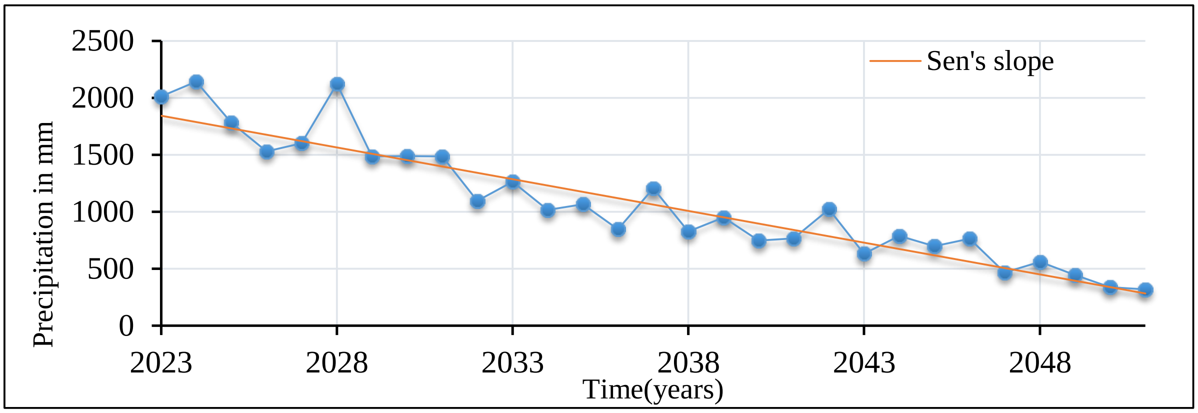

Figure 4.20 Yearly precipitation trends analysis time series for in period (2022-2051) under RCP8.5

Table 4.6 Precipitation trends analysis time series for in period (202-2051) under RCP8.5

No	Name	$P_{0.05}$	$\lvert Z \rvert$-value	P-value	Sen's slope	New-variance
1	Spring	1.96	2.24	0.000	6.9	3141.66
2	Summer	1.96	5.33	0.000	-63.5	4545.5
3	Autumn	1.96	2.28	0.022	-1.55	4428.2
4	Winter	1.96	4.53	0.000	3.17	3141.6
5	Annually	1.96	7.60	0.000	-56.91	2368.85

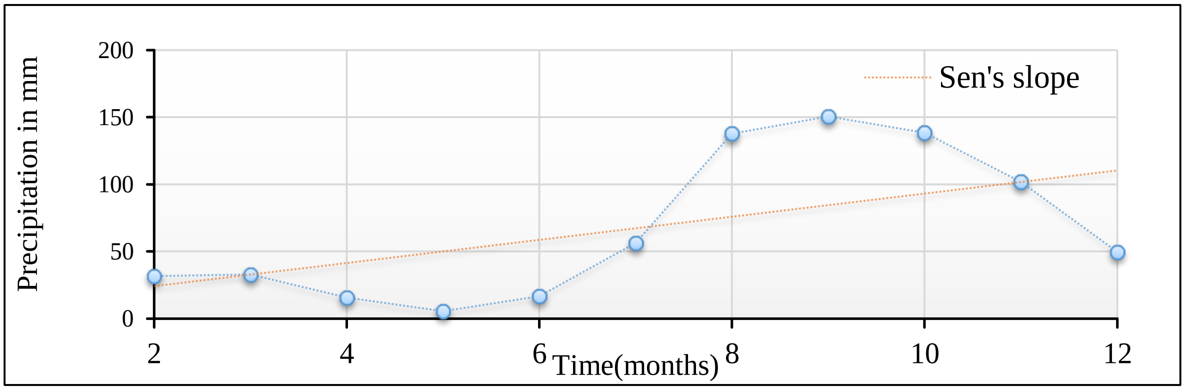

Figure 4.21 Yearly precipitation trends analysis for the period of (2052-2081) under RCP8.5

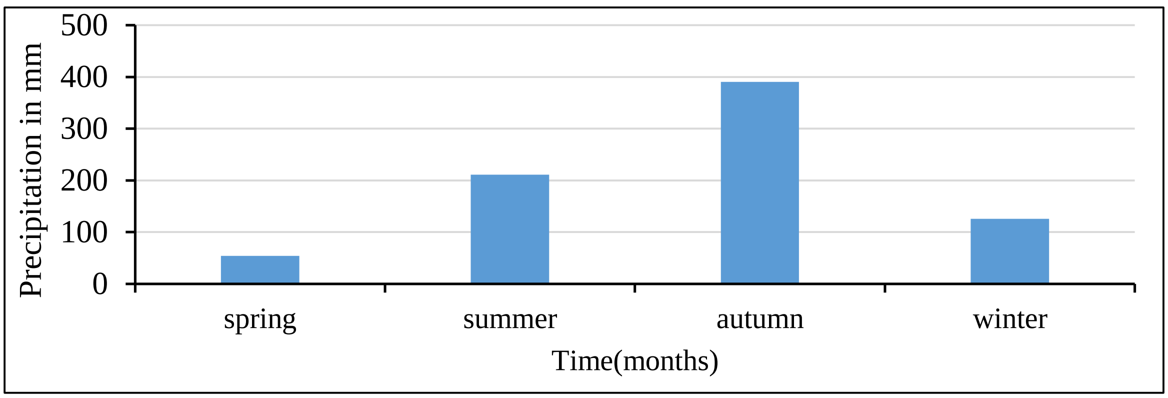

Figure 4.22 Seasonal precipitation trends analysis for the period of (2052-2081) under RCP8.5

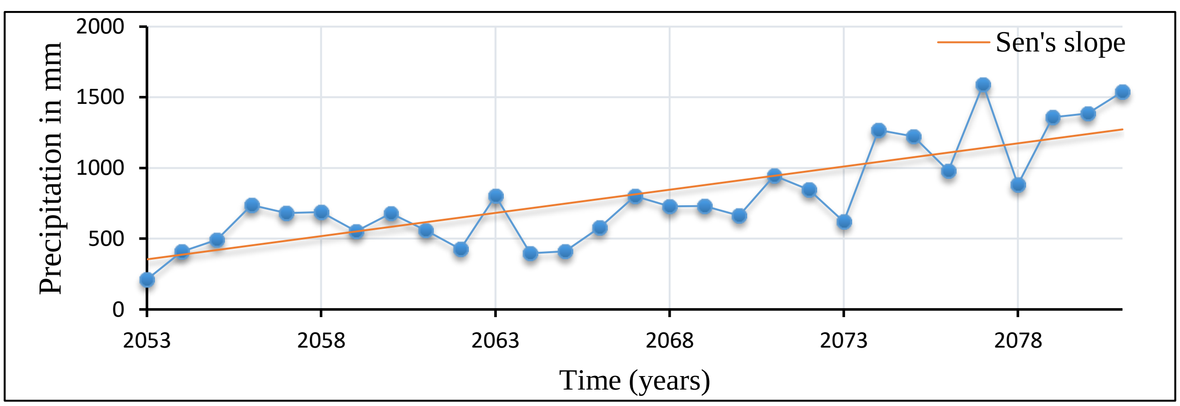

Figure 4.23 Yearly precipitation trends analysis for the period of (2052-2081) under RCP8.5

Table 4.7 Precipitation trends analysis time series for the period of (2052-2081) under RCP8.5

No	Name	$P_{0.05}$	$\lvert Z \rvert$-value	P-value	Sen's slope	New-variance
1	Spring	1.96	2.65	0.007	-3.81	5384.9
2	Summer	1.96	0.99	0.320	3.43	2842.0
3	Autumn	1.96	4.26	0.000	31.12	4985.7
4	Winter	1.96	0.84	0.39	-0.95	3344.6
5	Annually	1.96	4.55	0.000	30.64	2842.0

Table 4.8 The seasonal and annual trends of projected precipitation under (RCPs).

Name	RCP4.5 (2022-2051)	RCP4.5 (2052-2081)	RCP8.5 (2022-2051)	RCP8.5 (2052-2082)
Spring	✓	✓	✓	✓
Summer	✓	χ	✓	χ
Autumn	χ	✓	✓	✓
Winter	✓	✓	✓	χ
Annually	✓	✓	✓	✓

4.5 Impact of Climate Change on Temperature Trends.

Temperature trend analysis was conducted based on the measured data from the watershed area and the projected climate data from the regional climate models under different RCPs. Trend analysis of annual, seasonal, and monthly temperature data was undertaken to detect the variability and trend of temperature change in watershed areas for the future period of (2022-

2081). The future impact of climate change on temperature was done using the projected climate data from RCP4.5 and RCP8.5 scenarios. After the projected climate data was bias-corrected, the projected maximum and minimum temperature was a similar pattern with the observed historical climate data. The bias-corrected of under both of RCPs can be used in future hydrological impact assessment. The future climate data for the two climate variables (maximum and minimum temperature) were graphically plotted to detect the trend. The results show mean monthly increasing and decreasing trend of average minimum and maximum temperature were observed for both RCP4.5 and RCP8.5 all the time but in the summer and autumn season, the maximum temperature was high variation.

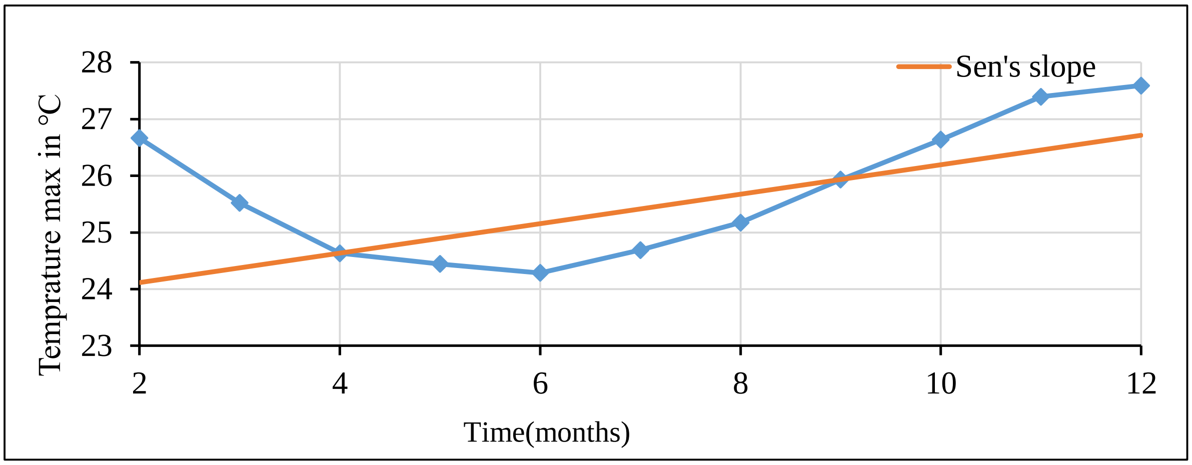

Figure 4.24 Monthly maximum temperature trends analysis for the period of(2022-2051) under RCP4.5

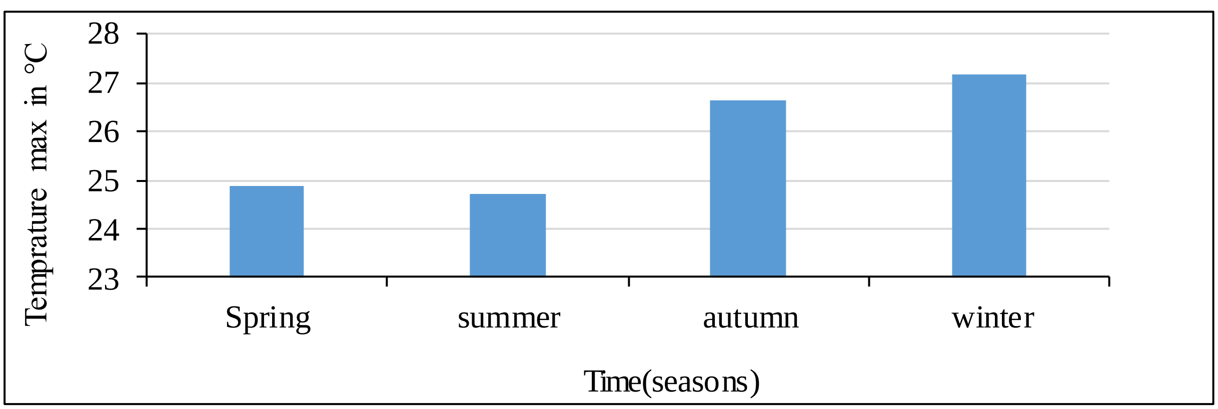

Figure 4.25 Seasonally maximum temperature trends analysis for the period of (2022-2051) under RCP4.5

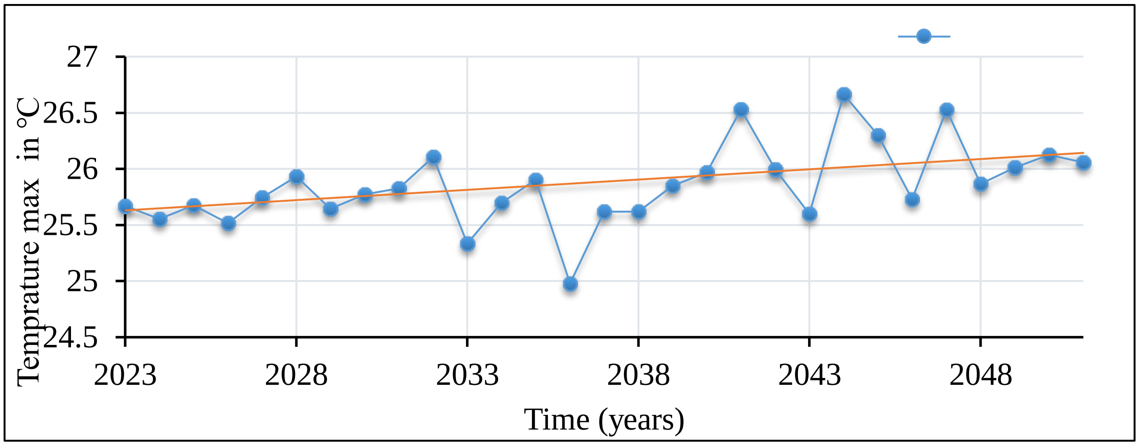

Figure 4.26 Yearly maximum temperature trends analysis for the period of (2022-2051) under RCP4.5

Table 4.9 Maximum temperature trends analysis for the period of (2022-2051) under RCP4.5

No	Name	$P_{0.05}$	$\lvert Z \rvert$-value	p-value	Sen’s slope	variance
1	Spring	1.96	2.77	0.006	-0.09	4458.5
2	Summer	1.96	7.76	0.000	0.112	1583.7
3	Autumn	1.96	5.38	0.000	0.132	3139.6
4	Winter	1.96	2.22	0.023	-0.08	7527.5
5	Annually	1.96	3.14	0.002	0.017	3139.6

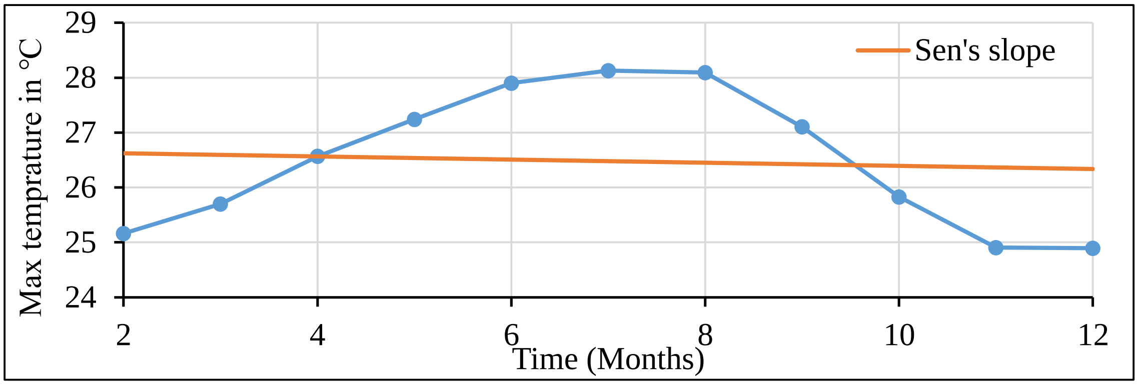

Figure 4.27 Monthly maximum temperature trends analysis for the period of (2052-2081) under RCP4.5

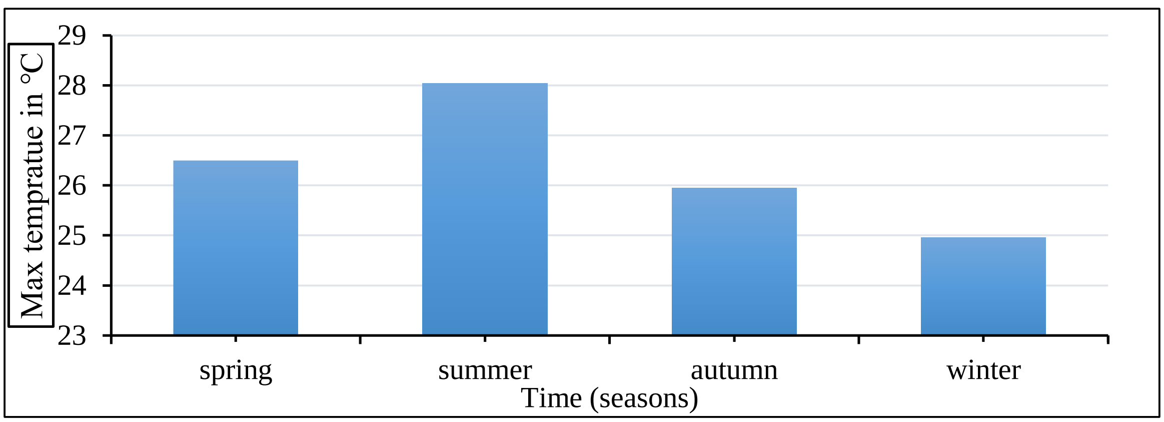

Figure 4.28 Seasonally maximum temperature trends analysis for the period of (2052-2081) under RCP4.5

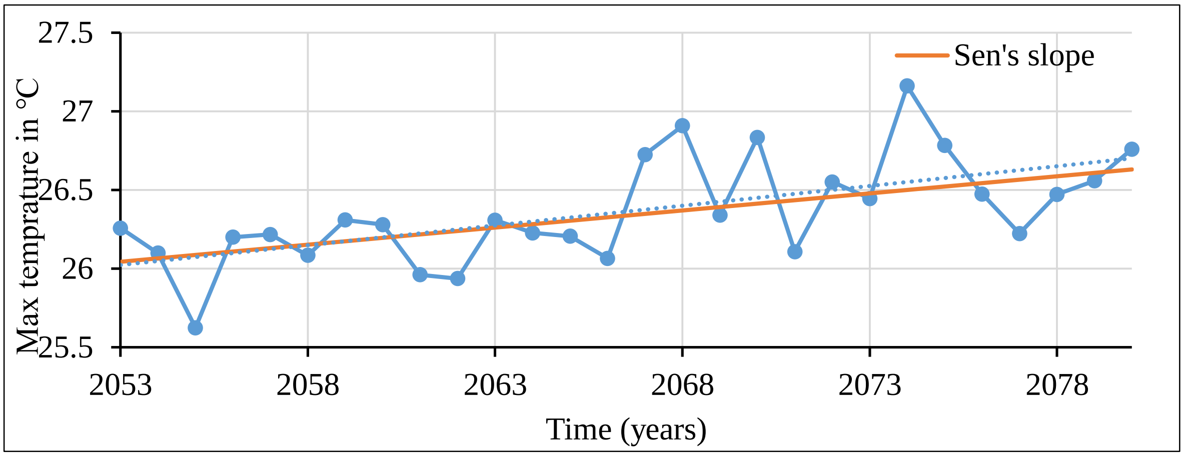

Figure 4.29 Yearly maximum temperature trends analysis time series for in period (2052-2081) under RCP4.5

Table 4.10 Maximum temperature trends analysis for the period of (2052-2081) under RCP4.5

No	Name	$P_{0.05}$	$\lvert Z \rvert$ -value	P-value	Sen's slope	variance
1	Spring	1.96	5.68	0.00	0.16	2842
2	Summer	1.96	0.58	0.56	0.02	6746.9
3	Autumn	1.96	5.51	0.00	-0.15	2841
4	Winter	1.96	3.43	0.006	0.09	2842
5	Annually	1.96	3.40	0.01	0.02	2838

.

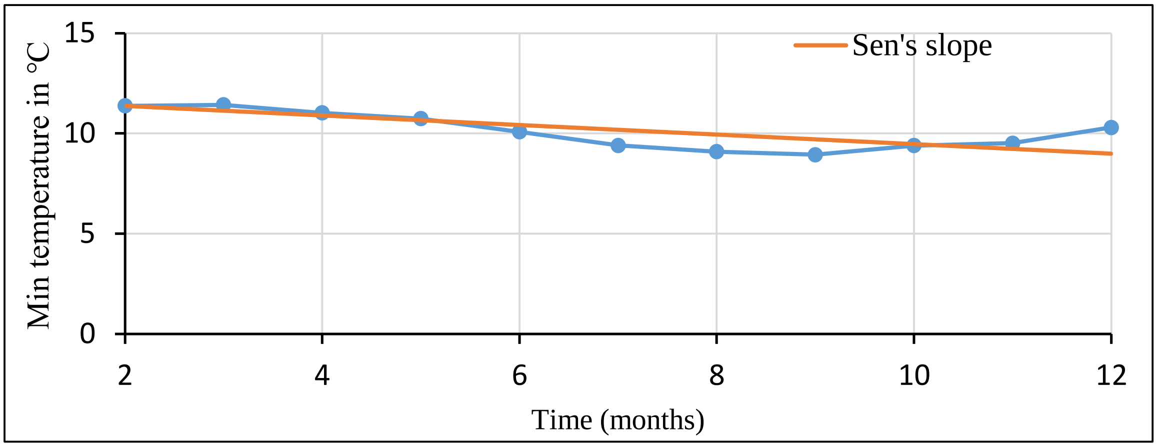

Figure 4.30 Monthly minimum temperature trends analysis for the period of (2022-2051) under RCP4.5

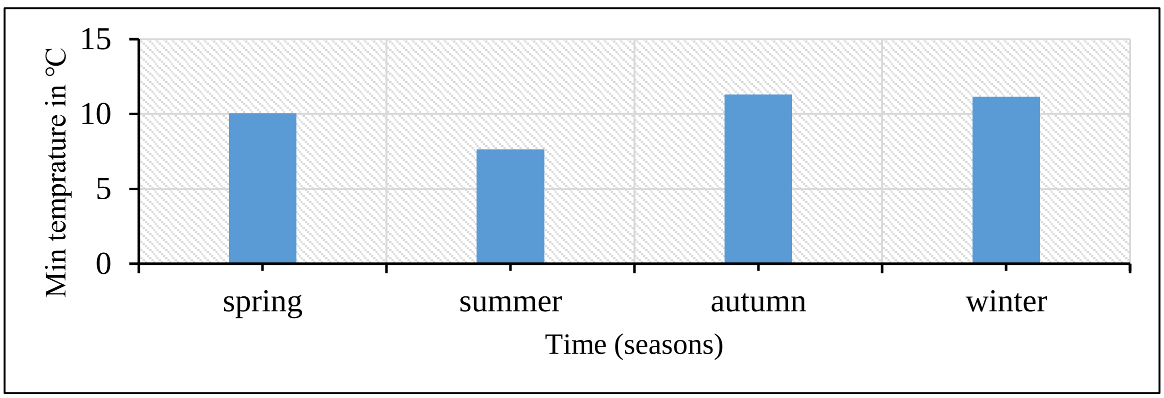

Figure 4.31 Monthly maximum temperature trends analysis for the period of(2022-2051) under RCP4.5

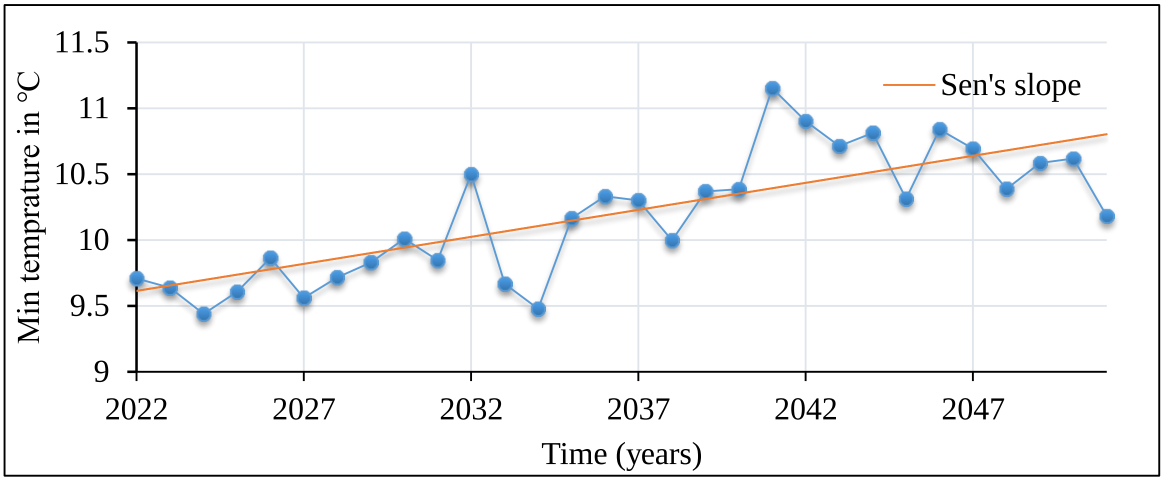

Figure 4.32 Monthly maximum temperature trends analysis for the period of (2022-2051) under RCP4.5

Table 4.11 Minimum temperature trends analysis for the period of (2022-2051) under RCP4.5

No	Name	$P_{0.05}$	$\lvert Z \rvert$-value	p-value	Sen's slope	variance
1	Spring	1.96	0.38	0.70	-0.007	4973.7
2	Summer	1.96	5.50	0.00	-0.085	3138.6
3	Autumn	1.96	5.20	0.002	-0.14	3141
4	Winter	1.96	3.73	0.002	0.117	7286
5	Annually	1.96	5.18	0.00	0.041	2158.5

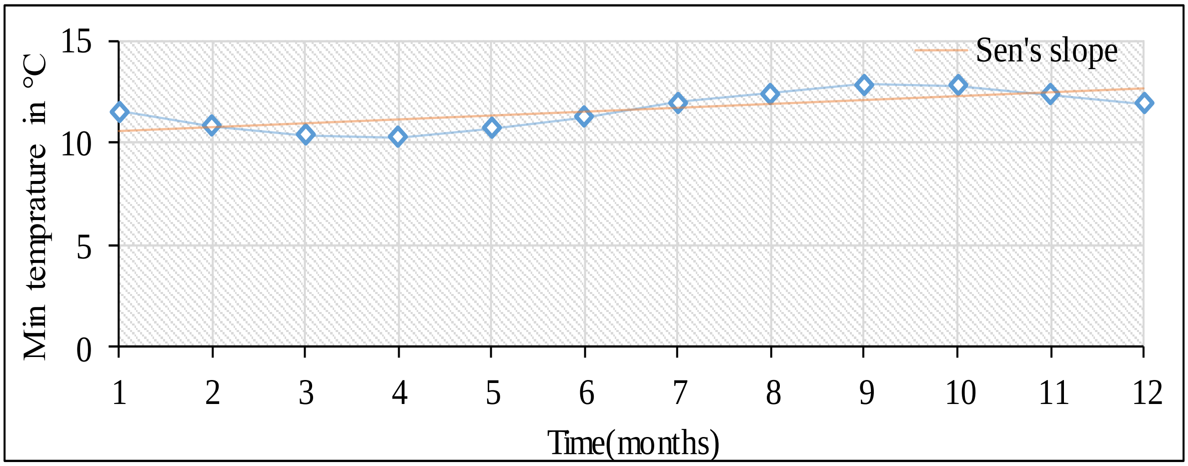

Figure 4.33 Monthly minimum temperature trends analysis time series for in period (2052-2081) under RCP4.5.

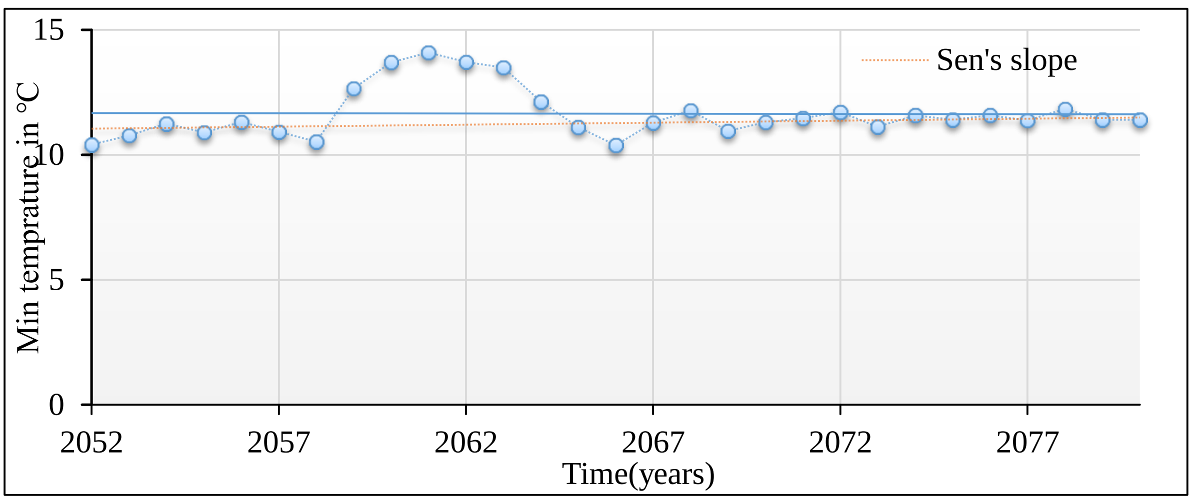

Figure 4.34 Yearly maximum temperature trends analysis for the period of (2052-2081) under RCP4.5

Table 4.12 Minimum temperature trends analysis for the period of (2052-2081) under RCP4.5

No	Name	$P_{0.05}$	$\lvert Z \rvert$ -value	P-value	Sen’s slope	variance
1	Spring	1.96	0.62	0.532	0.026	6165
2	Summer	1.96	2.54	0.011	0.12	4737.3
3	Autumn	1.96	1.2	0.208	-0.016	2842
4	Winter	1.96	3.75	0.0002	-0.108	4918
5	Annually	1.96	1.29	0.19	0.016	2848.

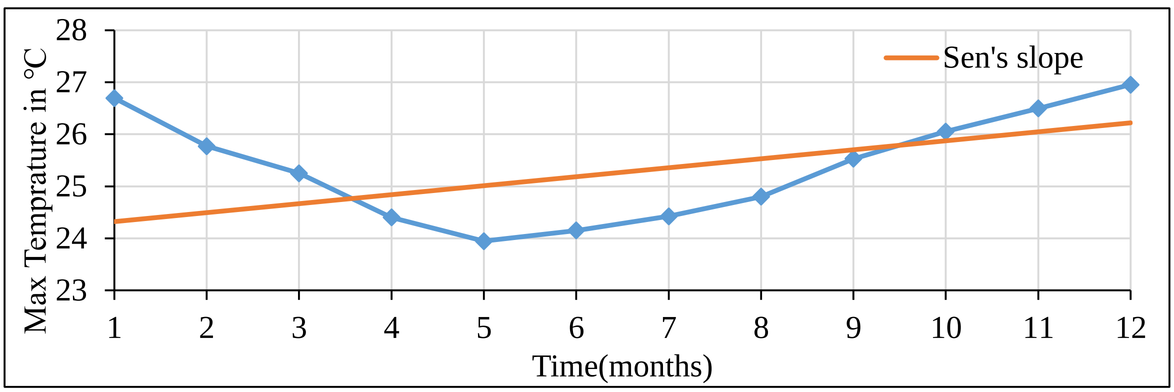

Figure 4.35 Monthly maximum temperature trends analysis time series for in period (2022-2051) under RCP8.5

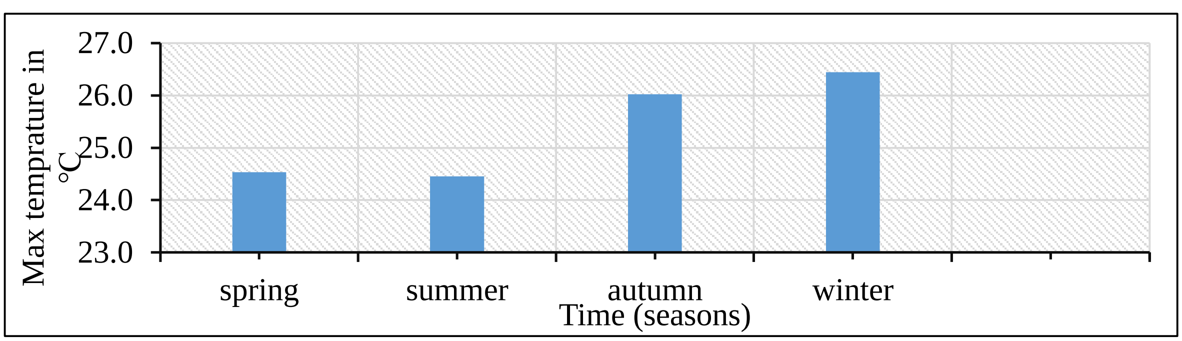

Figure 4.36 Seasonally maximum temperature trends analysis for the period of (2022-2051) under RCP8.5.

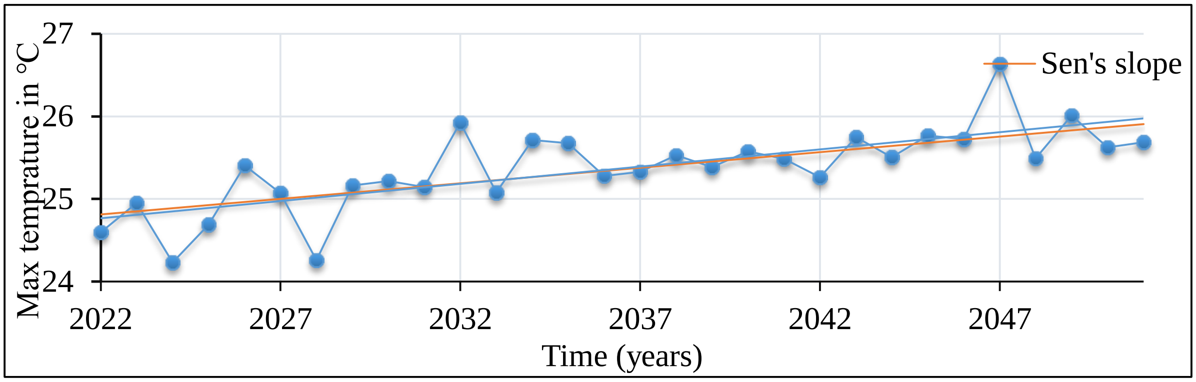

Figure 4.37 Yearly maximum temperature trends analysis for the period of (2022-2051) under RCP8.5

Table 4.13 Maximum temperature trends analysis for the period of (2022-2051) under RCP8.5

No	Name	$P_{0.05}$	$\lvert Z \rvert$ -value	p-value	Sen's slope	variance
1	Spring	1.96	3.71	0.0002	-0.018	3141.6
2	Summer	1.96	5.67	0.000	0.13	3141.6
3	Autumn	1.96	6.10	0.000	0.18	3141.6
4	Winter	1.96	2.14	0.031	-0.108	6135.8
5	Annually	1.96	5.06	0.000	0.038	2382.4

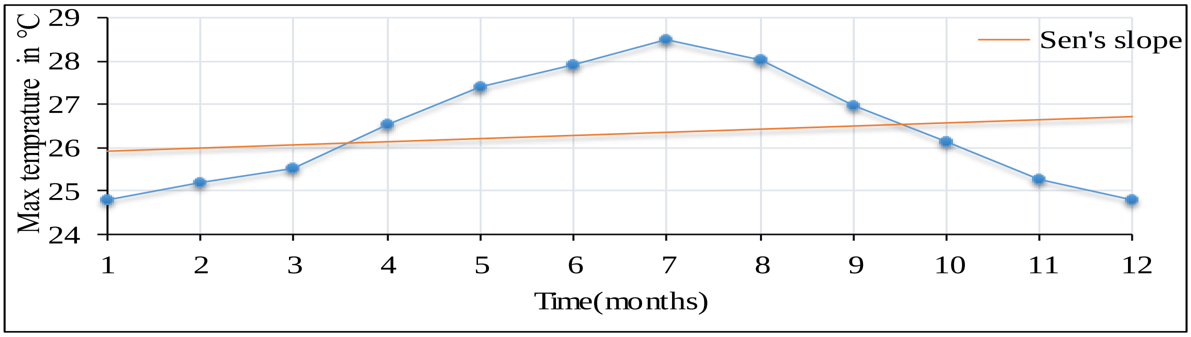

Figure 4.38 Monthly maximum temperature trends analysis for the period of (2052-2081) under RCP8.5

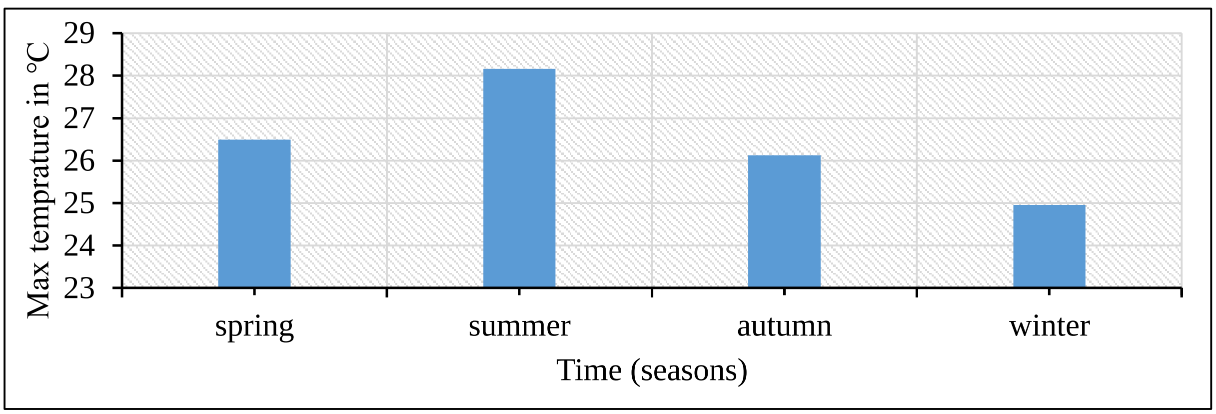

Figure 4.39 Seasonally maximum temperature trends analysis for the period of (2052-2081) under RCP8.5

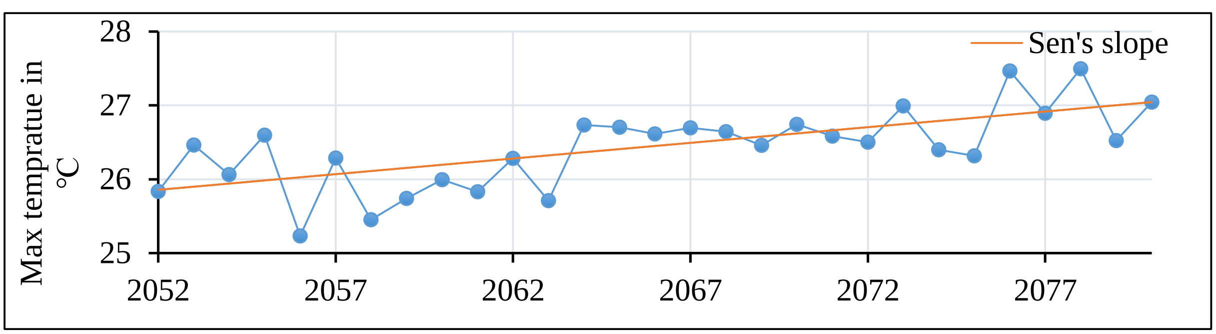

Figure 4.40 Yearly maximum temperature trends analysis for the period of (2052-2081) under RCP8.5

Table 4.14 Maximum temperature trends analysis for the period of (2022-2051) under RCP8.5

No	Name	$P_{0.05}$	$\lvert Z \rvert$ -value	p-value	Sen's slope	variance
1	Spring	1.96	5.57	0.000	0.16	2842
2	Summer	1.96	2.68	0.0072	0.089	5275.4
3	Autumn	1.96	5.08	0.000	-0.123	2842
4	Winter	1.96	3.307	0.001	0.042	1715.6
5	Annually	1.96	3.47	0.005	0.042	2842

The trends analysis is presented in figure 4.38,39,40 and table 4.12. The analysis has been done

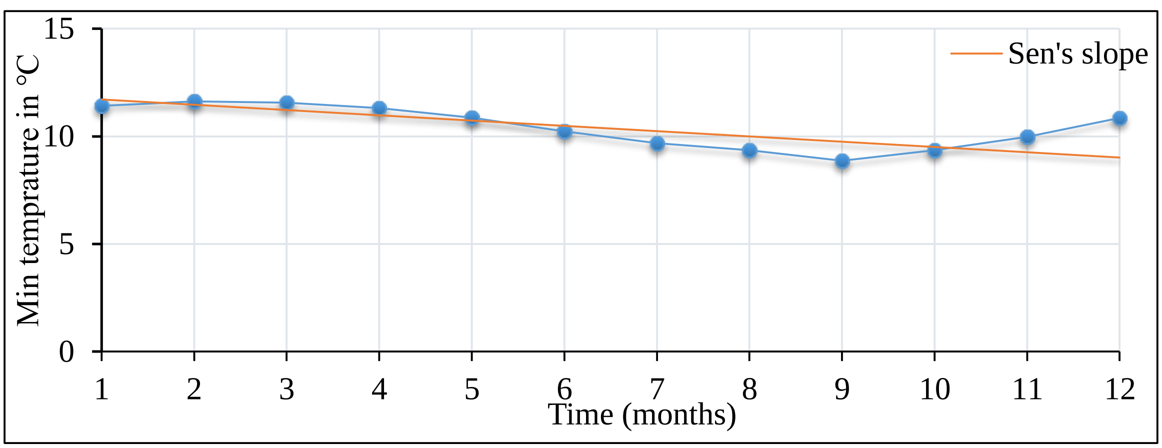

Figure 4.41 Monthly minimum temperature trends analysis time series for in period (2022-2051) under RCP8.5

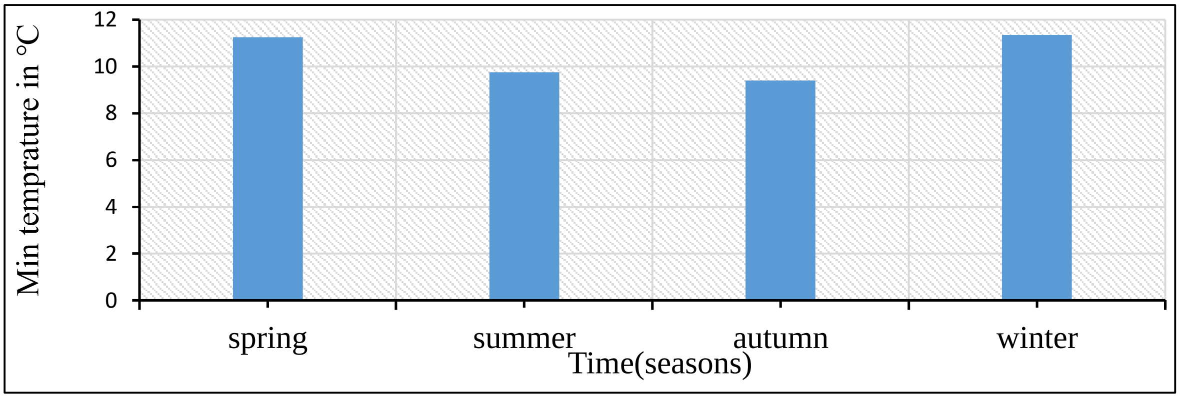

Figure 4.42 Seasonally minimum temperature trends analysis for the period of (2022-2051) under RCP8.5

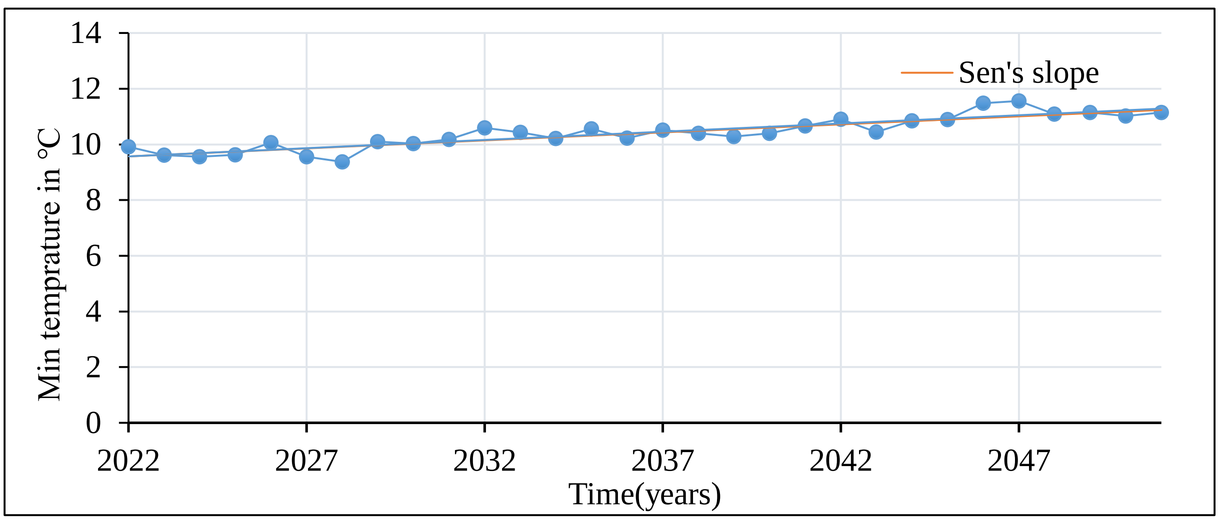

Figure 4.43 Yearly minimum temperature trends analysis for the period of (2022-2051) under RCP4.5

Table 4.15 Minimum temperature trends analysis for the period of (2022-2051) under RCP8.5

No	Name	$P_{0.05}$	$\lvert Z \rvert$	P-value	Sen's slope	variance
1	Spring	1.96	0.46	0.642	-0.004	3137.6
2	Summer	1.96	4.531	0.000	-0.061	3141.6
3	Autumn	1.96	3.22	0.0012	0.123	7891.8
4	Winter	1.96	3.29	0.001	0.123	9625.6
5	Annually	1.96	6.77	0.000	0.057	2257.4

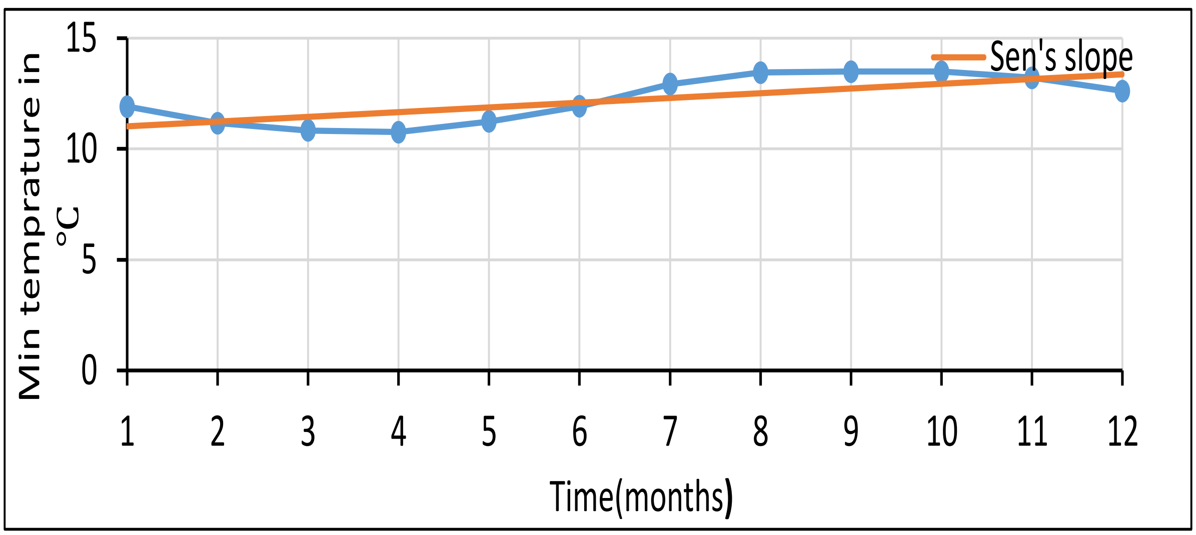

Figure 4.44 Monthly maximum temperature trends analysis for the period of (2052-2081) under RCP4.5

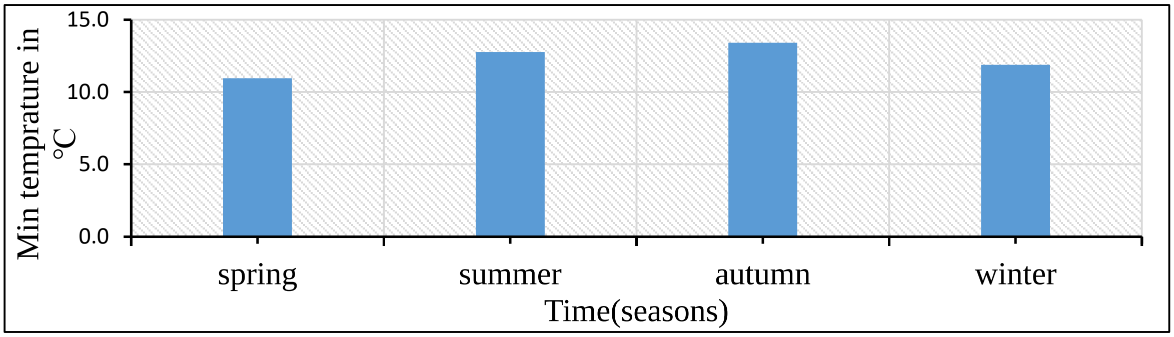

Figure 4.45 Seasonally minimum temperature trends analysis for the period of (2052-2080) under RCP8.5

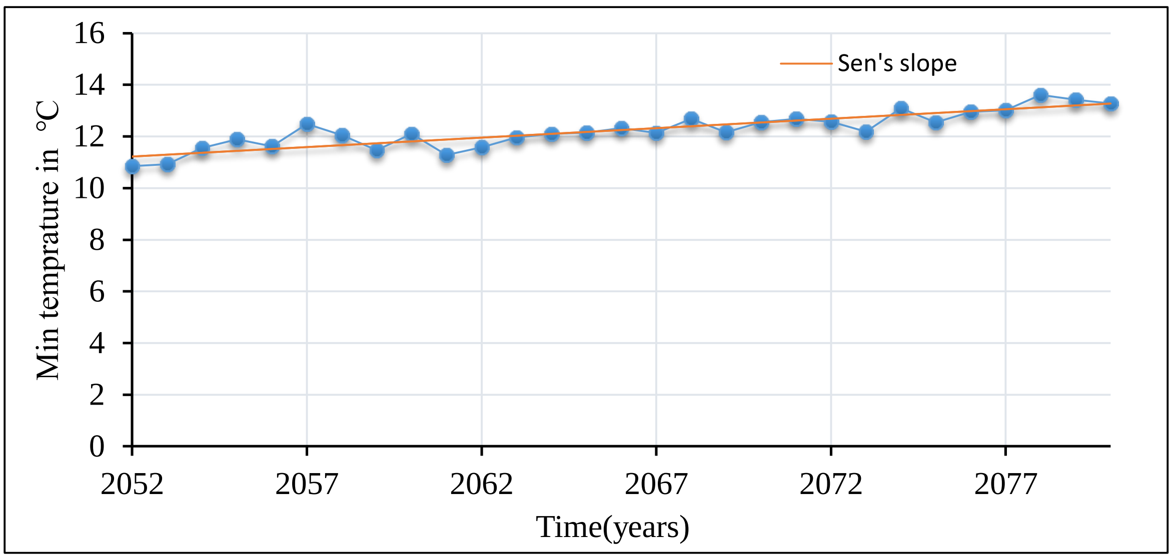

Figure 4.46 Monthly maximum temperature trends analysis time series for in period (2052-2081) under RCP8.5

Table 4.16 Minimum temperature trends analysis for the period of (2052-2081) under RCP8.5

No	Name	$P_{0.05}$	$\lvert Z \rvert$-value	p-value	Sen's slope	variance
1	Spring	1.96	1.97	0.048	0.109	9936.1
2	Summer	1.96	6.2	0.214	0.089	2841.0
3	Autumn	1.96	6.02	0.000	0.032	1014.0
4	Winter	1.96	5.02	0.001	-0.080	2841.0
5	Annual	1.96	7.4	0.000	0.073	1662.1

Table 4.17 The identified trend of maximum temperature was significant or not significant.

Name	RCP4.5 (2022-2051)	RCP4.5 (2052-2081)	RCP8.5 (2022-2051)	RCP8.5 (2052-2082)
Spring	✓	✓	✓	✓
Summer	✓	χ	✓	✓
Autumn	✓	✓	✓	✓
Winter	✓	✓	✓	✓
Annually	✓	✓	✓	✓

Table 4.18 The identified trend of minimum temperature was significant or not significant.

Name	RCP4.5 (2022-2051)	RCP4.5 (2052-2081)	RCP8.5 (2022-2051)	RCP8.5 (2052-2082)
Spring	χ	χ	χ	✓
Summer	✓	✓	✓	✓
Autumn	✓	χ	✓	✓
Winter	✓	✓	✓	✓
Annually	✓	χ	✓	✓

Whereas: χ Are non-significant trends

✓ Significant trends

4.6 Impact of Climate Change on Streamflow

The future impact of climate change on streamflow on mojo watershed was analyzed by comparing baseline river flow with the projected climate data in the future flow due to changes in precipitation, maximum and minimum temperature under RCP 4.5 and RCP 8.5 scenarios using SWAT model. The observed and projected climate data was analyzed. The SWAT model simulates streamflow of the watershed by using the observed data and bias-corrected of the projected climate data as input to hydrological models.

Based on the simulated SWAT result, the streamflow impact of the watershed was analyzed to sixty (60) years projected climate data including the warming up period. The baseline period of (2000-2015) and the future period of (2022 -2051) and (2052 -2081) and the hydrological model re-run for each case period for different scenarios. The observed streamflow of the (2000-2015) period is used as a baseline period against the future period of which the projected climate change impact evaluation. The mean projected volume streamflow is increasing for the period (2022-2051) and (2052-2081) under RCP4.5 scenarios by 55% and 57.06% and RCP8.5 scenarios 55.8% and 58% respectively as compared to baseline source. Also, the projected streamflow shows there was seasonal variation in both scenarios for the period of (2052-2081). The Streamflow of the Upper Awash River change, along with altered precipitation patterns and intensities, are likely to cause significant changes in streamflow volume and timing, attributes that are very important for proper water management and development (Tessema et al., 2020). Hence, future changes in streamflow and watershed hydrology caused by climate change have become increasingly important impressions for water resource management. Warmer and wetter scenarios of the Awash river basin are expected to increase the river discharge substantially and could serve to alleviate current local water shortages (Gedefaw *et al*., 2018) . There are highly seasonal variation of streamflow on the mojo watershed. The result indicate that in summer,spring and winter season the streamflow was increasing under both RCP4.5 and RCP8.5 and autumn season the streamflow decresing under both RCP4.5 and RCP8.5 sceanarios.

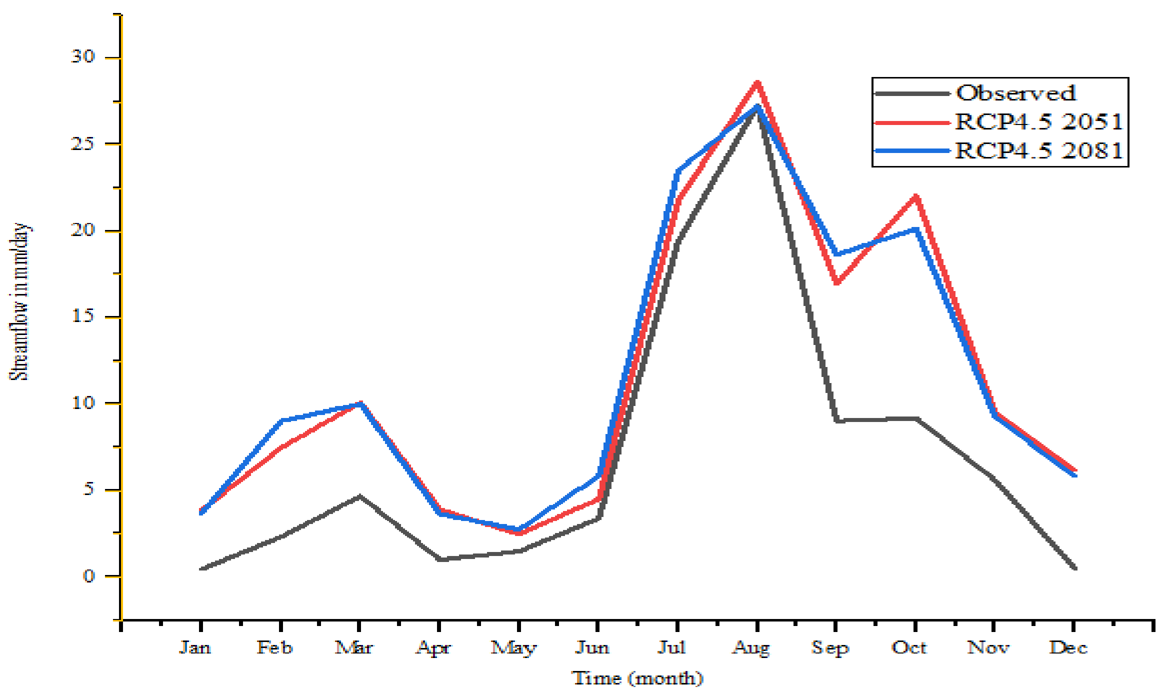

Figure 4.47 Comparison of observed and simulated monthly streamflow under RCP4.5 Scenarios

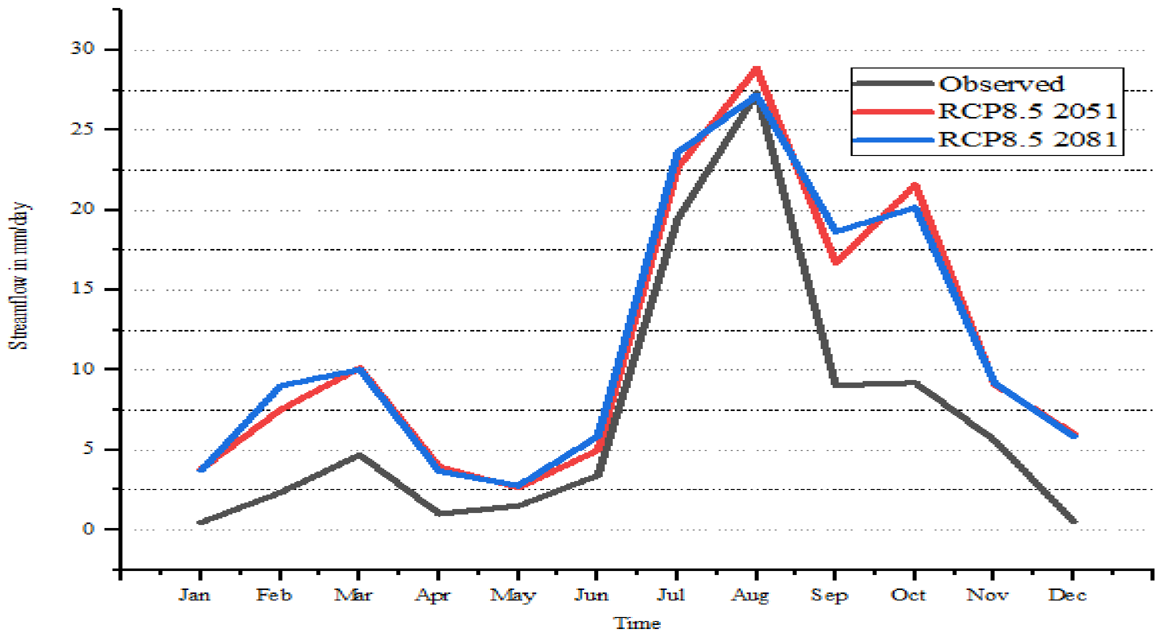

Figure 4.48 Comparison of observed and simulated monthly streamflow under RCP8.5 scenario

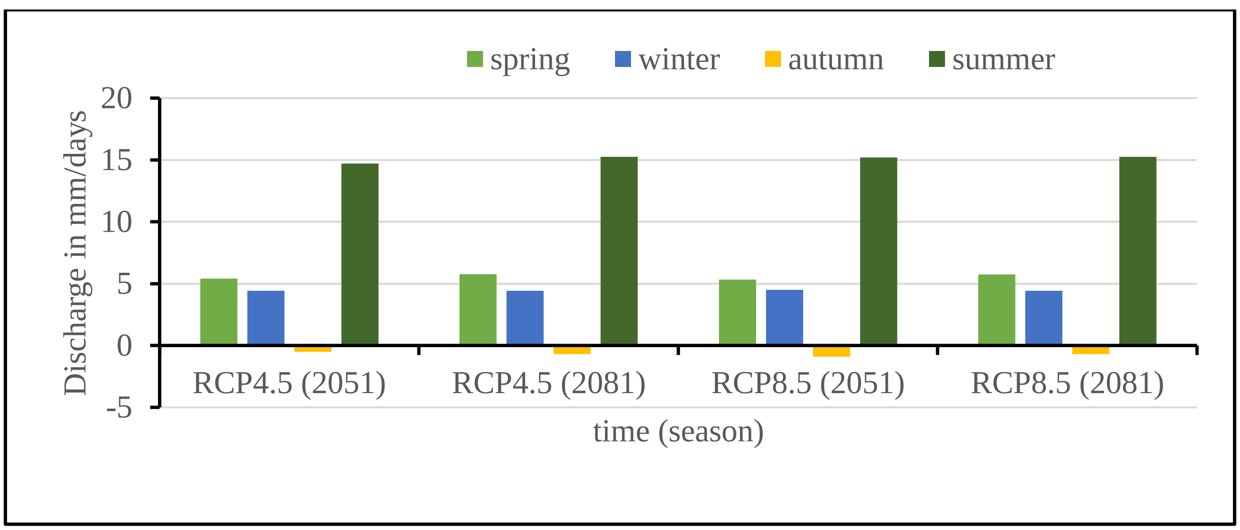

Figure 4.49 Season change streamflow under RCP4.5 and RCP8.5 for diffirent

4.7 Future Impact of Climate Change on Precipitation

Projected precipitation data on the Mojo river watershed indicated that a significant variation of monthly and seasonal as related to annual changes. The existing results displayed the fact that climate change is highly uncertain as the results were varying widely with models. Almost consistent results were obtained on projected temperature and precipitation changes with the models. The projected precipitation will be increasing under both RCP4.5 and RCP8.5 scenarios in the period of (2051). however, there will be high seasonally variation in the period of (2081) in both RCP4.5 and RCP8.5 scenarios. Compared to the baseline period the models indicate the total seasonal and annually projected precipitation show will be increasing in the period of (2051) compared to this period (2081) the projected under the RCP4.5 and RCP8.5 scenarios. For the period of (2081), the climate models projected precipitation will decrease in all seasons of the year except for the autumn and spring season under RCP4.5 and RCP8.5 scenarios. In the upper Blue Nile basin, which generates 43% of the country's total average runoff, climate change is projected to increase precipitation and streamflow by 7% to 48% and 21% to 97%, respectively, at end of the twenty-first century (Roth *et al*.,2018). Also, climate projections indicate that there will be a likely increase in rainfall amount extreme rainfall in the region by the 21st century (Bekele,2021).

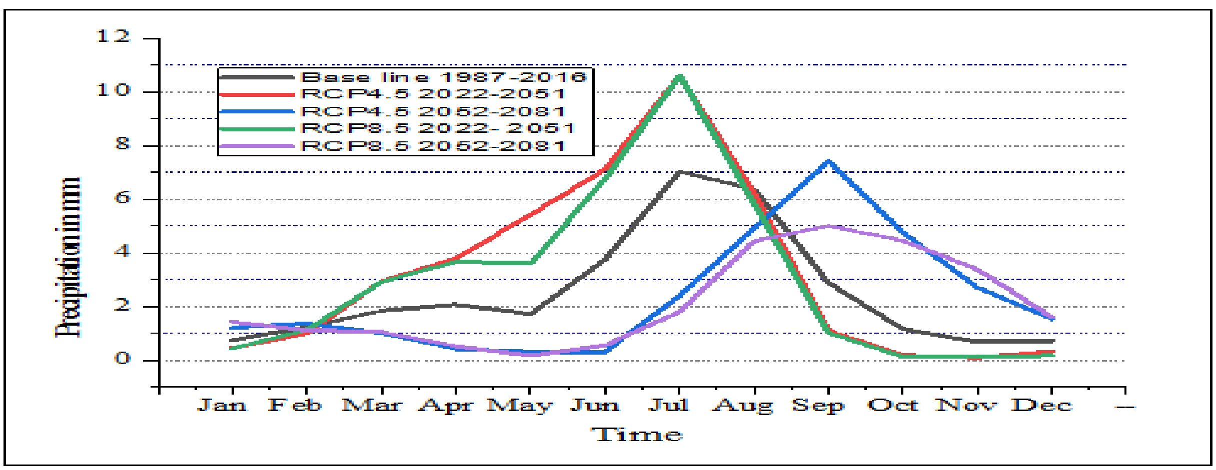

Figure 4.50 Comparison of the area means monthly precipitation of baseline period (1987-2016) and future (2051) and (2081) under two scenarios RCP4.5 and RCP8.5

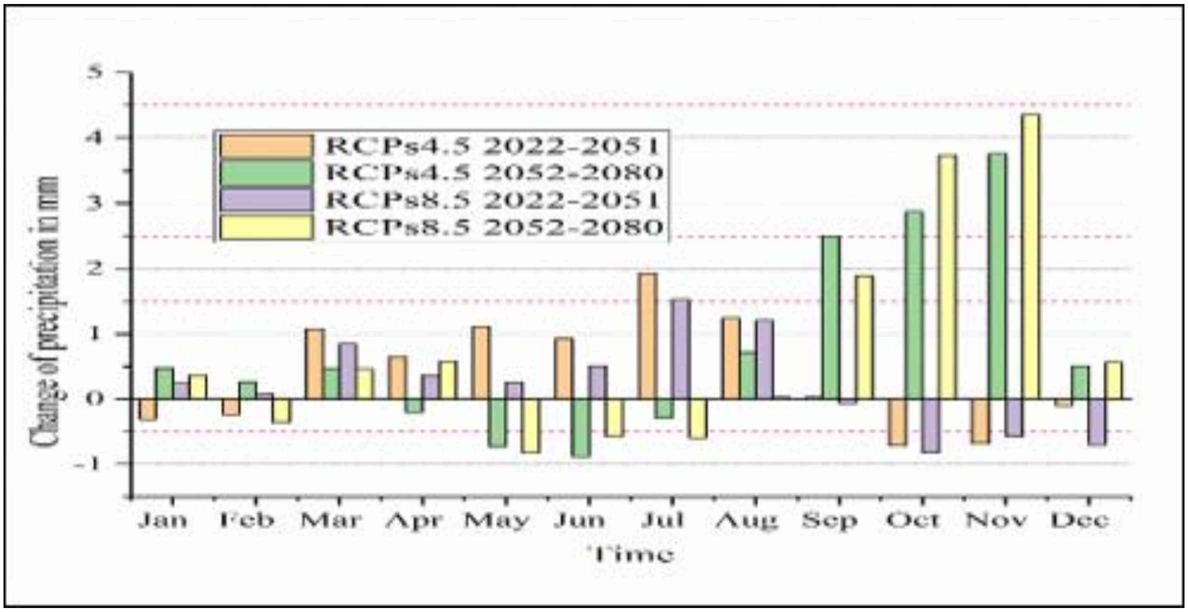

Figure 4.51 Change of mean monthly precipitation for a future (2051) and (2081) under two scenarios RCP4.5 and RCP8.5

Table 4.19 Average change of seasonally and annually precipitation under RCP4.5 and RCP8.5 scenarios

Name	RCP4.5 (2051)	RCP4.5 (2081)	RCP8.5(2051)	RCP8.5 (2082)
Spring	2.18	-1.3	1.5	-1.3
Summer	2.26	-3.0	2.0	-3.4
Autumn	-0.31	2.0	-1.15	0.8
Winter	-1.1	0.47	- 0.3	2.7
Annually	42%	32%	32.2%	27%

4.8 Future Impact of Climate Change on Temperature

For the mojo river watershed area, the overall maximum temperature showed that there is an increasing trend in both RCP4.5 and RCP8.5. The mean annual maximum temperature in the future period (2052) to (2081) will be increased by 0.14℃ and 0.7℃ under RCP4.5 and 0.4℃ and 1.3℃ under RCP8.5 scenarios respectively. Increasing maximum temperature showed more variation at the monthly and seasonal than annually. According to climate model predictors, using several scenarios of greenhouse gas emissions, the global mean temperature probably will increase from 1.1 to 6.4℃ in the next 100 years (IPCC,2007) (Kerim *et al.*, 2016).

Future temperature predictions show that both maximum and minimum temperature increase in magnitude and intensity in Addis Ababa up to the end of the 21st century (Feyissa, 2018). Temperature minimum shows a significantly increasing trend across all Wolaita Zone in Southern Nations and Nationalities People (SNNP) region, but Temperature maximum has revealed both increasing and decreasing trends (Esayas *et al*., 2019).

Table 4.20 Average yearly max and min temperature projected under both scenarios

No	Description	Year	Rcp4.5	Rcp8.5
1	Temp maximum	2051	0.14	0.4
2	Temp maximum	2081	0.7	1.3
3	Temp minimum	2051	-1.1	-0.7
4	Temp minimum	2081	1.3	1.3

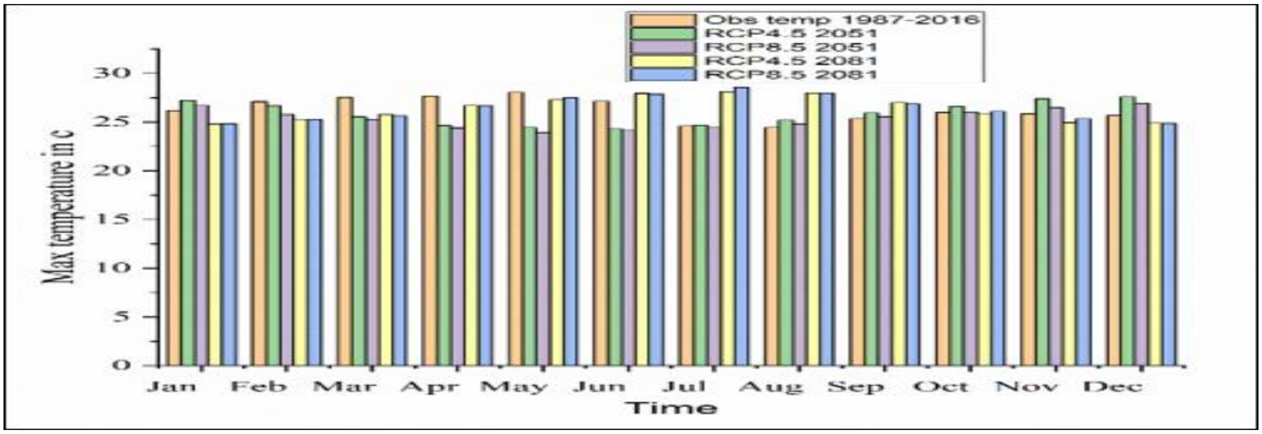

Figure 4.52 Comparison of the mean maximum temperature of the baseline period with future results of RCP4.5 and RCP8.5 scenarios

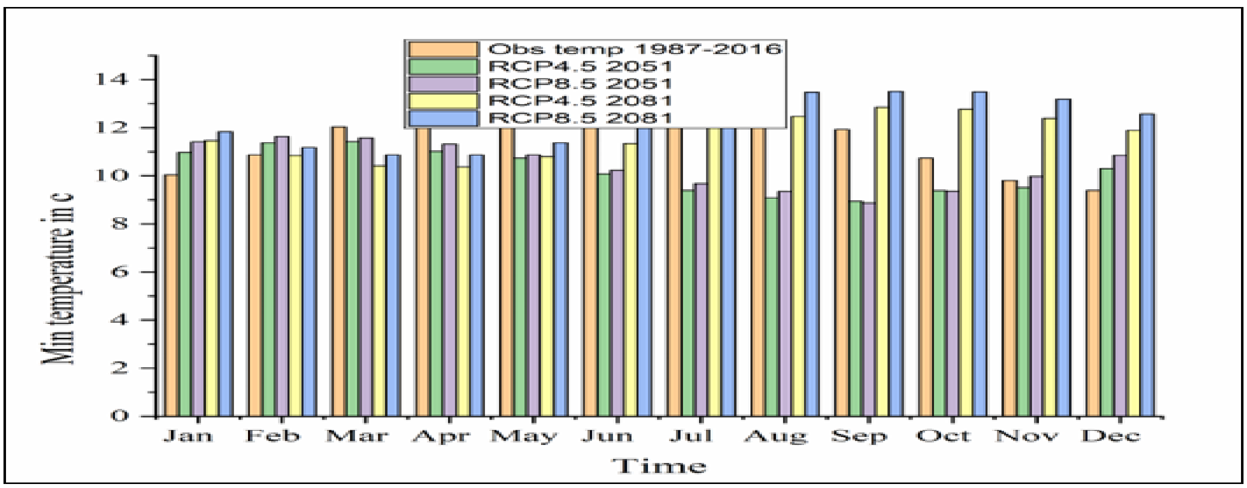

Figure 4.53 Comparison of the mean minimum temperature of the baseline period with future results of RCP4.5 and RCP8.5 scenarios

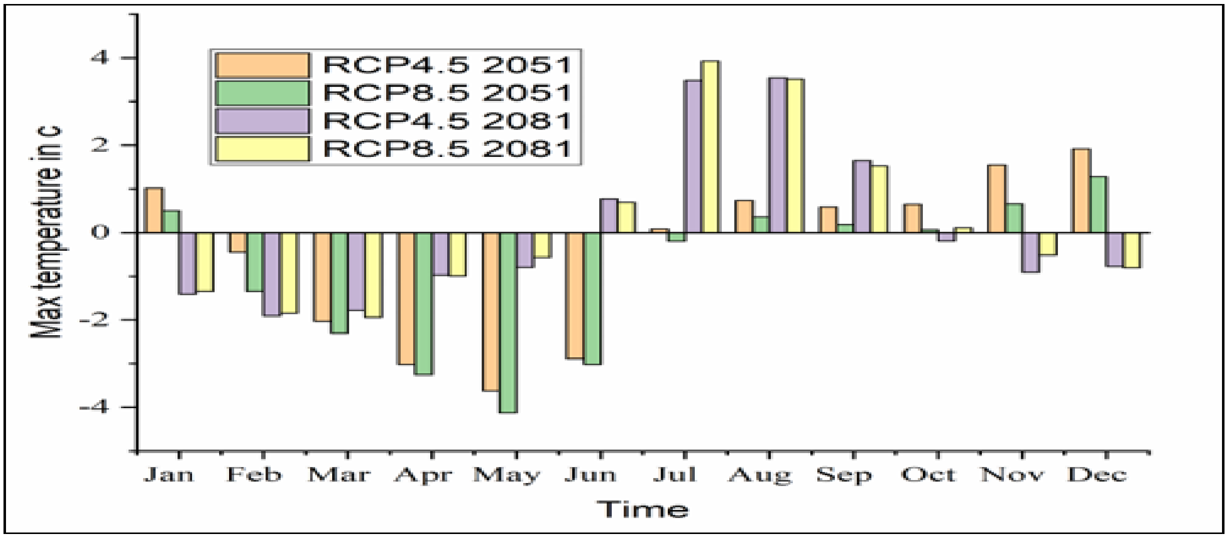

Figure 4.54. Change of mean monthly maximum temperature for a future (2051) and (2081) under two scenarios RCP4.5 and RCP8.5.

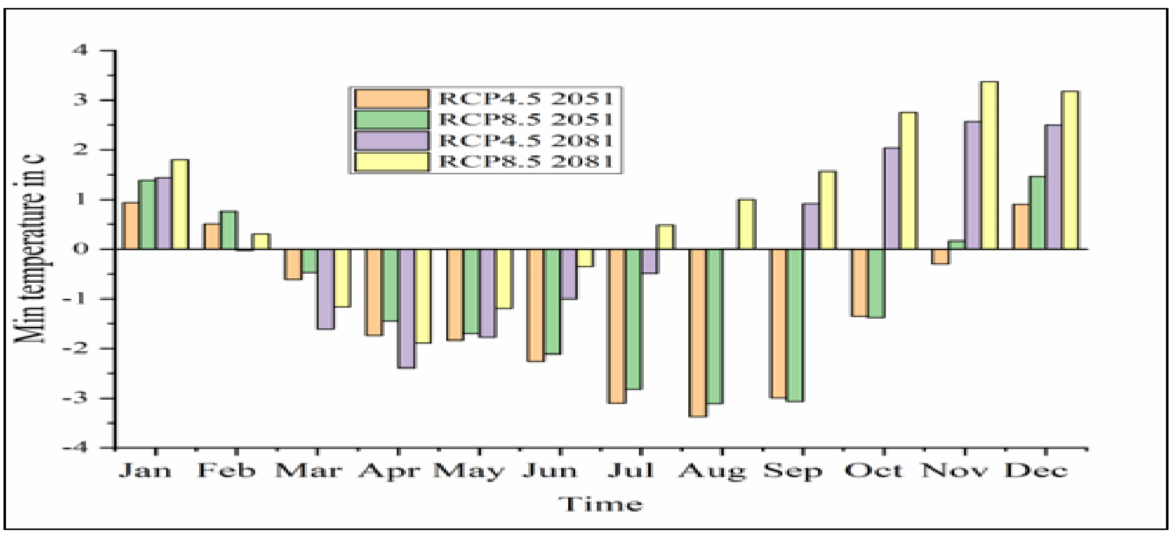

Figure 4.55 Change of mean monthly minimum temperature for a future (2051) and (2081) under two scenarios RCP4.5 and RCP8.5

5 CONCLUSION

The purpose of this thesis was to evaluate the impact of climate change on the streamflow of Mojo River using the SWAT model. Those RCMs (CCLM4-8, RAC4, and RAMCO22T) were used for performance evaluation. RAMCO22T model was the well-performed model among RCMs. The climate data were bias-corrected with power transformation and various scale methods. The SWAT model simulated with 30 years observed and 60 years of climate data under rcp4.5 and rcp8.5. The model was successfully calibrated and validated for the future period of (2000-2009) and (2010-2015) respectively excluding three (3) year warming up period every month of flow using SWAT CUP.SUFI-2 algorithms. During calibration of the streamflow, the sensitive parameters which were highly influenced by the results were identified using global sensitivity analysis. The results obtained from this study were shown that proper calibration of the SWAT model is appropriate for hydrology and impact assessment modeling at the watershed to minimize manual measurement that took place in the watershed.

The SWAT model performance was checked by using correlation coefficient (R^2), Nash–Sutcliffe simulation efficiency (ENS), PBIAS with value of 0.71,0.70, and -13.9 for calibration respectively and R^2, NSE, and PBIAS with value 0.70,0.66, and -4.7 for validation respectively. The trend time series was done using modified Mann-Kendall, Mann-Kendall, and sen’s slope for, precipitation and temperature under RCP4.5 and RCP8.5. The average yearly precipitation and temperature will significantly be increasing in (2022-2051) period in both scenarios and high seasonal variation in (2052-2081) period. The mean annual maximum temperature in the future period (2052) and (2081) will be increased by 0.14℃ and 0.7℃ under RCP4.5 and 0.4℃ and 1.3℃ under RCP8.5 scenarios respectively. While Minimum temperatures were decreasing in by (-1.1 and -0.7) for a future period (2051) and increased by (1.3 and 1.3) for the period of (2081) under both scenarios RCP4.5 and RCP8.5 respectively. Annual rainfall projected will be increase by 42% and 32% in the future period of (2051) and 32.9% and 27.1% of the future of (2081) under RCP4.5 and RCP8.5 scenarios respectively. The streamflow will be increased annually by 55% and 57.07% under RCP4.5 and 55.8% and 58% under RCP8.5 with the future period of (2051) and (2081) respectively.

6 RECOMMENDATION

Detailed climate models and long hydrological records are needed to predict future conditions in a changing world [Bayazit,2015]. The bias-corrected means of GCMs data using RCP4.5 and RCP8.5 were given as an input to the SWAT model for the periods of, 2051s, and 2081s. The remaining climatic and all other land use and soil hydrologic properties used in model development under current climate conditions were assumed to be constant and remain valid under conditions of future climate change. There is no consideration of changes in land use, soil properties, and other climatic variables, which could influence the hydrology of the basin. The assumption of stationarity, which has been made so far in runoff and streamflow forecasts studies, is now being challenged. Such a study should not be considered as actual accurate scenarios because the latter would need to include future soil and land-use change impact.

The outcome of this study is based on a single GCM with three RCMS under two (RCPs) scenarios, however, it is often recommended to apply different GCMs and concerning different RCMs to make the comparison between different models as well as to explore a wide range of climate change scenarios that would result in different hydrological impact.

The outcome of this study was statically performance of three RCMs was done, however, it is recommended to apply the performance of the RCMs with the simulation of all models to identify the most suitable model over the watershed.

The final result obtained from this study was addressed that the watershed exists under the climate change impact and also high variability of seasonal precipitation. Therefore decision-makers and stakeholders should minimize the sensitivity to climate change by climate policies and develop the sustainability of the watershed.

REFERENCES

Abera, F., 2011. *Assessment of Climate Change Impacts on the Hydrology of Upper Guder Catchment, Upper Blue Nile* (Doctoral dissertation, Msc. Thesis).

Addisu, S., Selassie, Y.G., Fissha, G. and Gedif, B., 2015. Time series trend analysis of temperature and rainfall in lake Tana Sub-basin, Ethiopia. *Environmental Systems Research*, *4*(1), pp.1-12.

Airey, M., & Hulme, M. (1995). Evaluating climate model simulations of precipitation: Methods, problems and performance. Progress in Physical Geography, 19(4), 427–448.

Akoko, G., Le, T.H., Gomi, T. and Kato, T., 2021. A Review of SWAT Model Application in Africa. *Water*, *13*(9), p.1313.

Al, E. E. T., Anitz, R. P., & Atthias, M. B. U. (2013). Assessment of the Performance of CORDEX Regional Climate Models in Simulating East African Rainfall.

Alemu, Z. A., & Dioha, M. O. (2020). Climate change and trend analysis of temperature: the case of Addis Ababa, Ethiopia. Environmental Systems Research, 9(1).

Amin, A., & Nuru, N. (2020). Evaluation of the Performance of SWAT Model to Simulate Stream Flow of Mojo River Watershed : In the Upper Awash River Basin , in Ethiopia. 8(1), 7–18.

Asare-nuamah, P., & Botchway, E. (2019). Heliyon Understanding climate variability and change : analysis of temperature and rainfall across agroecological zones in Ghana. Heliyon, 5(October), e02654.

Basin, A. (2018). Climate Change Impact on Water Resources in the Awash Basin, Ethiopia. 1–16.

Bates, B., Kundzewicz, Z. W., Wu, S., Burkett, V., Doell, P., Gwary, D., Hanson, C., Heij, B., Jiménez, B., Kaser, G., Kitoh, A., Kovats, S., Kumar, P., Magadza, C. H. D., Martino, D., Mata, L., Medany, M., Miller, K., & Arnell, N. (2008). Climate Change and Water. Technical Paper of the Intergovernmental Panel on Climate Change.

Bewket, W., Radeny, M., & Mungai, C. (n.d.). Agricultural Adaptation and Institutional Responses to Climate Change Vulnerability in Ethiopia. 106.

Beyer, R., Krapp, M., & Manica, A. (2020). An empirical evaluation of bias correction methods for palaeoclimate simulations. 1493–1508.

Birara, H., Pandey, R. P., & Mishra, S. K. (2018). Trend and variability analysis of rainfall and temperature in the tana basin region, Ethiopia. Journal of Water and Climate Change, 9(3), 555–569.

Biru, Z., & Kumar, D. (2018). Calibration and validation of SWAT model using stream flow and sediment load for Mojo watershed , Ethiopia. Sustainable Water Resources Management, 4(4), 937–949.

Bodian, A., Dezetter, A., Diop, L., Deme, A., Djaman, K., & Diop, A. (2018). Future climate change impacts on streamflows of Two Main West Africa River Basins: Senegal and Gambia. Hydrology, 5(1).

Capdevila, J., Sevilla, I., Alonso, V., Aparicio, L. A., Fonseca, P. J., Grande, E., Reina, J. J., Manzano, J. L., Domingo, J., Lájara, A., Barriuso, J., & Castellano, D. (2015). Evaluation of the efficacy and safety of lanreotide in combination with targeted therapies in patients with neuroendocrine tumours in clinical practice : a retrospective cross-sectional analysis. BMC Cancer, 1–11.

Carter, R. C., Parker, A., Carter, R. C., & Parker, A. (2016). Climate change , population trends and groundwater in Africa Climate change , population trends and groundwater in Africa. 6667(June).

Conway, D., & Schipper, E. L. F. (2011). Adaptation to climate change in Africa: Challenges and opportunities identified from Ethiopia. Global Environmental Change, 21(1), 227–237.

Dervis, K. (2007). Devastating for the World's Poor. UN Chronicle Online Edition, 1–4.

Dessu, S. B., & Melesse, A. M. (2013). Impact and uncertainties of climate change on the hydrology of the Mara River basin , Kenya / Tanzania. 2986(June 2012), 2973–2986.

Dibaba, W. T., Miegel, K., & Demissie, T. A. (2019). Evaluation of the CORDEX regional climate models performance in simulating climate conditions of two catchments in Upper Blue Nile Basin. Dynamics of Atmospheres and Oceans, 87, 101104.

Esayas, B., Simane, B., Teferi, E., Ongoma, V., & Tefera, N. (2019). Climate Variability and Farmers ' Perception in Southern Ethiopia. 2019.

FAO. (2016). Country Profile – Ethiopia. Food and Agriculture Organization of the United Nations (FAO). Rome, Italy. FAO,AQUSAT Reports, 11–12.

Fekadu, G., Zelalem, B., Gonfa, B., & Mamo, G. (2019). Impacts of climate change on stream flow and water availability in Anger sub - basin , Nile Basin of Ethiopia. Sustainable Water Resources Management, 5(4), 1755–1764.

Feyissa, G. (2018). Downscaling of Future Temperature and Precipitation Extremes in Addis Ababa under Climate Change. https://doi.org/10.3390/cli6030058

Gedefaw, M., Wang, H., Yan, D., Song, X., Yan, D., Dong, G., Wang, J., Girma, A., Ali, B. A., Batsuren, D., Abiyu, A., & Qin, T. (2018). Trend Analysis of Climatic and Hydrological Variables in the Awash River Basin ,Ethiopia. 1–14.

Group, T. C. (2018). SWAT Model Setup , Calibration , and Validation for the Upper Fox-Wolf Basins TMDL.

Gudu, F., Chala, T., & Sime, H. (2020). Stream flow modeling using SWAT model and the model performance evaluation in Toba sub - watershed , Ethiopia. Modeling Earth Systems and Environment, 0123456789.

Gurara, M. A., Jilo, N. B., & Tolche, A. D. (2021). Modelling climate change impact on the streamflow in the Upper Wabe Bridge watershed in Wabe Shebele River Basin, Ethiopia. International Journal of River Basin Management, 0 (0), 1–13.

Gutowski, W. J., Giorgi, F., Timbal, B., Frigon, A., Jacob, D., Krishnan, R., Lee, B., Lennard, C., Nikulin, G., & Rourke, E. O. (2016). WCRP Coordinated Reginal Downscaling Experiment (CORDEX): A Diagnostic MIP for CMIP6. 1–16.

Ibe, G.O. and Amikuzuno, J., 2019. Climate change in Sub-Saharan Africa: A menace to agricultural productivity and ecological protection. Journal of Applied Sciences and Environmental Management, 23(2), pp.329-335.

Ilori, O.W. and Ajayi, V.O., 2020. Change detection and trend analysis of future temperature and rainfall over West Africa. Earth Systems and Environment, 4(3), pp.493-512.

Kaluarachchi, J., & Smakhtin, V. (2008). Climate Change Impacts on Hydrology and Water Resources of the Upper Blue Nile River Basin, Ethiopia (Issue January 2014).

Kefeni, K., Dessalegn, T., & Roba, N. (2019). Evaluation of Climate Change Impact on Stream Flow in Upper Awash River Basin, Ethiopia. 10(8), 1448–1460.

Kefeni, K., Mokonnen, B., & Roba, N. (2020). Evaluation the Performance of Regional Climate Models in Simulating Rainfall Characteristics over Upper Awash Sub-Basin , Ethiopia. 5(1), 134–138.

Kerim, T., Abebe, A., & Hussen, B. (2016). Study of Water Allocation for Existing and Future Demands under Changing Climate Condition : Case of Upper Awash Sub River Basin. Journal of Environment and Earth Science, 6(10), 18–31.

Lenhart, T., Eckhardt, K., Fohrer, N. and Frede, H.G., 2002. Comparison of two different approaches of sensitivity analysis. Physics and Chemistry of the Earth, Parts A/B/C, 27(9-10), pp.645-654.

Luo, M., Liu, T., & Meng, F. (n.d.). Comparing Bias Correction Methods Used in Downscaling Precipitation and Temperature from Regional Climate Models : A Case Study from the Kaidu River Basin in Western China.

Melke, A. and Abegaz, F., 2017. Impact of climate change on hydrological responses of Gumara catchment, in the Lake Tana Basin-Upper Blue Nile Basin of Ethiopia. International Journal of Water Resources and Environmental Engineering, 9(1), pp.8-21.

Mengistu, A.G., Woldesenbet, T.A. and Dile, Y.T., 2021. Evaluation of the performance of bias-corrected CORDEX regional climate models in reproducing Baro–Akobo basin climate. Theoretical and Applied Climatology, 144(1), pp.751-767.

Moges, D.M. and Bhat, H.G., 2021. Climate change and its implications for rainfed agriculture in Ethiopia. Journal of Water and Climate Change, 12(4), pp.1229-1244.

Niang, I., Ruppel, O. C., Abdrabo, M. A., Essel, A., Lennard, C., Padgham, J., & Urquhart, P. (2015). Africa. Climate Change 2014: Impacts, Adaptation and Vulnerability: Part B: Regional Aspects: Working Group II Contribution to the Fifth Assessment Report of the Intergovernmental Panel on Climate Change.

Of, R. E., Ibe, O. M. O., & Asin, R. I. B. (2017). School of gradute studies .

Pohlert, T., 2020. trend: non-parametric trend tests and changepoint detection.–R package ver. 1.1. 2.

Quansah, J. E., Naliaka, A. B., Fall, S., Ankumah, R., & Afandi, G. El. (2021). Assessing future impacts of climate change on streamflow within the alabama river basin. Climate, 9(4), 1–19.

Roth, V., Lemann, T., Zeleke, G., & Teklay, A. (2018). Effects of climate change on water resources in the upper Blue Nile Basin of Ethiopia. Heliyon, November 2017.

Saharia, A.M. and Sarma, A.K., 2018. Future climate change impact evaluation on hydrologic processes in the Bharalu and Basistha basins using SWAT model. Natural Hazards, 92(3), pp.1463-1488.

Seibert, J. (2011). Introduction to hydrological modelling and the HBV model How do we see reality ? How does a hydrologist see reality ? System and model.

Sisay, E. (2017). Hydrological modelling of ungauged urban watershed using SWAT model. Modeling Earth Systems and Environment, 0(0), 0.

Stevenson, R.L., 2020. Climate change: evidance and cause: update 2020.

Strickland, T. C., & Bosch, D. D. (2013). Evaluation of SWAT Manual Calibration Sensitivity in the Little River Watershed. May 2007. https://doi.org/10.13031/2013.23149

Tadese, M.T., Kumar, L. and Koech, R., 2020. Climate change projections in the Awash River

Basin of Ethiopia using Global and Regional climate models. International Journal of Climatology, 40(8), pp.3649-3666.

Tadese, M.T., Kumar, L., Koech, R. and Zemadim, B., 2019. Hydro-climatic variability: a characterisation and trend study of the Awash River Basin, Ethiopia. Hydrology, 6(2), p.35.

Tadesse, D., 2010. The impact of climate change in Africa. Institute for Security Studies Papers, 2010(220), p.20.

Taesombat, W., & Sriwongsitanon, N. (2009). Areal rainfall estimation using spatial interpolation techniques. 35, 268–275.

Taye, M.T. and Willems, P., 2013. Identifying sources of temporal variability in hydrological extremes of the upper Blue Nile basin. *Journal of hydrology*, *499*, pp.61-70.

Tessema, N., Kebede, A., & Yadeta, D. (2020). Modeling the Effects of Climate Change on Streamflow Using Climate and Hydrological Models : The case of the Kesem Sub-basin of the Awash River Basin , Ethiopia. International Journal of River Basin Management, 0(0), 1–46.

Tessema, S.M., 2011. Hydrological modeling as a tool for sustainable water resources management: a case study of the Awash River Basin (Doctoral dissertation, KTH Royal Institute of Technology).

Teutschbein, C. and Seibert, J., 2013. Is bias correction of regional climate model (RCM) simulations possible for non-stationary conditions?. Hydrology and Earth System Sciences, 17(12), pp.5061-5077.

Teutschbein, Claudia, & Seibert, J. (2012). Bias correction of regional climate model simulations for hydrological climate-change impact studies: Review and evaluation of differen methods. Journal of Hydrology, 456–457, 12–29.

Uniyal, B., & Jha, M. K. (2015). Assessing Climate Change Impact on Water Balance Components of a River Basin Using SWAT Model. 4767–4785 .

Van Vooren, S., Van Schaeybroeck, B., Nyssen, J., Van Ginderachter, M., & Termonia, P. (2019). Evaluation of CORDEX rainfall in northwest Ethiopia: Sensitivity to the model representation of the orography. International Journal of Climatology, 39(5), 2569–2586.

Vuuren, D. P. Van, Edmonds, J., Kainuma, M., Riahi, K., Nakicenovic, N., Smith, S. J., & Rose, S. K. (2011). The representative concentration pathways : an overview. 5–31.

WaleWorqlul, A., Taddele, Y. D., Ayana, E. K., Jeong, J., Adem, A. A., & Gerik, T. (2018). Impact of climate change on streamflow hydrology in headwater catchments of the upper Nile Basin, Ethiopia. Water (Switzerland), 10(2).

Wang, Z., Ficklin, D. L., Zhang, Y., & Zhang, M. (2011). Impact of climate change on stream fl ow in the arid Shiyang River Basin of northwest China.

Weldearegay, S. K., & Tedla, D. G. (2018). Impact of climate variability on household food availability in Tigray, Ethiopia. Agriculture and Food Security, 7(1), 1–9.

Yaseen, M., Nabi, G., & Latif, M. (2014). Assessment of Climate Change at Spatiao-Temporal Scales and its Impact on Stream Flows in Mangla Watershed. 15, 17–36.

Zegeye, H., 2018. Climate change in Ethiopia: impacts, mitigation and adaptation. International Journal of Research in Environmental Studies, 5(1), pp.18-35.

Zeleke, T. T., Giorgi, F., Diro, G. T., & Zaitchik, B. F. (2017). Trend and periodicity of drought over Ethiopia. International Journal of Climatology, 37(13), 4733–4748.

Zhang, H., Xu, W., Xu, X., & Lu, B. (2017). Responses of Streamflow to Climate Change and Human Activities in a River Basin, Northeast China. Advances in Meteorology, 2017.

APPENDIX

Average yearly temperature.

				Bias corrected tasmax4.5									
year	Jan	Feb	Mar	Apr	May	Jun	Jul	Aug	Sep	Oct	Nov	Dec	av yea
2022	27.0	27.7	29.5	27.8	26.7	24.2	23.4	23.2	23.7	23.7	25.1	25.4	25.6
2023	26.0	28.6	27.1	26.8	26.5	23.3	23.0	24.5	24.8	26.0	25.1	26.3	25.7
2024	27.6	28.4	27.8	25.8	24.4	23.1	23.3	23.4	25.6	25.8	25.6	26.0	25.6
2025	26.9	28.6	28.5	28.4	24.5	23.0	22.6	23.5	24.3	25.6	25.4	26.6	25.7
2026	27.9	28.8	27.0	24.5	24.5	23.3	23.3	24.6	26.2	24.7	24.9	26.4	25.5
2027	28.3	29.4	28.3	26.0	24.4	24.2	23.2	22.9	24.4	25.2	26.1	26.7	25.7
2028	27.7	27.1	28.5	25.8	23.1	22.7	24.6	25.5	25.8	26.3	26.1	28.1	25.9
2029	28.6	29.4	25.4	25.9	24.0	23.6	23.5	24.0	25.9	24.5	26.5	26.4	25.6
2030	28.3	28.9	26.3	25.6	23.5	24.1	23.2	25.1	24.8	24.7	26.6	28.2	25.8
2031	28.4	27.0	27.5	24.3	23.7	23.7	24.2	24.6	26.0	26.0	27.0	27.5	25.8
2032	28.9	28.2	27.6	26.3	24.8	23.2	24.9	25.1	25.6	24.6	26.1	28.2	26.1
2033	27.8	27.4	24.9	23.3	22.4	23.2	24.3	24.6	24.7	26.0	27.2	28.3	25.3
2034	27.4	26.9	25.1	23.4	23.5	24.0	24.8	26.3	25.2	25.5	27.4	28.9	25.7
2035	28.3	26.7	25.4	23.6	23.9	23.8	25.2	25.1	25.5	26.4	28.3	28.6	25.9
2036	28.6	27.6	25.1	23.3	23.0	24.3	23.0	22.6	22.9	24.9	27.7	26.9	25.0
2037	27.3	27.4	25.1	24.1	23.7	23.0	25.0	25.9	23.2	25.9	27.6	29.3	25.6
2038	28.7	25.5	25.0	23.3	24.1	23.1	24.1	25.1	24.7	26.5	28.3	29.1	25.6
2039	25.8	27.8	25.7	23.4	23.4	23.3	25.1	25.3	26.7	27.3	28.5	28.0	25.8
2040	27.0	27.0	23.7	23.4	23.5	24.6	25.1	25.3	26.0	27.8	28.8	29.5	26.0
2041	26.6	27.7	25.1	23.2	25.6	26.0	26.9	25.7	26.3	28.4	27.7	29.0	26.5
2042	28.0	25.5	23.8	24.5	24.6	24.5	24.9	24.8	26.5	26.8	29.8	28.3	26.0
2043	26.5	24.3	23.3	23.3	23.6	25.3	25.7	24.9	26.0	28.0	28.4	27.8	25.6
2044	26.9	25.6	24.0	25.4	26.4	25.9	25.7	26.2	27.0	29.6	28.8	28.4	26.7
2045	28.5	23.4	23.2	23.5	24.0	24.8	26.1	26.6	27.8	29.0	30.0	28.6	26.3
2046	26.0	24.9	23.0	23.3	23.7	23.6	25.3	25.2	27.2	28.5	29.3	28.8	25.7
2047	27.2	24.9	23.8	24.1	26.3	25.9	26.4	27.0	28.4	28.1	28.6	27.6	26.5
2048	25.3	24.1	24.1	23.2	24.8	26.1	25.9	26.7	28.9	29.1	27.4	24.9	25.9
2049	24.4	23.4	24.0	24.8	24.3	25.8	25.8	27.0	27.2	29.0	27.9	28.5	26.0
2050	25.3	24.2	23.8	24.0	25.9	26.2	25.7	26.7	28.5	27.3	28.7	27.1	26.1
2051	25.2	23.7	24.1	24.8	26.5	26.5	26.7	27.9	28.3	28.0	26.8	24.1	26.1
averag	27.2	26.7	25.5	24.6	24.4	24.3	24.7	25.2	25.9	26.6	27.4	27.6	

			Bias corrected tasmax4.5										
year	Jan	Feb	Mar	Apr	May	Jun	Jul	Aug	Sep	Oct	Nov	Dec	av.yea
2052	23.9	23.2	24.9	26.4	25.8	25.6	26.1	28.2	29.3	28.8	25.8	25.4	26.1
2053	24.1	24.3	23.9	25.1	24.9	26.1	26.5	28.5	29.0	28.7	27.4	26.8	26.3
2054	24.0	24.1	24.0	24.9	26.0	25.4	26.7	28.1	30.5	28.1	26.6	24.9	26.1
2055	23.7	23.8	23.4	23.3	23.8	25.9	27.3	27.0	29.3	29.4	25.4	25.1	25.6
2056	23.4	23.3	23.8	25.2	25.7	25.7	26.3	27.8	29.5	28.7	29.6	25.4	26.2
2057	23.9	24.2	25.3	26.4	26.9	27.4	28.0	28.9	29.9	26.5	24.5	22.9	26.2
2058	22.9	24.1	25.1	26.7	25.8	26.2	28.5	29.6	28.7	25.7	24.8	25.0	26.1
2059	24.5	24.5	24.9	24.0	25.7	27.1	28.8	30.6	30.1	26.8	24.7	23.9	26.3
2060	24.0	23.8	24.7	25.9	25.7	27.1	28.9	29.9	27.6	26.3	26.9	24.9	26.3
2061	24.8	24.1	24.1	25.0	24.4	25.3	28.6	29.5	29.3	28.6	24.6	23.3	26.0
2062	23.3	25.9	26.1	26.7	25.1	27.4	28.6	29.9	25.5	26.5	24.1	22.2	25.9
2063	24.8	24.7	26.2	26.1	26.5	27.5	29.4	28.0	27.7	26.3	25.0	23.6	26.3
2064	24.7	26.2	25.6	24.9	26.8	28.0	30.1	29.8	27.6	24.0	23.2	23.7	26.2
2065	24.7	24.4	25.5	25.6	26.9	28.4	30.0	29.5	27.5	24.6	23.7	23.6	26.2
2066	23.6	25.7	26.2	26.7	26.7	28.7	28.4	29.3	26.7	23.7	22.7	24.4	26.1
2067	25.0	26.4	26.0	25.2	27.2	29.3	30.7	27.8	28.5	25.0	24.8	24.8	26.7
2068	26.8	25.8	26.5	27.4	27.5	29.2	28.8	28.4	28.0	25.8	24.3	24.3	26.9
2069	23.4	23.8	25.1	25.2	28.4	29.5	29.3	28.7	28.0	24.7	25.1	24.9	26.3
2070	25.4	26.6	27.3	26.9	28.8	29.8	29.2	27.9	25.6	25.6	24.4	24.5	26.8
2071	23.0	23.2	24.7	26.6	28.9	29.1	27.9	27.1	27.2	25.7	24.3	25.6	26.1
2072	24.8	24.7	25.7	27.8	27.6	29.9	28.8	28.7	26.1	23.5	24.6	26.2	26.6
2073	26.7	27.0	26.7	27.4	28.8	28.0	27.5	24.7	24.1	24.9	24.6	26.9	26.4
2074	27.2	26.8	27.3	28.3	29.7	30.4	29.3	29.6	25.2	24.2	23.8	24.1	27.2
2075	24.8	26.1	27.1	28.6	29.2	30.5	27.0	29.3	25.6	24.0	24.1	25.1	26.8
2076	25.6	25.4	24.6	28.1	29.7	29.6	27.3	27.3	24.4	24.3	25.1	26.4	26.5
2077	26.2	26.0	26.8	28.5	28.6	27.6	26.6	25.5	23.7	24.6	24.5	26.1	26.2
2078	25.8	27.4	27.8	29.1	30.1	27.7	26.5	24.6	24.1	24.6	24.3	25.7	26.5
2079	25.3	27.2	27.9	29.3	30.0	27.5	28.1	25.3	23.3	24.0	24.5	26.4	26.6
2080	26.8	27.0	28.1	29.3	28.8	29.2	26.6	25.1	24.2	25.5	24.7	25.9	26.8
2081	26.6	26.6	28.0	30.0	28.3	29.3	27.2	24.8	23.7	25.0	25.8	25.3	26.7
averag	24.8	25.2	25.8	26.7	27.3	27.9	28.1	28.0	27.0	25.8	24.9	24.9	

			Bias corrected tasmax8.5										
year	Jan	Feb	Mar	Apr	May	Jun	Jul	Aug	Sep	Oct	Nov	Dec	av year
2022	26.5	28.4	27.4	27.4	23.4	23.6	22.9	22.5	22.7	23.7	22.4	24.3	24.6
2023	25.3	27.5	28.4	26.6	26.2	23.7	21.6	22.1	23.7	24.3	24.8	25.2	25.0
2024	25.5	27.2	26.5	26.0	23.2	22.5	22.5	22.3	22.6	23.7	23.2	25.5	24.2
2025	26.6	27.4	27.3	23.1	23.9	22.0	22.5	23.8	24.6	24.5	24.6	26.0	24.7
2026	27.3	28.1	28.6	26.2	24.0	22.8	22.9	25.0	24.0	25.1	24.6	26.3	25.4
2027	26.7	27.6	27.0	26.6	23.3	23.0	22.7	22.8	24.5	25.3	25.7	25.6	25.1
2028	27.2	27.8	25.5	24.5	23.1	22.8	22.3	22.6	22.0	23.2	23.9	26.1	24.3
2029	28.0	27.3	28.1	25.1	23.1	23.1	22.7	24.0	24.5	23.7	25.3	27.0	25.2
2030	28.6	27.5	26.3	26.3	23.8	23.1	23.3	23.8	24.4	23.8	24.4	27.4	25.2
2031	28.2	27.7	25.9	25.3	23.4	23.9	22.8	23.3	23.9	24.3	25.1	28.0	25.1
2032	28.0	26.7	26.6	25.4	23.9	24.3	25.0	26.1	25.7	25.6	26.4	27.4	25.9
2033	27.9	26.7	26.8	24.3	22.8	22.9	24.0	24.8	25.2	23.4	25.4	26.9	25.1
2034	28.9	27.8	25.0	23.6	23.3	23.9	24.1	25.0	25.6	25.8	26.7	28.8	25.7
2035	29.5	24.5	25.0	23.6	24.1	24.5	25.6	25.5	25.1	25.6	27.4	27.8	25.7
2036	28.7	24.4	25.9	22.9	22.8	24.3	25.3	25.9	25.1	25.4	26.6	26.0	25.3
2037	26.1	25.1	25.5	22.7	23.4	24.0	25.1	24.7	25.4	26.4	27.2	28.4	25.3
2038	26.9	24.1	23.7	23.6	24.2	24.3	25.5	25.3	25.9	26.9	28.5	27.5	25.5
2039	28.3	24.9	24.0	23.4	23.1	23.5	24.4	24.4	25.6	26.1	27.4	29.6	25.4
2040	26.3	26.2	23.9	24.4	23.4	24.5	25.4	24.9	26.2	26.3	27.7	27.8	25.6
2041	24.6	24.1	23.6	22.8	23.2	25.0	25.8	25.7	26.3	27.4	29.2	28.1	25.5
2042	26.6	25.3	24.1	23.8	23.5	23.4	23.2	24.8	25.3	26.3	29.1	27.8	25.3
2043	26.6	24.2	23.2	22.7	23.7	25.6	26.3	26.1	26.3	27.9	28.7	27.6	25.7
2044	25.6	23.4	22.8	23.2	24.4	25.9	25.2	25.1	26.6	28.7	28.0	27.1	25.5
2045	25.2	25.0	23.3	23.4	25.5	25.6	25.7	24.4	27.2	28.0	28.9	27.1	25.8
2046	27.1	23.8	23.4	23.8	24.7	25.0	25.4	26.1	27.0	27.0	27.6	27.9	25.7
2047	26.4	24.8	24.2	24.6	27.1	26.0	25.6	26.5	28.2	29.3	28.4	28.5	26.6
2048	24.8	24.1	23.8	23.4	24.3	25.5	26.4	26.9	27.3	27.7	25.4	26.3	25.5
2049	25.8	24.8	24.5	24.6	25.8	26.2	26.5	25.7	27.4	27.9	27.7	25.2	26.0
2050	24.5	23.2	23.4	24.3	22.9	24.4	25.9	27.1	28.9	28.2	28.0	26.6	25.6
2051	23.3	23.4	23.7	24.8	24.7	25.3	26.0	26.7	28.9	30.0	26.7	24.9	25.7
average	26.7	25.8	25.2	24.4	23.9	24.1	24.4	24.8	25.5	26.1	26.5	27.0	

					Bias corrected tasmax8.5								
year	Jan	Feb	Mar	Apr	May	Jun	Jul	Aug	Sep	Oct	Nov	Dec	av yea
2052	23.1	24.0	23.1	24.5	24.8	25.7	25.5	28.0	28.4	28.2	28.7	26.2	25.8
2053	25.1	25.0	24.1	25.7	25.7	26.0	27.1	28.5	29.2	29.0	25.7	26.4	26.5
2054	23.8	23.7	24.4	26.2	25.8	26.5	26.1	26.6	29.1	26.5	27.1	26.9	26.1
2055	24.7	24.6	25.6	26.7	26.1	26.6	26.9	27.2	29.6	28.7	25.9	26.5	26.6
2056	23.6	23.2	24.5	22.6	23.0	24.7	26.4	28.6	27.4	27.5	27.4	23.8	25.2
2057	23.8	25.0	23.9	25.7	26.3	26.6	27.8	27.3	26.4	28.9	28.1	25.6	26.3
2058	24.4	24.0	24.2	24.0	24.7	25.3	28.0	28.4	28.2	26.5	23.8	23.9	25.5
2059	23.9	23.7	23.8	25.2	25.4	26.5	28.7	28.9	26.3	26.2	25.6	24.7	25.7
2060	24.4	24.3	25.2	26.8	27.1	25.6	28.5	27.0	27.5	27.6	25.0	22.9	26.0
2061	24.0	23.5	25.2	26.1	26.0	26.7	28.2	29.2	27.6	26.6	23.6	23.3	25.8
2062	24.6	24.3	25.3	25.9	26.7	27.0	29.1	29.1	28.6	26.6	25.0	23.2	26.3
2063	24.4	23.7	23.3	23.4	25.5	26.3	28.4	27.5	29.4	27.8	24.9	24.1	25.7
2064	24.9	26.3	26.5	26.5	26.7	27.4	29.1	30.3	29.5	26.1	23.8	23.9	26.7
2065	24.9	24.4	26.3	26.7	26.4	28.0	30.0	29.3	29.0	26.4	24.8	24.2	26.7
2066	24.7	25.1	25.4	26.5	25.9	28.8	29.1	28.4	29.0	27.2	25.3	23.9	26.6
2067	25.0	26.6	26.7	26.2	28.0	29.5	29.9	26.6	25.6	26.7	24.7	25.0	26.7
2068	26.8	26.5	26.1	26.5	27.8	28.8	29.5	29.0	26.2	24.6	23.9	24.2	26.6
2069	25.2	26.2	25.9	25.9	28.3	29.0	28.8	28.7	25.9	24.6	24.5	24.4	26.5
2070	23.3	24.7	26.1	27.7	29.3	30.1	30.1	29.9	26.7	24.5	24.3	24.3	26.7
2071	24.5	26.0	26.4	28.3	28.7	29.5	29.6	26.7	25.6	25.6	24.4	23.7	26.6
2072	24.3	25.7	25.3	27.5	28.4	29.8	29.4	28.3	26.6	24.5	24.3	24.1	26.5
2073	25.0	26.3	24.8	27.7	28.8	28.8	29.5	29.8	27.7	25.1	24.6	25.7	27.0
2074	23.8	24.7	26.4	28.5	30.5	29.9	29.7	26.5	25.0	23.5	24.1	24.2	26.4
2075	23.9	25.3	24.6	27.7	29.7	29.6	28.6	27.2	23.8	24.5	26.4	24.6	26.3
2076	26.3	27.2	27.6	28.3	29.8	28.4	29.0	28.6	25.8	25.0	26.4	27.2	27.5
2077	27.3	27.5	28.7	28.6	29.8	28.9	24.8	27.0	23.9	24.6	24.9	26.7	26.9
2078	26.5	27.5	28.4	29.2	30.3	29.3	30.2	28.3	24.3	25.5	25.6	25.0	27.5
2079	26.0	25.1	24.8	27.4	29.9	30.3	29.0	27.0	24.9	25.0	24.7	24.2	26.5
2080	26.4	26.3	27.3	28.0	30.0	30.1	30.0	25.3	24.6	24.7	25.4	26.6	27.0
2081	27.2	27.7	28.5	30.0	29.9	26.2	29.4	25.2	24.4	25.0	27.0	26.9	27.3
averag	24.9	25.3	25.6	26.7	27.5	27.9	28.5	28.0	26.9	26.1	25.3	24.9	

Table: Precipitation Bias correction method used known as power transformation

Day	YEAR	Month	Ob.RainFall	RCP(mm)	RCP^b	a*RCP^b
	2/1/1987	2	0	0	0	0
	2/2/1987	2	0	0	0	0
	2/3/1987	2	0	0	0	0
	2/4/1987	2	0	0	0	0
	2/5/1987	2	0	0	0	0
	2/6/1987	2	0	0	0	0
	2/7/1987	2	0	0	0	0
	2/8/1987	2	0	0	0	0
	2/9/1987	2	0	0	0	0
	2/10/1987	2	0	0	0	0
	2/11/1987	2	0	0	0	0
	2/12/1987	2	0	0	0	0
	2/13/1987	2	0	0	0	0
	2/14/1987	2	0	0	0	0
	2/15/1987	2	0	0	0	0
	2/16/1987	2	0	0	0	0
	2/17/1987	2	0	0	0	0
	2/18/1987	2	0	0	0	0
	2/19/1987	2	0	0	0	0
	2/20/1987	2	0	0.5768	0.239147	0.000256
	2/21/1987	2	0	6.015	106.1726	0.113605
	2/22/1987	2	0	0.0824	0.001518	1.62E-06
	2/23/1987	2	0	0	0	0
	2/24/1987	2	0	0	0	0
	2/25/1987	2	0.113809	0	0	0
	2/26/1987	2	0	0	0	0
	2/27/1987	2	0	0	0	0
	2/28/1987	2	0	0	0	0
Sum			0.11	6.67	106.41	0.11
Mean			0.00	0.24	3.80	0.00
Std			0.02	1.14	20.06	0.02
Cv(Std/Mean)			5.29	4.77	5.28	5.28
Cvob -CvRCP^b		0.001	0bs	RCP	RCP^b	a*RCP^b
a=(MOb/MRCP^b)		0.00107				
b		0.01				

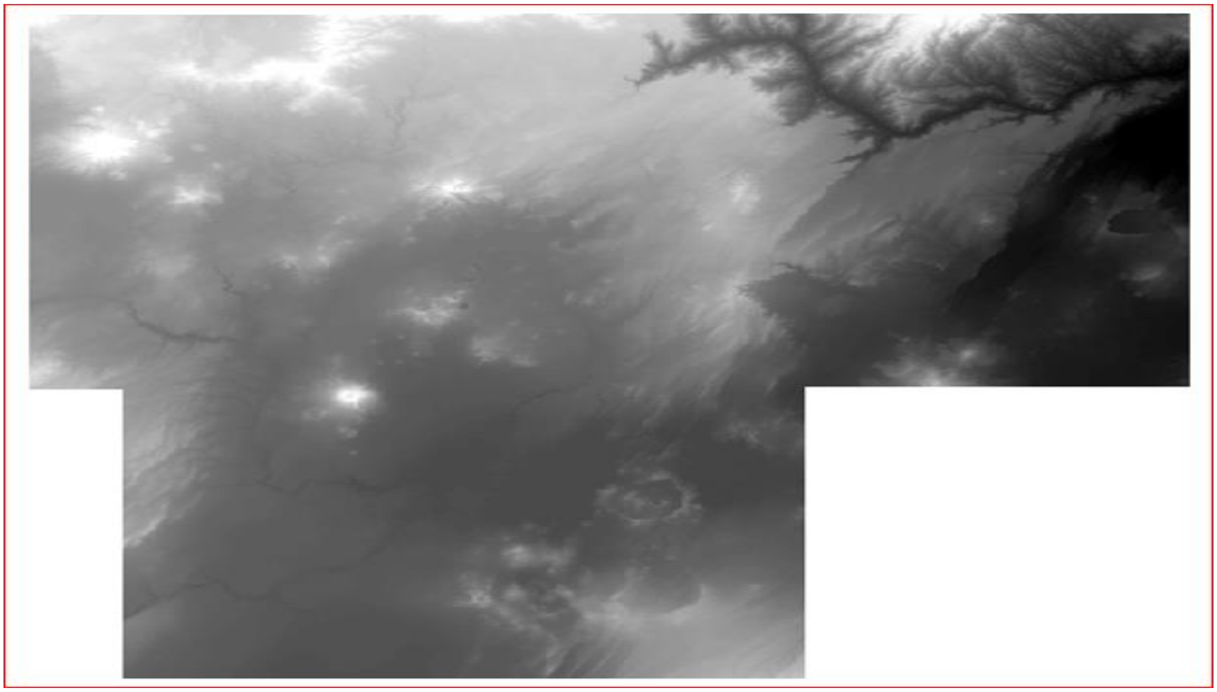

Digital Elevation Model Downloaded from https://asf:alaska.edu.

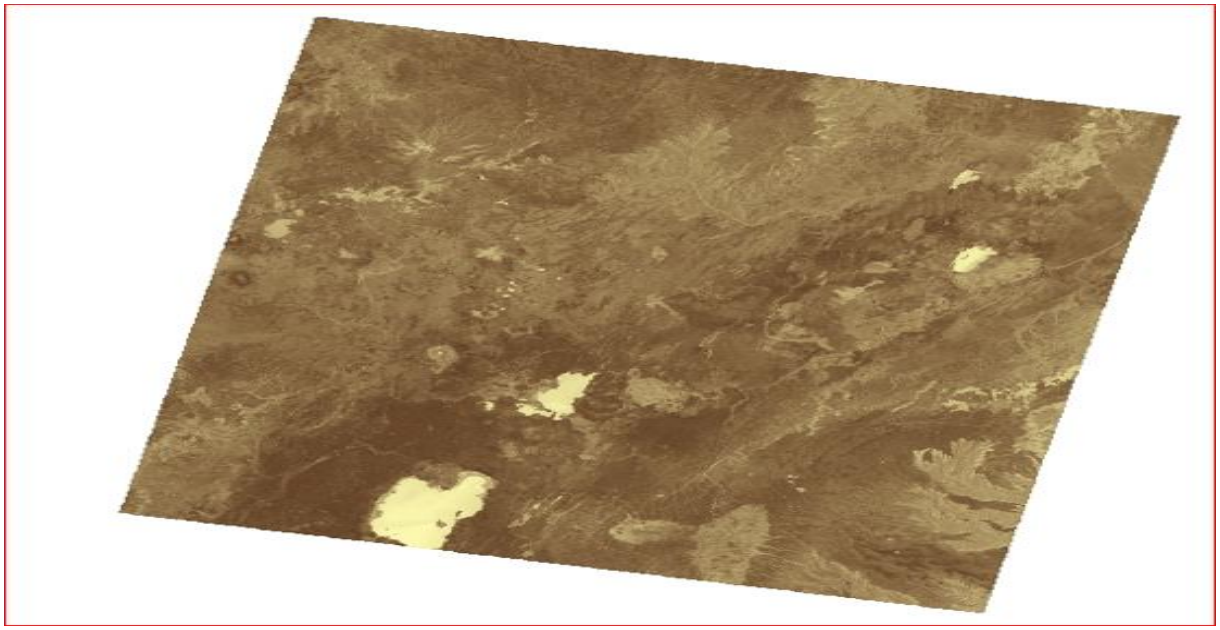

Land Use Land Cover in Downloaded Form https://earthexplorer.usgs.gov.